To the Graduate Council:

I am submitting herewith a thesis written by Ying Feng entitled "Determination of Neutron Dose from Criticality Accident with Bioassays for Blood-^{24}Na and Hair-^{32}P." I have examined the final copy of this thesis for form and content and recommend that it be accepted in partially fulfillment of the requirements for the degree of Master of Science, with a major in Nuclear Engineering.

L. F. Miller , Major Professor

We have read this thesis
and recommend its acceptance:

Accepted for the Council:

Associate Vice Chancellor
and Dean of the Graduate School

STATEMENT OF PERMISSION TO USE

In presenting this thesis in partial fulfillment of the requirements for a Master's Degree at the University of Tennessee, Knoxville, I agree that the Library shall make it available to borrowers under rules of the Library. Brief quotation from this thesis is allowable without special permission, provided that accurate acknowledgement of the source is made.

Permission of extension quotation from or reproduction of this thesis may be granted by my major professor, or in his absence, by the head of Interlibrary Services when, in the opinion of either, the proposed use of the material is for scholarly purpose. Any copying or use of the material in this thesis for financial gain shall not be allowed without my written permission.

Signature Ying Feng

Date Nov. 26, 1991

DETERMINATION OF NEUTRON DOSE FROM CRITICALITY ACCIDENTS WITH BIOASSAYS FOR BLOOD ^{24}Na AND HAIR ^{32}P

A Thesis

Presented for the

Master of Science Degree

The University of Tennessee

Knoxville

Ying Feng

December 1991

ACKNOWLEDGEMENTS

I wish to express my sincere gratitude to my major professor, Dr. L. F. Miller, for his guidance, advice, inspiration, and valuable suggestions during my graduate study and research. Dr. Miller was instrumental in changing my career direction. I would also like to express my sincere gratitude to other committee members, Dr. J. E. Turner and Dr. D. J. Downing, for their wonderful teaching, their comments and suggestions on my thesis.

Appreciation is also expressed to the department head, Dr. T. W. Kerlin, for providing me a chance to study at this department. I would also like to thank Dr. G. Mei, Dr. W. Casson, Dr. J. S. Bogard, Dr. M. Thein, and the ORNL for the financial and technical support to this research. Appreciation is also expressed to Mr. Osborne, Radiation Safety Officer at UTK and Dr. Schwietzer in the Chemistry Department of UTK for their kindness and assistance for this research.

Special thanks to my husband, A. Wei.

ABSTRACT

The possible occurrence of a criticality accident cannot be entirely disregarded even through the advanced technology has been developed for preventing accidents. The necessary procedures and facilities for dealing with criticality accidents must be provided to obtain a rapid dose assessment following a criticality accident for doctors to determine treatment methods for each victim.

A comprehensive study of the accident neutron dosimetry using blood and hair was performed and the results of this study are presented in this thesis. The primary objectives of this research are to establish blood-^{24}Na and hair-^{32}P activity measurement procedures for the accident dosimetry system at the Oak Ridge National Laboratory and to develop an accident neutron dosimetry system using blood and hair. These were accomplished through experiments conducted at the University of Tennessee, Knoxville and through calculations of blood and hair activations for 98 different neutron spectra.

A measurement procedure of blood-^{24}Na was established based on a HPGe detector system. The sensitivity of the measurement process for a 20 ml sample is one to two rads of total neutron dose for hard spectra and below 0.5 rads for soft spectra based on 30 to 60 minute counting.

A procedure for direct counting hair samples using a liquid scintillation detector was established. About six to ten rads of total neutron dose can be measured from one gram of hair sample using this procedure. Detailed procedures

for chemical dissolution and ashing hair samples were documented.

The established neutron dose assessment system using blood and hair is based on a collection of 98 neutron spectra. Ninety-eight blood activity-to-dose conversion factors were calculated. This dosimetry system make it possible to estimate the individual's neutron dose within a few hours after an accident if the accident spectrum can be approximated from one of the tabulated 98 neutron spectra.

TABLE OF CONTENTS

CHAPTER PAGE

I. INTRODUCTION 1

1.1 Nuclear Criticality Accidents 1

1.2 Characteristics of an Accident Dosimetry System 3

1.3 Types of Accident Dosimetry Systems 4

1.4 Overview of Previous Work in Body Activation 5

1.5 Objectives of Present Research 6

1.6 Contributions of this Thesis 7

1.8 Organization of this Thesis 8

II. DEVELOPMENT OF BLOOD SODIUM MEASUREMENT PROCEDURES 10

2.1 Introduction 10

2.2 Blood-Sodium Measurement System 11

2.2.1 Components of Measurement System 12
2.2.2 Performance Tests of Measurement Systems 14
2.2.3 Calibration of Detection System 15

2.2.3.1 Two Point Energy Calibration 15
2.2.3.2 Efficiency Calibration 16

2.3 Saline Sample Irradiation and Counting 19

2.4 Blood Na-24 Concentration Calculation 24

2.5 Counting Statistics and Error Analysis 30

2.6 Sensitivity of Measurement Process 32

III.DEVELOPMENT OF HAIR P-32 MEASUREMENT PROCEDURES 39

3.1 Introduction 39

3.2 Hair-Phosphorus Measurement System 41

3.2.1 Liquid Scintillation Counting 41
3.2.2 Components of Counting System 45
3.2.3 Performance Tests of Detector 46

3.3 P-32 Counting Efficiency Determination 46

3.3.1 Quenching 46
3.3.2 Counting Interference 49
3.3.3 Tracing Hair-^{32}P Counting Efficiency 50

3.4 Hair Sample Preparation 53

3.4.1 Hair Washing 55
3.4.2 Chemical Dissolution of Hair 55
3.4.3 Ashing Hair 57

3.5 Hair Sample Counting
and ^{32}P Activity Calculation 58

3.6 Sensitivity of Measurement System 62

**IV. DEVELOPMENT OF ACCIDENT
NEUTRON DOSE ASSESSMENT SYSTEM** 67

4.1 Introduction 67

4.2 Discussion of Neutron Spectra 68

4.2.1 Spectrum Description 68
4.2.2 Plots of Representative Spectra 69

4.3 Neutron Dosimetry Using Blood 73

4.3.1 Blood Activity-to-Fluence 73

4.3.1.1 Capture Probability 73
4.3.1.2 Relation between Fluence and ^{24}Na Activation 76

4.3.2 Fluence-to-Neutron Dose Conversion Factors 80
4.3.3 ^{24}Na Activity-to-Dose Conversion Factors for Different Spectra 81

4.4 Estimation of Accident Neutron Dose Using Blood and Hair Activation 92

4.5 Interpretation of the Derived Neutron Dose 102

4.5.1 Floor Scattering Neutrons 102
4.5.2 Orientation of Individual in the Moment of Excursion 103
4.5.3 Person's Size 105

V. CONCLUSIONS AND SUGGESTIONS FOR FURTHER WORK . . . 106

5.1 Conclusions 106

5.2 Suggestions for Further Work 107

REFERENCES 108

APPENDIXES 111

Appendix A: Blood Activity Measurement Procedure 112

Appendix B: Hair Activity Measurement Procedure 118

Appendix C: Computer Programs
Developed for this Research 124

Appendix D: Additional Bibliography 135

VITA 136

LIST OF TABLES

Table		Page
1.1	Summary of Radiation Accident	2
2.1	Efficiency Calibration Standard	18
2.2	The Measured and Calculated Results for Saline Samples	28
2.3	Results of Counting Error Analysis	33
2.4	Minimum Detectable Activity for Saline Samples Counted at UT	37
3.1	Relationship between Quenching and Hair Sample Weight	54
3.2	Description of Chemical Materials Used	56
3.3	Measured and Calculated Results for Hair Samples Irradiated by Different Neutron Doses	60
3.4	Background Count Rate from Chemically Dissolved "Blank" Hair Samples with Different Amount of Hair and Counting Time in Window 5-1700 KeV	63
3.5	Background Count Rate from Ashed "Blank" Hair Samples with Different Amount of Hair and Counting Time in Window 5-1700 KeV	65
3.6	Minimum Detectable Activity for Hair ^{32}P Counting	66
4.1	Spectra Description	70
4.2	Capture Probabilities for a Bomanb Phantom	74
4.3	Neutron Fluence to Dose Conversion Factors	83

4.4 Activity to Depth Dose Conversion Factors for 98 Neutron Spectra 86

4.5 Activity to Surface Absorbed Recoil Dose Conversion Factors for 98 Neutron Spectra 89

4.6 Ratio of Activation between Hair and Blood & Ratio between Fluence above 2.5 MeV and Total Fluence for 98 Neutron Spectra 95

LIST OF FIGURES

Figure		Page
2.1	Connection of Components in HPGe System	13
2.2	Efficiency Curve Using QCY.48	20
2.3	Bare Cf-252 Spectrum	21
2.4	D_2O Moderate Cf-252 Spectrum	22
2.5	A Schematic of Blood Samples Irradiation	23
2.6	Relationship among the LLD, Type I Error, and Type II Error	36
3.1	Illustration of the Collision Process	43
3.2	A Schematic of Liquid Scintillation Counting	44
3.3	Quenching Effect	48
3.4	Efficiency Curves for Tritium and Carbon-14	58
4.1	Uncollided Fission Spectrum (original)	71
4.2	Uncollided Fission Spectrum (interpolated)	72
4.3	A Schematic of Bomab Phantom	75
4.4	Capture Probability as a Function of Neutron Energy	77
4.5	Cross Section of $^{23}Na(n,\gamma)^{24}Na$	78
4.6	Fluence-to-Dose Conversion Factors	82
4.7	Cross Section of ^{32}S (n,p) ^{32}P	93
4.8	Relationship between Activity Ratio (A_{P-32}/A_{Na-24}) and Depth Dose for 98 Neutron Spectra	97

4.9 Relationship between
Activation Ratios and Depth Dose 98

4.10 Spectra of the "Direct" and Floor-Scattered
Components of Neutrons Striking a Phantom
3 M from a Fission Source. The Source
is 1.5 m above the Floor 104

CHAPTER I

INTRODUCTION

1.1 Nuclear Criticality Accidents

A criticality accident is defined as "an unplanned or uncontrolled nuclear excursion resulting from the assembly of a quantity of fissile material. In some cases the mass of the material may have a sufficient excess of reactivity to become prompt-critical and result in a very fast pulse of energy accompanied by a field of thermal and ionizing radiation. [1]" A radiation risk to workers and the public can arise from the possibility of a criticality excursion.

Techniques and procedures for preventing the occurrence of such accidents have reached very high standards. Despite advanced technology and administrative controls aimed at preventing criticality accidents, the possible occurrence of such an accident cannot be entirely disregarded.

About 36 separate criticality accidents have occurred since 1945 [1]. Thirteen occurred in the U.S.A, and most happened before 1964. Table 1.1 lists some accidents that occurred in the U.S.A. and Yugoslavia [2].

The principal concern for the victims is for those whose integral absorbed doses are greater than 25 rads to the whole body or a major part. The occurrence of fatalities is considered generally to begin at about 200 rads. A fatal outcome is probably inevitable at about the 800 rad dose level [2].

The necessary procedures and facilities for dealing with criticality accidents

Tablele 1.1 Summary of Radiation Accidents

Accident	Date	Type	Pt. Code	Calculated Total Body Dose		
				Neutron	Gamma	Total (rad)
Los Alamos I	August 21	Criticality	LA1	297 (rad)	?	297+ (rad)
	1945	(Experimental Assembly)	LA2	18.2	2	20.2
Los Alamos II	May 21	Criticality	LA3	1230	120	1350
	1946	(Experimental Assembly)	LA4	220	22	242
			LA6	120	12	142
			LA7	50	5	55
			LA8	33	3	36
			LA9	25	2.5?	27.5?
Argonne	June 2	Criticality	A1	14.2	145	159
	1952	(Reactor)	A2	9.6	116	126
			A3	5.5	55	60.5
			A4	0.8	10	10.8
Oak Ridge	June 16	Criticality	OR1	96	269	365
	1958	(Processing)	OR2	89	250	339
			OR3	86	241	327
			OR4	71	199	270
			OR5	62	174	236
			OR6	18	50.5	68.5
			OR7	18	50.5	68.5
Yugoslavia	October 15	Criticality	Y1	320	320	640
	1958	(Reactor)	Y2	250	250	500
			Y3	290	290	580
			Y4	300	300	600
			Y5	210	210	420
			Y6	175	175	350
Los Alamos III	December 30	Criticality	LA11	2300	6900	9200
	1958	(Processing)	LA12			

must be provided to obtain a rapid dose assessment following a criticality accident for doctors to determine the treatment methods for each victim. This is called the accident dosimetry system.

1.2 Characteristics of an Accident Dosimetry System

Criticality accidents present a number of dosimetry problems that differ markedly from those encountered in routine personnel dosimetry. Some characteristics of criticality accidents are as follows.

1. The probability for the occurrence of criticality accidents is very low.
2. The radiation field has a complex spectrum due to the mixture of neutrons and gammas,
3. The neutron spectrum varies markedly regarding the types of critical assembly, the moderator, and the nature of shielding.
4. The initial radiation intensity in an accident is extremely high.
5. Criticality accidents involve an acute exposure to gamma and neutron radiation for which the concept of dose-equivalent is invalid. The dose equivalent is meaningful for low level chronic exposures. Dose from nuclear accidents should be given in terms of absorbed dose to the body (rads).

In addition, the accident dosimetry system should permit an initial dose determination to be completed within 48 hours with an uncertainty of less than 50% and less than 25% within one week of the accident [1].

1.3 Types of Accident Dosimetry Systems

Nuclear accident dosimetry systems fall into the following three categories.

1. Personnel dose meters worn on the body such as activation and fission detectors, nuclear track detectors for neutron measurement, and thermoluminescent dose meters (TLDs) for gamma measurement.

2. Area dose meters installed in the general vicinity where a potential criticality accident could occur.

3. Activation of body components such as whole-body sodium, blood sodium and hair phosphorus by neutrons.

The installed area dosimetry systems give spectral information over the whole accident area. However, it could be of little value if the system cannot cover the accident area, or if more than one excursion occurs. A simple personnel dose meter gives the dose received by the individual. But, it could provide fairly unaccurate results if the information of the person's orientation to the critical system at the time of the accident is not known. It is also possible that the individual may not be wearing a dosimeter when an accident occurs. Under these circumstances, body activation will be the best technique to access the individual's neutron dose received in an accident.

1.4 Overview of Previous Work in Body Activation

Body activation in determining the induced neutron dose in irradiated

personnel was first implemented by Hempelmann and his associates in 1952 [3]. In the 1960's and 1970's, Los Alamos Scientific Laboratory (LASL), Oak Ridge National Laboratory (ORNL), Atomic Energy Research Establishment (AERE) of the United Kingdom, International Atomic Energy Agency (IAEA), and others continuously conducted research work in this field. The mechanisms of body activation by neutrons have been developed. Experiments on phantoms under several simulated critical assemblies have been conducted. One of the important contributions from this research is the concept of body capture probability. Capture probability accounts for body moderation to the incident neutrons. Mechanisms of body activation and other results will be utilized in this research work. Due to the lack of the information on accident neutron spectra, the previous research for accident neutron dosimetry was limited to a certain degree. In the early 1980's, the progress in this field was lessened because of little concern about criticality accidents.

In the later 1980's, research work on criticality accidents became active after the Chernoble accident in the U.S.S.R. in 1986. Within one decade, more advanced nuclear measurement equipment has been developed. In 1990, IAEA published more detailed information for different neutron spectra [4]. All of these make it necessary and feasible to update and improve the accident neutron dosimetry system.

1.5 Objectives of Present Research

The Department of Energy (DOE) required its contractors to establish radiation protection standards and programs with respect to the protection of the

worker from ionizing radiation through DOE Order 5480.11 in 1988. The ORNL is required to update its nuclear accident dosimetry system. The updated nuclear accident dosimetry system will include following five basic elements [22]:

(a) A method to conduct initial "screening" of personnel involved in nuclear accidents to determine if they have received a significant radiation exposure.

(b) Methods for analysis of biological materials (including sodium-24 activity in blood and phosphorus-32 activity in hair).

(c) A system of fixed units capable of yielding estimated radiation dose and the approximate neutron spectrum at their locations.

(d) Personnel dosimeters capable of furnishing sufficient information to determine neutron and gamma dose and/or dose equivalent.

(e) Counting facilities to evaluate personnel dosimeters, sodium in blood, and phosphorus in hair.

The research described herein fulfills items (b) and (e).

The objectives of this research are to study the principles of the accident neutron dosimetry using bioassay materials (blood and hair), to establish the measurement procedures of blood Na-24 and hair P-32 induced by neutrons, and to develop a practical and rapid accident neutron dose assessment process based on the blood and hair for the accident dosimetry system at ORNL. The following detailed tasks have been identified to accomplish these objectives.

1. Review the previous work on accident neutron dosimetry.
2. Study the principles of experimental facilities used in this research.

3. Conduct experiments to develop suitable methods for hair sample treatment.

4. Establish measurement procedures of blood Na-24 activity induced by neutrons.

5. Establish measurement procedures of hair P-32 activity induced by high energy neutrons.

6. Determine the sensitivities of the two established measurement procedures.

7. Develop an accident neutron dosimetry system which can quickly access neutron doses from the activation of the blood and hair with or without detailed knowledge of the accident neutron spectrum.

8. Analyze the factors affecting the accident neutron dose determination qualitatively.

1.6 Contributions of this Thesis

This thesis is mainly composed of two parts: the establishment of detailed blood Na-24 and hair P-32 measurement procedures, and the development of an accident neutron dosimetry system using the blood and hair.

The first contribution of this thesis is that it provides detailed and accurately documented activity measurement procedures of the blood and hair for an accident neutron dosimetry system at ORNL. Both procedures include sample preparation, requirements for materials and equipments, preparation of the detection system, activity analysis methods, and requirements of the Minimum Detectable Activity

(MDA).

The second contribution of this thesis is the establishment of a dosimetry system using blood and hair. The activation of the blood and hair is a strong function of neutron spectra. However it is very difficult to obtain detailed and accurate information on an accident spectrum in a short period of time after the accident. This dosimetry system can be used with or without detailed information on the accident neutron spectrum. Activity-to-dose conversion factors were calculated for 98 neutron spectra, which encompass the most likely neutron spectra expected to be encountered in criticality accidents. Calculated activity ratios between the hair and blood can be used to select the most appropriate accident spectrum.

The third contribution is that the computer codes developed to complete this research will be useful for data processing in a real accident.

1.7 Organization of this Thesis

This thesis is presented in five chapters and four appendixes. Following this introductory chapter, the development of the measurement procedures of blood ^{24}Na is discussed in Chapter II. A description of the experimental facility and measurement system used for this study is included, and the discussion of Minimum Detectable Activity (MDA) is also presented in this chapter. A similar discussion for the hair ^{32}P is given in Chapter III. This chapter also discusses the pretreatment methods for hair samples. Chapter IV describes the development of the dosimetry system. The methodology for calculating the 98 blood activity-to-dose conversion

factors is presented in this chapter. The special functions of the hair as a bioassay material in an accident are addressed. The uncertainty of this dosimetry system is qualitatively discussed in Chapter IV. Concluding remarks and suggestions for future research are presented in Chapter V. The established measurement procedures for blood-^{24}Na and hair-^{32}P are presented in Appendix A and Appendix B separately. The computer codes developed for this research are presented in Appendix C. Appendix D lists an additional bibliography.

CHAPTER II

DEVELOPMENT OF
BLOOD SODIUM MEASUREMENT PROCEDURES

2.1 Introduction

A human body normally contains about 1.4 grams sodium-23 per kg of weight. The concentration of sodium-23 in blood is 1.91 mg per ml blood [5]. Sodium-23 will produce sodium-24 when it absorbs neutrons. Sodium-24 is a gamma-ray emitter with a 14.8 hour radioactive half-life. Sodium-24 decays by emitting a beta particle and two gamma-rays, having energies 1.369 MeV and 2.754 MeV. Both blood-sodium and body-sodium activity measurements can be used as an indication of neutron exposure in an accident.

The measurement of blood-sodium is more reliable than the whole body-sodium measurement since the whole body measurement results are affected by the radioactive contamination of the body surface. In this research, a NaCl solution was used instead of real human blood.

The blood-sodium measurement system, neutron sources, activity counting process, the methodology of ^{24}Na activity calculation, and MDA are studied in this chapter. The quantities that influence the determination of blood-sodium activities are discussed.

2.2 Blood-Sodium Measurement System

Measurements of blood-sodium activities are usually made by measuring the gamma activity of small samples of blood. Gamma activities can be measured by a NaI(TL) crystal scintillator with a multichannel-channel analyzer or by a High Purity Germanium detector with a multi-channel analyzer (HPGe). HPGe is utilized in this research for two reasons.

First, most of sodium-23 in blood is in the form of NaCl. When irradiated by neutrons, ^{37}Cl will become ^{38}Cl, and ^{38}Cl is a gamma emitter with radioactive half-life of 33 minutes. It has two energy gamma-rays, 1.64 MeV and 2.17 MeV, which are close to gamma-ray energies of ^{24}Na. The main portion of gamma activity of blood during the first four hours after excursion is due to ^{38}Cl. To avoid the interface of ^{38}Cl gamma-ray with the ^{24}Na measurement, a high energy resolution detector is needed. The resolution of a detector reflects the width of its photopeaks. The narrower the peak, the more capable the system to distinguish different gamma rays of closely spaced energies. Energy resolution is defined as the width of a peak half-way between its top and base. HPGe systems have a typical energy resolution of a few tenths of a percent compared with 5-10% for NaI detectors.

Second, the HPGe spectrometers used in laboratories for routine measurements usually are routinely calibrated over a broad band of gamma-ray energies under quality assurance program. Thus, these systems can be immediately utilized after accidents.

2.2.1 Components of Measurement System

A schematic of the measurement system is shown in Figure 2.1. The spectrometry system consists of lead shielding, a GMX n-type high-purity Germanium detector, a preamplifier, a high voltage filter, a high voltage bias supply, a main amplifier, and the Advanced Data Collection and Management (ADCAM) system from EG&G ORTEC.

The ADCAM system integrates a personal computer with a multichannel analyzer, several computer-controlled instruments and software to provide a workstation for performing high quality measurements. The workstation uses a personal computer for data acquisition and data reduction for experiments.

The detector absorbs the energy from the incident gamma ray and produces a current pulse which is proportional to the absorbed energy. This pulse is integrated, converted to a voltage pulse, and shaped by the preamplifier. Additional amplification and pulse shaping is provided by the main amplifier (shaping amplifier). Output pulses from this amplifier go to the multichannel analyzer (MCA). The MCA has two basic functions. First, it counts the number of pulses from the detector. The number of pulses (counts) are related to the number of gamma rays coming from the sample and to the disintegration rate (activity) of the source. Second, the MCA measures the amplitude of each pulse which is proportional to the deposited gamma-ray energy. This process is referred to as pulse height analysis(PHA). Since the size of the pulse can be related back to the gamma-ray energy, PHA can identify different radionuclides in the sample.

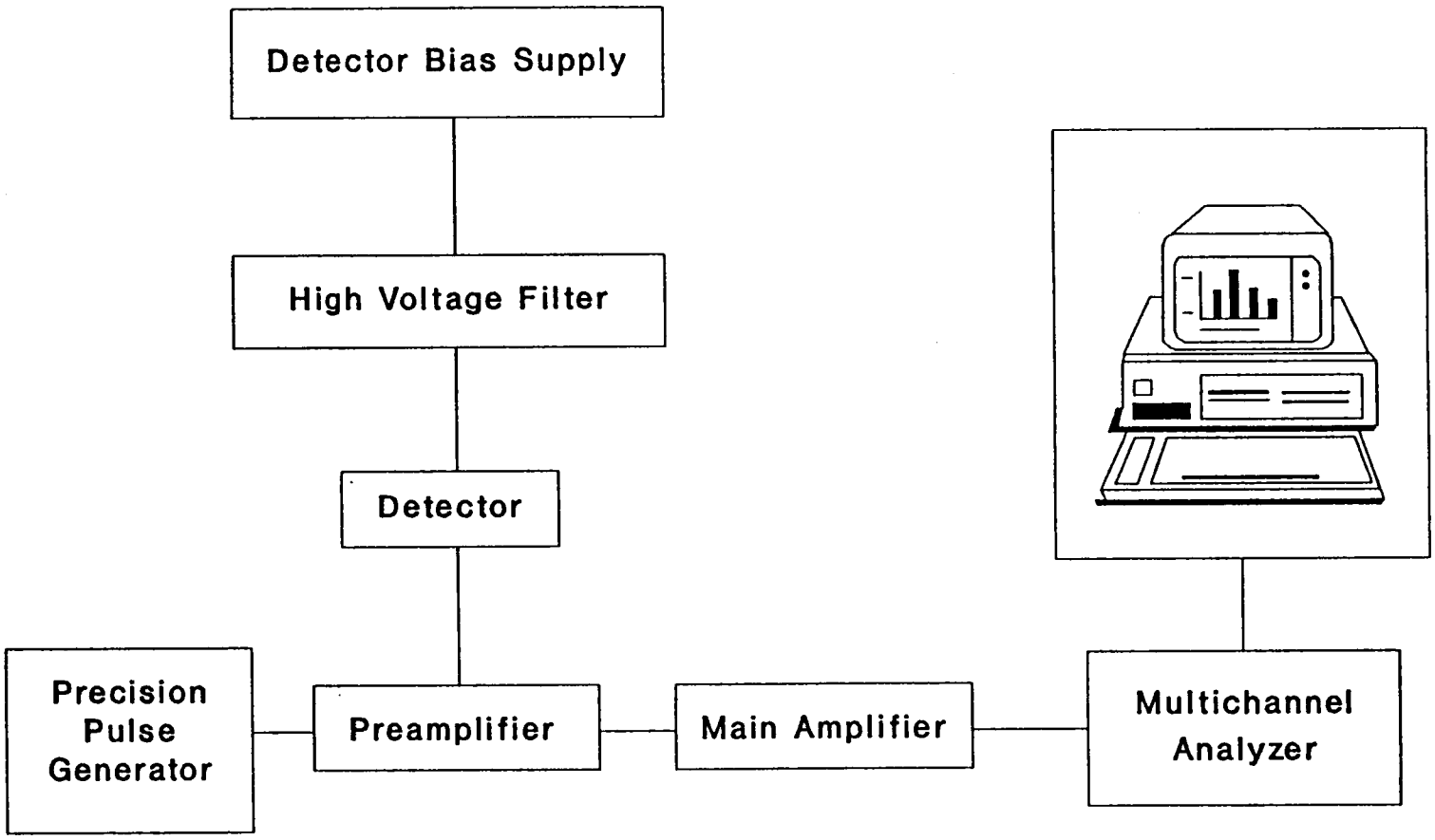


Figure 2.1 Connection of Components in HPGe System

The print-out from the ADCAM system includes the identified gamma-ray energy, the gross counts and net counts corresponding to the identified gamma-ray peak, live time, and centroid channel number.

2.2.2 Performance Tests of Measurement System [25]

Performance characteristics include: energy resolution, peak shape, and relative detection efficiency.

The energy resolution is determined by the full width at half maximum (FWHM) of a spectral peak at 1.33 Mev from a calibrated Co-60 source. At least 4000 counts in the peak channel are needed. Detailed measurement procedures are provided in the user's manual. The measured resolution should be compared with the Quality Assurance Data Sheet in the manual to determine if there is a significant discrepancy.

The spectral peaks should be nearly symmetrical, approaching a Gaussian shape. The quality of the peak shape is determined at a specific height other than the half maximum. The full width at tenth maximum (FWTM) is measured, and the tenth-to-half ratio (FWTM/FWHM) is calculated. The ratio of FWTM/FWHM for a Gaussian peak is 1.823.

Detector efficiency is usually quoted by specifying the photopeak efficiency relative to that of a standard NaI(Tl) scintillation crystal. "A calibrated Co-60 point source is placed 25 cm from the center of the detector to determine the absolute efficiency of the germanium detector for 1.33 MeV photons. At least 20,000 counts

should be accumulated in the 1.33 MeV peak. [25]" The ratio of the absolute germanium detector efficiency to the efficiency of a 3 in. × 3 in. NaI scintillation detector at 25 cm (known to be 1.2E-3) is calculated. This ratio, expressed as a percentage, gives the relative efficiency of the detector ($R.E_f$):

$$R.E_f = \frac{(peak\ area)/[(activity)\times(live\ time)]}{1.2\times10^{-3}} \times 100 \quad (2.1)$$

where the peak area is the number of counts at the peak, the activity is the disintegrations per second, and the live time is the real time minus total system dead time in seconds.

2.2.3 Calibration of Detection System

It is necessary to relate the channel number of a photopeak to the energy of the gamma ray that produced it prior to calibrating the detector. The efficiency of the detector is calibrated with a National Institute of Standards and Technology (NIST) traceable source.

2.2.3.1 Two Point Energy Calibration of the MCA

The process of determining the relationship between channel number and energy is called the MCA energy calibration. Over the energy range of most interest, the relationship between channel number and energy is close to a straight line. This relationship can be expressed as:

$$E_r = mX + E_0 \quad (2.2)$$

where E_r is gamma ray energy (keV), X is the channel number of photopeak centroid, m is slope (keV/channel), and E_0 is the intercept (keV). The slope and intercept are usually determined by a linear least square analysis, which is automatically calculated by the system. Quadratic fits are often used in research laboratories.

Two peaks are needed for the straight-line energy calibration. The calibration standard source of the used is Eu-154, whose energy range covers from 123.1 keV to 1274.4 keV. The system is calibrated at a specified amplifier gain, and the cursor reads in KeV.

2.2.3.2 Efficiency Calibration

It is customary to choose the Full-Energy-Peak Efficiency (E_P) as the detection system efficiency for a semiconductor detector. The E_P is defined as the probability that a gamma ray of energy E_r, emitted from the source, will appear in the photopeak of the observed pulse-height spectrum. This efficiency is a function of photon energy and usually determined experimentally by using a selected NIST traceable gamma-ray standard source with precisely known gamma-ray emission rates. Factors affecting the detector efficiency are the detector itself, the detector-to-source geometry, the materials surrounding the detector, and the absorption in the source material.

Source-detector geometry is an important consideration in the efficiency calibration of detector systems and must be reproducible with good precision. Rate-dependent factors, such as dead-time and summation effects, are also important in accurate efficiency determinations. Since the irradiated blood sample usually contains low level activity, the dead time and coincidence summation effects can be neglected. These facts allow the blood sample to be counted at the center of the end cap of the detector. For the experiments conducted herein, saline solution were contained in a 20 ml scintillation glass vial. To keep the same source-detector geometry, absorption in the source material, and the level of emission rate as the blood sample, the traceable calibration gamma-ray source was diluted and contained in a similar glass vial and counted on the top center of the detector.

The gamma-ray reference standard used for this calibration consists of QCY.48 solution in 4M HCL [23]. Eight mixed radio-nuclide in solution are listed in Table 2.1. The 0.2 ml of QCY.48 was diluted by 20 ml of distilled water in a 20 ml glass vial. The emission rates from nuclides in the calibration source are also described in Table 2.1. The formula for calculating efficiencies is

$$E_{pi} = \frac{C_i}{T \times I_{pi} \times A_{oi} e^{-\lambda t}} \qquad (2.3)$$

where E_{pi} is the efficiency corresponding to each nuclide decay in the calibration source, C_i is the net counts under each peak, T is the live time (real time minus total system dead time), I_{pi} is the gamma-ray decay intensity, λ is the decay constant of each nuclide, and A_{oi} is the emission rate of each nuclide in the calibration source.

Table 2.1 Efficiency Calibration Standard

(0.2 ml of Liquid QCY.48)

Parent nuclide	Gamma-ray energy (MeV)	Gamma-ray per second & gm of solution	Half-life	Efficiency
Cadmium-109	0.088	636	515 days	5.925E-2
Cobalt-57	0.122	585	271 days	5.250E-2
Cerium-139	0.166	725	137.6 days	4.610E-2
Tin-113	0.392	2144	115 days	1.895E-2
Cesium-137	0.662	2486	30 years	9.667E-3
Cobalt-60	1.173	3272	5.27 years	5.440E-3
Cobalt-60	1.333	3276	5.27 years	4.918E-3
Yttrium-88	1.836	6553	106.6 days	3.345E-3

The efficiency curve as a function of gamma ray energy is shown in Figure 2.2. The lower the energy of the gamma ray, the more likely the photoelectric effect will occur, so the detector has higher efficiency at lower energy. The efficiency will drop off below 90 -100 keV because the lower energy gamma-rays tend to interact with the cryostat end cap or the detector's outer electrode before reaching the detector active volume. Counting efficiency for a specified peak can be determined from an efficiency curve or from the mathematical equation.

2.3 Saline Sample Irradiation and Counting

The saline sample used in experiments consists of 0.16 gram salt and 20 ml distilled water since 100 ml blood for a reference man contains 0.8 gram of salt [6]. The neutron sources for irradiation are bare Cf-252 and D_2O moderated Cf-252. They are traceable to NIST and are located in the Radiation Calibration Facility (RADCAL) at Oak Ridge National Laboratory. The bare Cf-252 neutron spectrum, as shown in Figure 2.3, is similar to an unshielded fission spectrum with an average energy of 2.5 MeV. The D_2O moderated Cf-252 is a relatively soft spectrum and is illustrated in Figure 2.4.

Irradiation positions of saline samples are shown in Figure 2.5. Samples are placed on a standard 40×40 cm plexiglass phantom. The distance from the source center (not the geometric center of the source capsule) to the center of the front face of the phantom varies from 10 cm to 25 cm for bare Cf-252, and 50 cm for D_2O moderated Cf-252. These irradiation situations are not the actual accident situations

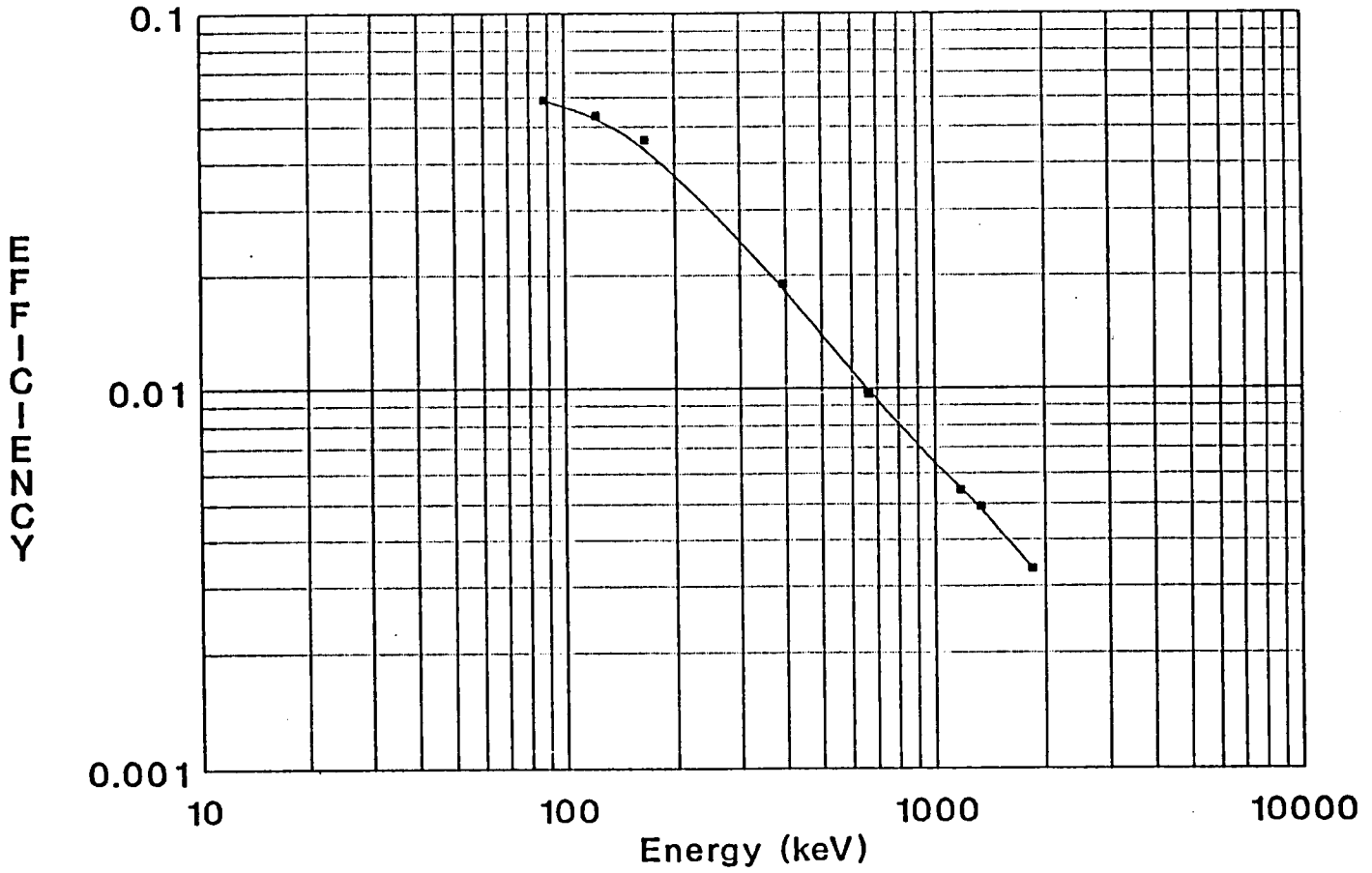


Figure 2.2 Efficiency Curve Using QCY.48
(same volume and shape as blood samples)

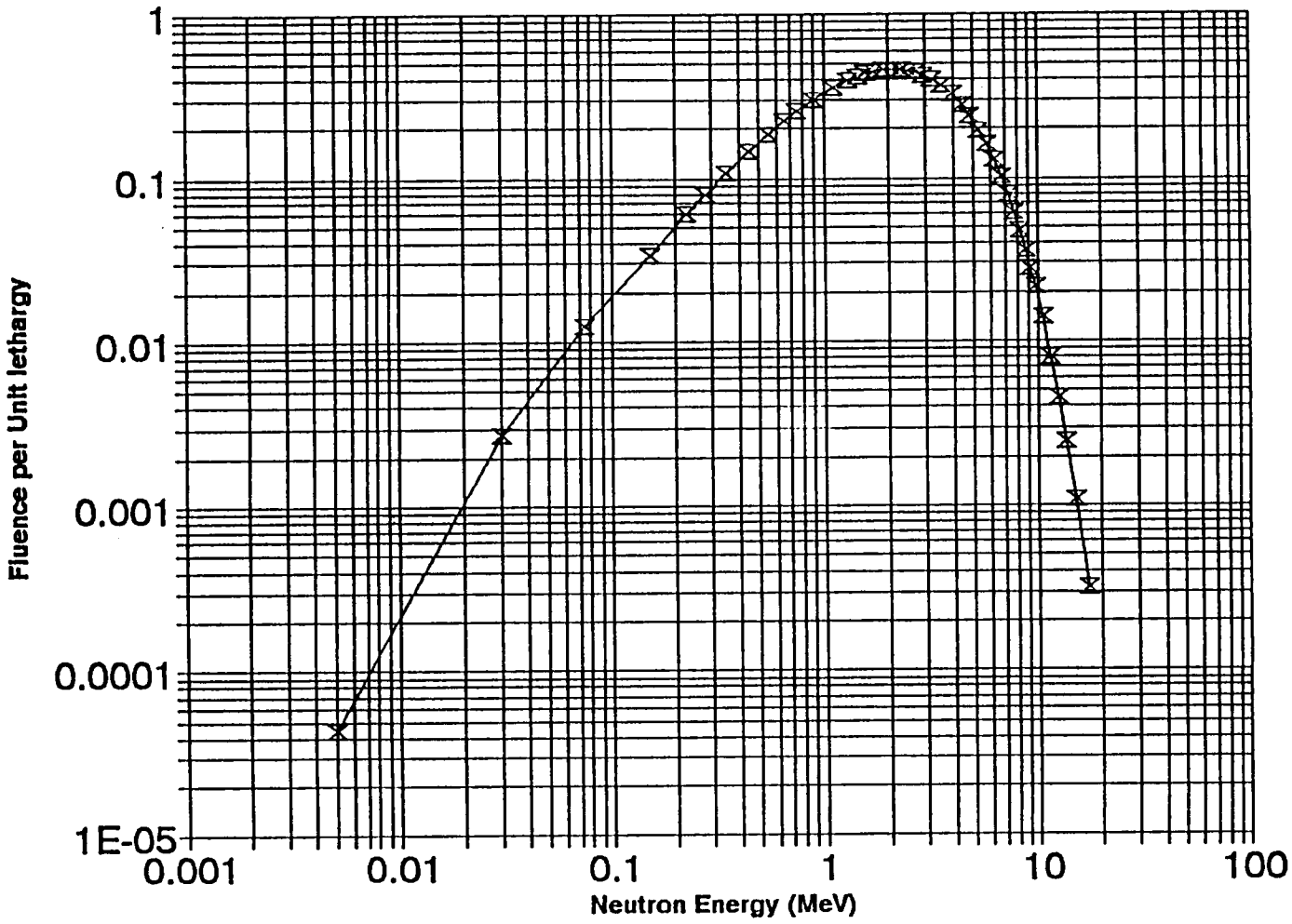


Figure 2.3 Bare Cf-252 Spectrum

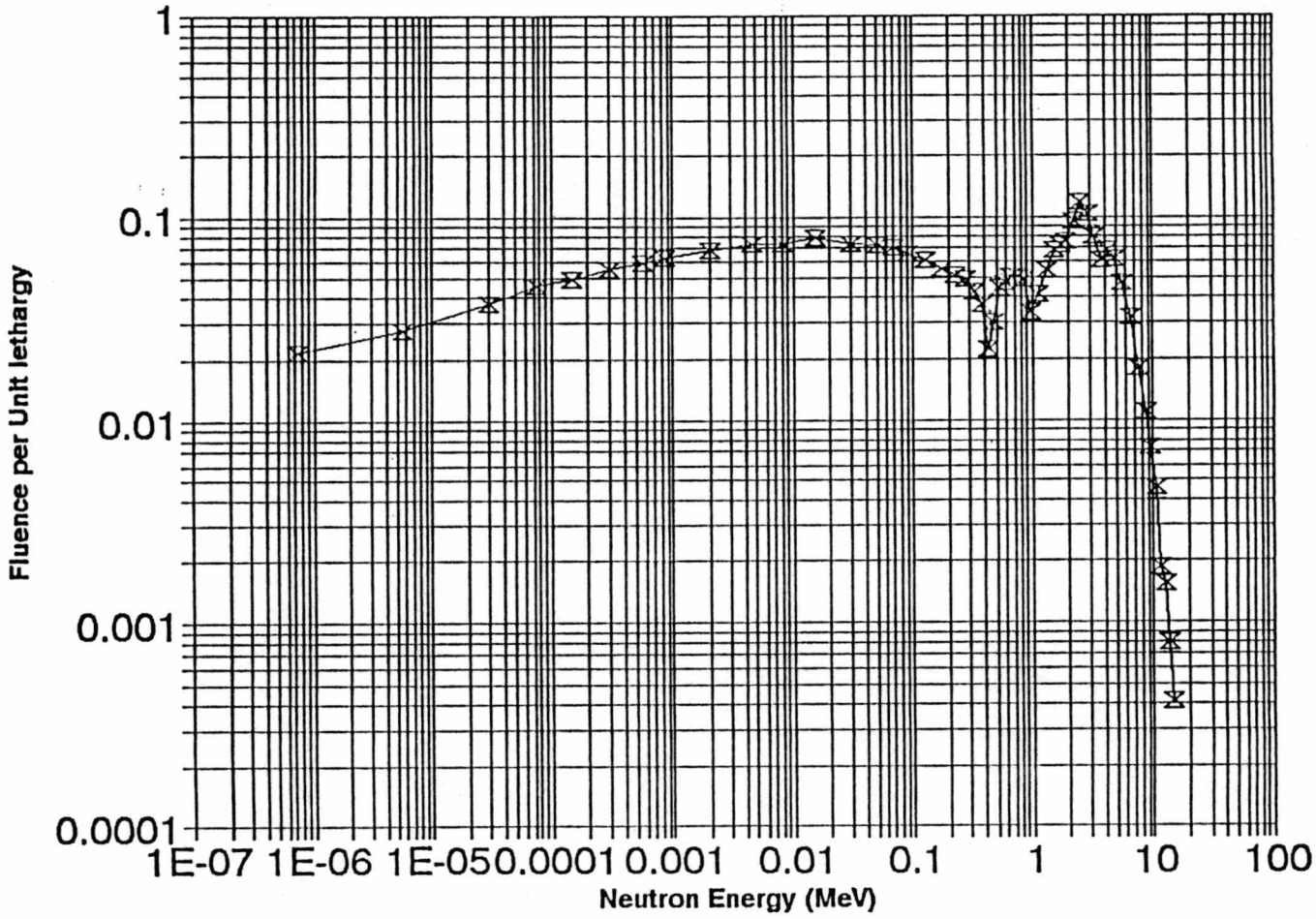


Figure 2.4 D_2O Moderated Cf-252 Spectrum

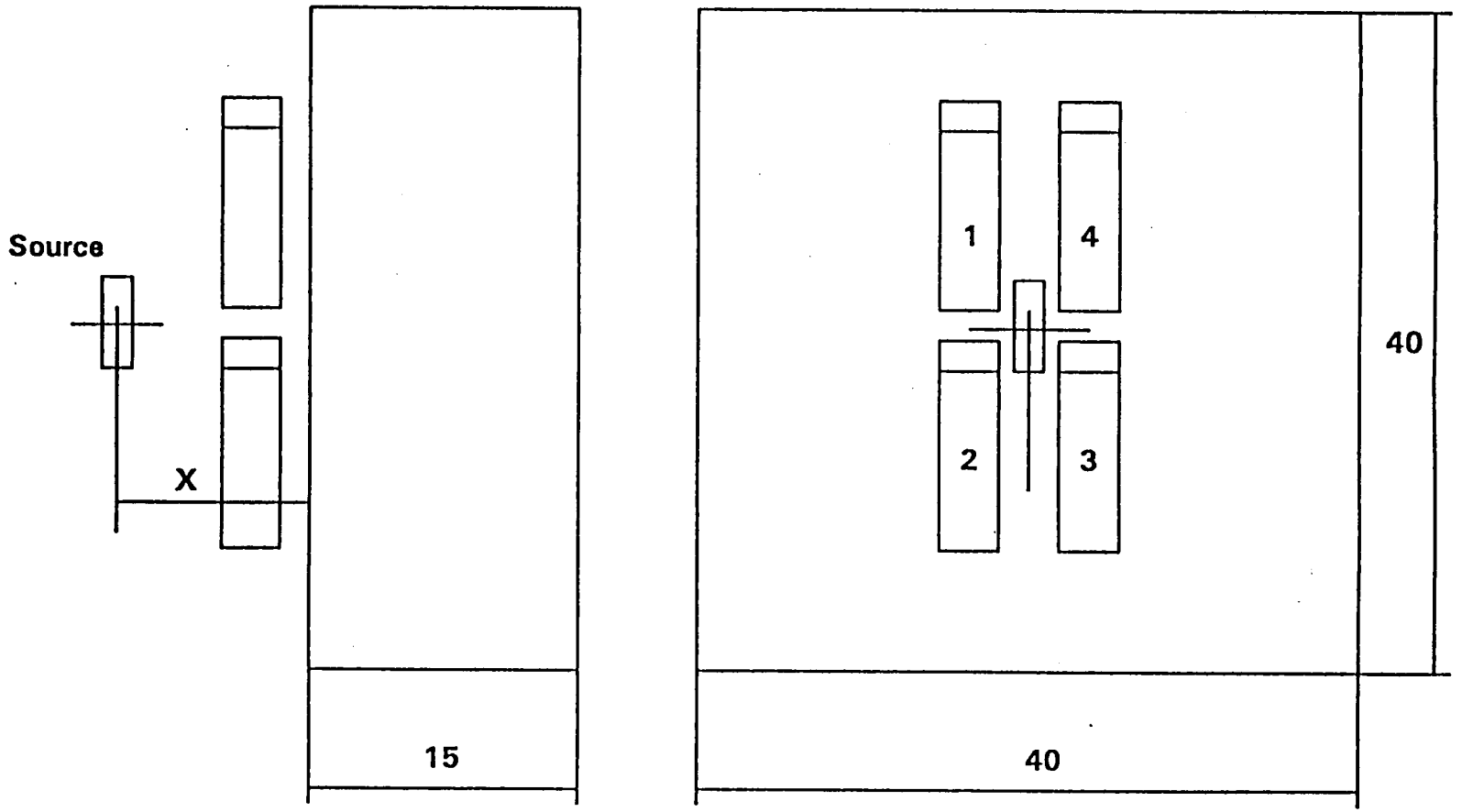


Figure 2.5 A Schematic of Blood Samples Irradiation

since a small bottle of saline on the phantom surface is used instead of a "reference man" phantom. However these situations will not affect the reliability and accuracy for establishing activity measurement procedures.

The 1.368 MeV photopeak is used for counting ^{24}Na since it has a higher efficiency than its 2.75 MeV photopeak. Seventeen saline samples were irradiated by bare Cf-252 and D_2O moderated Cf-252 for different irradiation times and were counted at several different counting times.

2.4. Blood Na-24 Concentration Calculation

The specific sodium-24 activity (A_{Na}) in blood is derived from the following equations:

$$A_1 = A_{Na} e^{-\lambda t_1}, \tag{2.4}$$

and

$$A_2 = A_{Na} e^{-\lambda t_2}, \tag{2.5}$$

and

$$A_1 - A_2 = \lambda C, \tag{2.6}$$

where A_1 and A_2 are the activities at the time of the start of counting and the end of counting respectively. The difference, A_1-A_2, is the decayed activity during the counting period, A_{Na} is the activity at the time of the end of irradiation by neutrons, t_1 is the elapsed time between the end of irradiation and the start of counting, t_2 is

the elapsed time between the end of irradiation and the end of the counting, C is the Na-24 counts for the peak at 1.368 MeV corrected for background and counting efficiency, and λ is the ^{24}Na decay constant. Thus, we obtain,

$$A_{Na} = \frac{\lambda C}{e^{-\lambda t_1} - e^{-\lambda t_2}}. \qquad (2.7)$$

There are two other important factors which affect the ^{24}Na concentration in blood. One is the sodium-24 biological decay. The other is radioactive decay during a extended irradiation time.

If the blood sample is not collected until some days after the accident it is necessary to correct for the excretion of ^{24}Na from the body. The biological decay of sodium activity in the body can be represented by the sum of three exponential terms [1]. The fraction (R_t) of ^{24}Na retained in the body is given by

$$R_t = 0.487e^{-0.0815t} + 0.510e^{-0.0513t} + 0.0027e^{-0.0015t} \qquad (2.8)$$

where t is the time elapsed from incident to collection of blood sample (days). The biological half-life is about 11 days, contrasting with the radioactive half-life of 14.7 hours. Normally, the blood sample is taken within a few hours of the accident, and such a correction is not necessary. Since we use saline samples in the experiments, biological decay is not considered.

Most criticality accidents happen in a very short time with an intensive high dose rate. However, the dose rate of neutron sources in RADCAL is lower. To give a high dose for the sample, a few hours or a few days irradiation of the sample is needed. The short half-life of ^{24}Na will cause some loss of Na-24 activity in a longer

irradiation time. The lost activity must be compensated by a decay correction factor. The factor was derived from following equations,

$$\frac{dN(t)}{dt} = \phi\sigma N_T(t) - \lambda N(t), \tag{2.9}$$

where dN(t)/d(t) is the change rate of ^{24}Na produced at any irradiation time. The $\varphi\sigma N_T(t)$ is the product rate of ^{24}Na at any irradiation time, $\lambda N(t)$ is the radioactive decay rate, $N_T(t)$ is the concentration of ^{23}Na at any irradiation time, and $N_T(t)$ is assumed to be constant. Solving equation (2.9), we obtain

$$A = \phi\sigma N_T(1 - e^{-\lambda t}) \tag{2.10}$$

where A is the ^{24}Na activity at the end of irradiation time, excluding the decayed activity. If we exponentially expand $e^{-\lambda t}$, then we obtain

$$A = \phi\sigma N_T\lambda t - \phi\sigma N_T \left[\frac{(\lambda t)^2}{2!} - \frac{(\lambda t)^3}{3!} + \frac{(\lambda t)^4}{4!} - \frac{(\lambda t)^5}{5!} - \ldots \right] \tag{2.11}$$

and

$$A_{Na} = \phi\sigma N_T\lambda t \tag{2.12}$$

where A_{Na} is the total ^{24}Na activity produced at the end of irradiation time, including the decayed ^{24}Na activity. Comparing Equations (2.10) and (2.12), the decay correction factor (F_a) is

$$F_a = \frac{\lambda t_a}{1 - e^{-\lambda t_a}}, \tag{2.13}$$

where t_a is the irradiation time.

Thus, the equation for calculating ^{24}Na activity in a blood sample is given by

$$A_{Na} = \frac{\lambda C_{net} F_a}{2.22 * 10^6 E_f I_r V R_t (e^{-\lambda t_1} - e^{-\lambda t_2})} \quad (\mu Ci / ml) \qquad (2.14)$$

where C_{net} = ^{24}Na net counts corrected for background,

E_f = efficiency of detector for 1.368 MeV gamma-rays,

I_r = fraction of gamma-rays per disintegration (100%),

V = volume of blood sample (ml),

F_a = radioactive decay correction factor during the irradiation period,

and

R_t = fraction of ^{24}Na retained in the blood at the time of collecting the blood sample.

Seventeen saline samples were irradiated by bare Cf-252 and D_2O moderated Cf-252 . The highest neutron dose given to a saline sample was 642 rads from bare Cf-252 at 10 cm. The lowest dose was 1.865 rads from D_2O moderated Cf-252. The measured data and calculated results are listed in Table 2.2.

The relatively consistent ratio between the neutron dose and measured ^{24}Na activity for the samples irradiated by the same neutron source indicates an acceptable repeatability of the ^{24}Na measurement process. Minor variations may be caused by: 1) variation of salt concentration in different saline samples, 2) uncertainty of measured dose, 3) counting geometry change, and 4) counting statistic variation, which will be discussed in next section.

Table 2.2 The Measured and Calculated Results for Saline Samples.

Including Neutron Dose, ^{24}Na Activity, and Ratios between Dose and Activity

Sample ID	Neutron source*	t_a (min.)	t_1 (min.)	T (min.)	C_{net}	F_a	A_{Na} (μCi/ml)	Dose (rad)	D/A**
A	1	1256	364	90	704	1.56	1.62E-4	190	1.17E+6
B	1	190	267	90	200	1.07	2.95E-5	30	1.02E+6
C	1	277	458	90	153	1.11	3.06E-5	38	1.24E+6
D	1	1574	588	90	781	1.73	2.09E-4	252	1.20E+6
E	1	4223	743	90	1401	3.38	5.49E-4	642	1.17E+6
F	1	2360	881	90	1234	2.17	3.44E-4	390	1.13E+6
G	1	1153	524	90	1024	1.51	1.51E-4	175	1.16E+6
H	1	235	426	90	326	1.09	3.23E-5	36	1.12E+6
AA-1	1	1976	224	10	166	1.95	2.18E-4	251	1.15E+6
AA-2	1	1976	236	30	540	1.95	2.40E-4	251	1.05E+6
AA-3	1	1976	374	60	1022	1.95	2.29E-4	251	1.10E+6

Note: *. Neutron source 1 is bare Cf-252 at 10 cm.
Neutron source 2 is bare Cf-252 at 25 cm.
Neutron source 3 is D_2O moderated Cf-252 at 50 cm.

**. D/A is the ratio between neutron dose and ^{24}Na activity in 20 ml of saline sample, rad per μCi/ml.

Table 2.2 (Continued)

Sample ID	Neutron source	t_a (min.)	t_1 (min.)	T (min.)	C_{net}	F_a	A_{Na} (μCi/ml)	Dose (rad)	D/A
BB-1	2	1360	81	30	370	1.61	1.21E-4	38.7	3.20E+5
BB-2	2	1360	121	60	774	1.61	1.32E-4	38.7	2.93E+5
CC-1	2	1444	389	30	333	1.66	1.41E-4	40.7	2.89E+5
CC-2	2	1444	424	60	657	1.66	1.45E-4	40.7	2.81E+5
*I	2	3840	1560	30	2.57E4	3.12	2.34E-4	67.9	2.90E+5
DD-1	3	538	218	120	1171	1.22	8.30E-5	1.865	2.24E+4
DD-2	3	538	1548	166	1714	1.22	8.99E-5	1.865	2.07E+4
FF-1	3	6216	111	10	121	4.83	1.04E-3	21.55	2.07E+4
FF-2	3	6216	168	60	1932	4.83	1.02E-3	21.55	2.11E+4
FF-3	3	6216	123	30	1032	4.83	1.04E-3	21.55	2.07E+4
GG-1	3	7237	349	10	263	5.59	1.09E-3	25.08	2.30E+4
GG-2	3	7237	1402	60	684	5.59	1.08E-3	25.08	2.32E+4
*HH-1	3	5654	1456	60	601	4.41	8.17E-4	18.76	2.29E+4
*HH-2	3	5654	1518	60	591	4.41	8.36E-4	18.76	2.24E+4

Note: The samples with mark "*" were counted at ORAU

2.5 Counting Statistics and Error Analysis

Radioactive decay is a random process. Thus, any measurement based on observing the radiation emitted in nuclear decay is subject to certain degree of statistical fluctuation. This fluctuation will cause an unavoidable uncertainty in a nuclear measurement. The fluctuation from a measurement can be analyzed using counting statistics analysis. Counting statistics analysis has two main functions in nuclear measurements. One is to determine if the fluctuation observed from a counting system is consistent with expected statistical fluctuation by counting the same sample repeatedly under the same counting condition. That is usually applied in the quality control procedures for counting equipment. The other function is to estimate how close a single measurement is to its "true" value when only one measurement of a particular quantity is available. The blood sample measurement in this research is a single measurement.

Since a nuclear transformation is a random, independent event, with a low probability for any one atom, the Poisson or Gaussian distribution (if the count of a sample is greater than 20) will be carried out to perform the counting statistic error analysis. We generally assume that a single count of a radioactive sample is an estimate for the mean of a Poisson or Gaussian distribution, and the square root of the count is the standard deviation. It is conventional to simply present the error of a single measurement as one standard deviation.

The estimated standard deviation of ^{24}Na activity (σ_A) is calculated from the standard deviation of the net counts (σ_{net}). The net counts (C_{net}) do not directly

represent the number of counts from a specific source in a given counting time. The net count, C_{net}, is derived from gross counts (C_{B+C}) and background counts (C_B). Since we cannot associate the standard deviation with the square root of any quantity that is not a directly measured number of counts, the standard deviation of net counts, C_{net}, must be calculated according to the error propagation formula, Equations (2.14) and (2.15),

$$\mu = x + y + z \tag{2.15}$$

$$\sigma_\mu^2 = \left(\frac{\delta\mu}{\delta x}\right)^2\sigma_x^2 + \left(\frac{\delta\mu}{\delta y}\right)^2\sigma_y^2 + \left(\frac{\delta\mu}{\delta z}\right)^2\sigma_z^2 \tag{2.16}$$

where x, y, and z are directly measured counts, and μ is the quantity derived from these counts.

Thus, the standard deviation of C_{net} is given by

$$\sigma_{net} = \sqrt{C_{B+C}+C_B} \tag{2.17}$$

and

$$\sigma_A = \frac{\lambda F_a \sigma_{net}}{2.2*10^6 E_f I_r (e^{-\lambda t_1} - e^{-\lambda t_2})} \tag{2.18}$$

or in the form of specific activity,

$$\sigma_A = A_{Na}\sqrt{\frac{C_{B+C}+C_B}{C_{net}^2}} \quad \mu Ci/ml \tag{2.19}$$

Sometimes, it is convenient to express the statistical error as a percent

variation, that is, the standard deviation of the activity divided by the activity itself. It is expressed as

$$\% \ \sigma_A = 100\frac{\sigma_A}{A_{Na}}. \tag{2.20}$$

The calculated standard deviation and per cent variation of saline samples are listed in Table 2.3. The higher the accumulated net counts in samples, the lower the variation. The largest per cent variation is 11.5% for sample C. It is caused by its very high background count and low net count. The exact reasons that sample C has a very high background count are unknown. The incident such as removing the cover of the lead shielding during counting or the buffer not being cleared may result in high background count, and therefore a large deviation.

2.7 Sensitivity of Measurement Process

The sensitivity of the measurement process is referred to as the required minimum detectable activity in a sample (MDA) to be detected with a given statistical confidence level. The lower the MDA, the higher the sensitivity of the measurement process. The MDA is expressed as

$$MDA = \frac{Constant \times Lower\ Limit\ Detection}{Sample\ Size \times Efficiency \times Counting\ Time}, \tag{2.21}$$

where the Lower Limit of Detection (LLD) of a detector is determined by the statistical maximum acceptable risk of making a Type I error, α (of concluding there are sample counts when there are none) and a Type II error, β (of concluding there

Table 2.3 Results of Counting Error Analysis

Sample ID	Gross counts	Background counts	Net Counts	T (min.)	A_{Na} (μCi/ml)	σ_A (μCi/ml)	σ_A / A_{Na} (%)
A	750	46	704	90	1.62E-4	6.31E-6	4.0%
B	244	44	200	90	2.95E-5	2.12E-6	7.2%
C	247	94	153	90	3.06E-5	3.52E-6	11.5%
D	848	67	781	90	2.09E-4	7.94E-6	3.8%
E	1469	68	1401	90	5.49E-4	1.54E-5	2.8%
F	1285	51	1234	90	3.44E-4	1.02E-6	2.96%
G	1080	56	1024	90	1.51E-4	4.97E-6	3.29%
H	373	47	326	90	3.23E-5	2.03E-6	6.28%
AA-1	177	11	166	10	2.18E-4	1.87E-5	8.26%
AA-2	552	13	540	30	2.40E-4	1.05E-5	4.4%
AA-3	1062	40	1022	60	2.29E-4	7.33E-6	3.2%

Table 2.3 (continued)

Sample ID	Gross Counts	Background counts	Net Counts	T (min.)	A_{Na} (μCi/ml)	σ_A (μCi/ml)	σ_A / A_{Na} (%)
BB-1	392	22	370	30	1.21E-4	6.65E-6	5.5%
BB-2	801	27	774	60	1.30E-4	4.81E-6	3.7%
CC-1	355	22	333	30	1.41E-4	8.17E-6	5.8%
CC-2	684	27	657	60	1.45E-4	5.89E-6	4.06%
DD-1	1299	128	1171	120	8.31E-5	2.67E-6	3.22%
DD-2	691	67	624	166	8.98E-5	3.96E-6	4.41%
FF-1	387	37	350	60	1.04E-3	6.11E-5	5.88%
FF-2	1068	36	1032	10	1.02E-3	3.28E-5	3.22%
FF-3	1991	59	1932	30	1.04E-3	2.43E-5	2.34%
GG-1	287	24	263	10	1.09E-3	7.30E-5	6.7%
GG-2	756	72	684	60	1.08E-3	4.53E-5	4.2%

are no counts when there are some). The relationship between the LLD, Type I, and Type II errors is shown in Figure 2.6 [7]. The LLD at the 95% confidence level is, approximately,

$$LLD = (K_\alpha + K_\beta)\sqrt{2C_B} \tag{2.22}$$

where $K_\alpha = K_\beta = 1.645$. These values of K_α and K_β are based on a standard normal distribution and correspond to case when the probability that making the Type I and Type II errors (α,β) is 5%. Equation (2.22) is suitable for the measurement situation where the background counts (C_B) in the region of interest is not accurately known beforehand. So, the MDA for our measurement system will be calculated using the following equation.

$$MDA = \frac{4.66\sqrt{C_B}}{2.22\times10^6 E_f T V} \quad (\mu Ci/ml) \tag{2.23}$$

where E_f is the efficiency at 1.368 MeV energy, T is the counting time in minutes, and V is the volume of saline samples. The MDA is directly proportional to the standard deviation of background counts and inverse to counting time, efficiency of detector and sample size. The four variables on the right hand side of Equation (2.23) are usually interrelated. For instance, the background and efficiency depend on the sample size, and the counting time will affect the total background counts. The calculated MDA for saline samples counted at UTK are listed in Table 2.4. The MDAs vary slightly for the same counting time since the background changes. Approximately, the MDA is about 2.1E-6 μCi/ml for counting 90 minutes, 2.4E-6

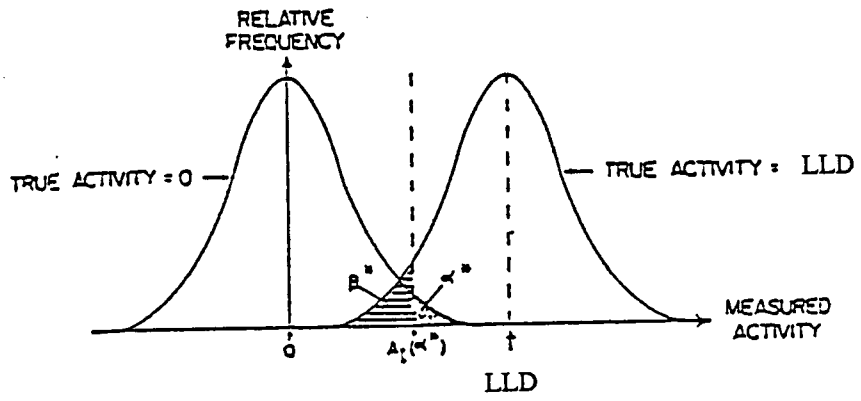


Figure 2.6 Relationship among the LLD, Type I Error, and Type II Error

Table 2.4 Minimum Detectable Activity

for Saline Samples Counted at UT

Sample ID	Counting Time (min.)	MDA (μCi/ml)
A	90	1.97E-6
B	90	1.87E-6
C	90	2.82E-6
D	90	2.38E-6
E	90	2.4E-6
F	90	2.07E-6
G	90	2.11E-6
H	90	1.99E-6
AA-1	10	8.67E-6
AA-2	30	3.15E-6
AA-3	60	2.76E-6
BB-1	30	4.09E-6
BB-2	60	2.27E-6
CC-1	30	4.11E-6
CC-2	60	2.27E-6
DD-1	120	2.47E-6
DD-2	166	1.29E-6
FF-1	60	2.65E-6
FF-2	10	1.57E-5
FF-3	30	6.7E-6
GG-1	10	1.28E-5
GG-2	60	3.7E-6

μCi/ml for counting 60 minutes, 4.0E-6 μCi/ml for counting 30 minutes, and 1.4E-5 μCi/ml for counting 10 minutes for a system with an efficiency of 4.5E-3. Depending on the moderation of the neutron spectrum, one to two rads of total neutron dose from the hardest spectrum can be detected for counting 30 to 60 minutes with a 95% confidence level. For soft spectra, the neutron dose below one rad can be readily detected with 10 minutes counting.

CHAPTER III

DEVELOPMENT OF

HAIR P-32 MEASUREMENT PROCEDURES

3.1 Introduction

One of the most important components of an accident neutron dosimetry system is to measure the fast neutron fluence. The first reason is that most of the recoil dose in actual accidents is received from neutrons with energies greater than 100 keV. Second, the initial estimation of an accident neutron spectrum requires fast neutron information. To date, the $^{32}S(n,p)^{32}P$ reaction in the hair with a threshold neutron energy, 2.5 MeV, is the best choice for determining the fast neutron information using the body activation [1]. P-32 is a pure beta emitter with a maximum energy of 1.7 MeV and 14.3 day half-life.

Hair and nails occurring on the surface of the body all possess sufficient sulfur for incident fast neutron fluence estimates. However, only hair, especially on the head, is readily available in sufficient quantity to permit analysis after an accident. Sulphur is naturally present in the hair of the human body with a composition of 45 mg/g hair with little variation from individual to individual or with anatomical distribution [8]. By contrast, hair contains almost no phosphorus except that contributed by epidermal cell fragments and external contamination. The almost complete absence of natural phosphorus in the hair permits the use of hair as a

biological sulfur threshold detector for determination of the incident dose of neutrons with energies in excess of 2.5 MeV [8]. The measurements of the hair samples taken from around the head, front, left, right, and back, also can provide important information about the person's orientation at the time of the accident based on the relative specific activity of the four samples.

After the accident, if the individual has not been contaminated by fission products or fissile material, the ^{32}P activity can be counted directly on a beta detector. If the person has been contaminated very seriously, a more complicated chemical separation procedure may be required [9]. In most cases, the technique preferred, because of accuracy and simplicity, is the direct counting of the hair. In the 1960's, scientists conducted several experiments on hair with direct counting using a low-background beta counter. The sensitivity of the process is 20 rads (above 2.9 MeV) for a one gram sample [10]. Since the preference for medical treatment after accidents is determined by the dose a person received, a higher sensitivity of the activity measurement process is required. In the past decade, the multichannel liquid scintillation spectrometer was developed with a low background and high efficiency. This development provides the possibility for improving the hair activity measurement process. Another advantage of liquid scintillation counting is that it can easily cut off the ^{32}P counts below certain beta energy. Since most of the contaminating activity is of much lower energy than ^{32}P, the absence of some low energy activity can still provide an accurate preliminary estimate of ^{32}P activity directly without the chemical treatment when the sample is lightly contaminated. The lost activity can be made up

when calculating ^{32}P activity if it is necessary.

The hair ^{32}P activity measurement system, hair sample preparation, activity counting process, calculation of ^{32}P activity, and MDA of hair measurements are discussed in this chapter.

3.2 Hair-Phosphorus Measurement System

This section introduces the liquid scintillation counting principles, the components of counting system, calibration and verification of performance tests of counting system, and hair ^{32}P counting efficiency determination.

3.2.1 Liquid Scintillation Counting

A liquid scintillation sample usually consists of the radioactive material to be counted and the scintillation solution. The scintillation solution is also referred to as the cocktail. The cocktail is a mixture of a solvent and a solute, all contained in a sample vial. The main functions of the solvent is to help dissolve the sample and solute and absorb the kinetic energy from beta particles. Ninety to ninety-five percent of the concentration in the cocktail is solvent. When a radioactive atom decays in the sample, the following events take place. Some of the radiant energy released in the decay process is transferred to the solvent molecules which, in turn, transfer this energy to solute molecules. The solute molecules become excited by accepting this extra energy from the solvent. The excited molecules quickly return

to the ground state releasing this excess energy in the form of photons, see Figure 3.1. It takes about 150 electron volts to produce one photon [24]. "The intensity of photons in the scintillation is proportional to the initial energy of the beta particle. These photons escape from the vial and impinge on the face of the photo-multiplifier tube and then cause the release of a photoelectron inside the tube. Each of these photoelectrons is then multiplied within the tube. This multiplication process results in the production of a measurable electrical signal which can be processed. [24]"

Usually, there are two types of solutes in the cocktail. The primary solute is sensitive to absorb the energy from the solvent and emits photons with 3500-3700 Å wave lengths. However, the sensitive range of the PMT photocathode is 4200-4500 Å. The secondary solute (wave length shifter) is needed to absorb the short wave length photons and then emit the long wave length photons for producing a greater response from the PMT.

"In terms of liquid scintillation counting, all radioactive decay are multi-photon events. The scintillation counter takes advantage of this fact and uses two PMTs to separate the real nuclear decay events from non-decay events. The energy of a nuclear decay event is dissipated in a period of time on the order of 5.0E-9 second. Thus, a beta decay having a multiplicity of photons will stimulate both PMTs at the same instant in time. The signal from each PMT is fed into a circuit which produces an output only if the two signals occur together, that is within the resolving time of the circuit, approximately 20.0E-9 second. [11]" This is termed a coincidence circuit, as shown in Figure 3.2, and the output of the circuit is a coincidence pulse. figure

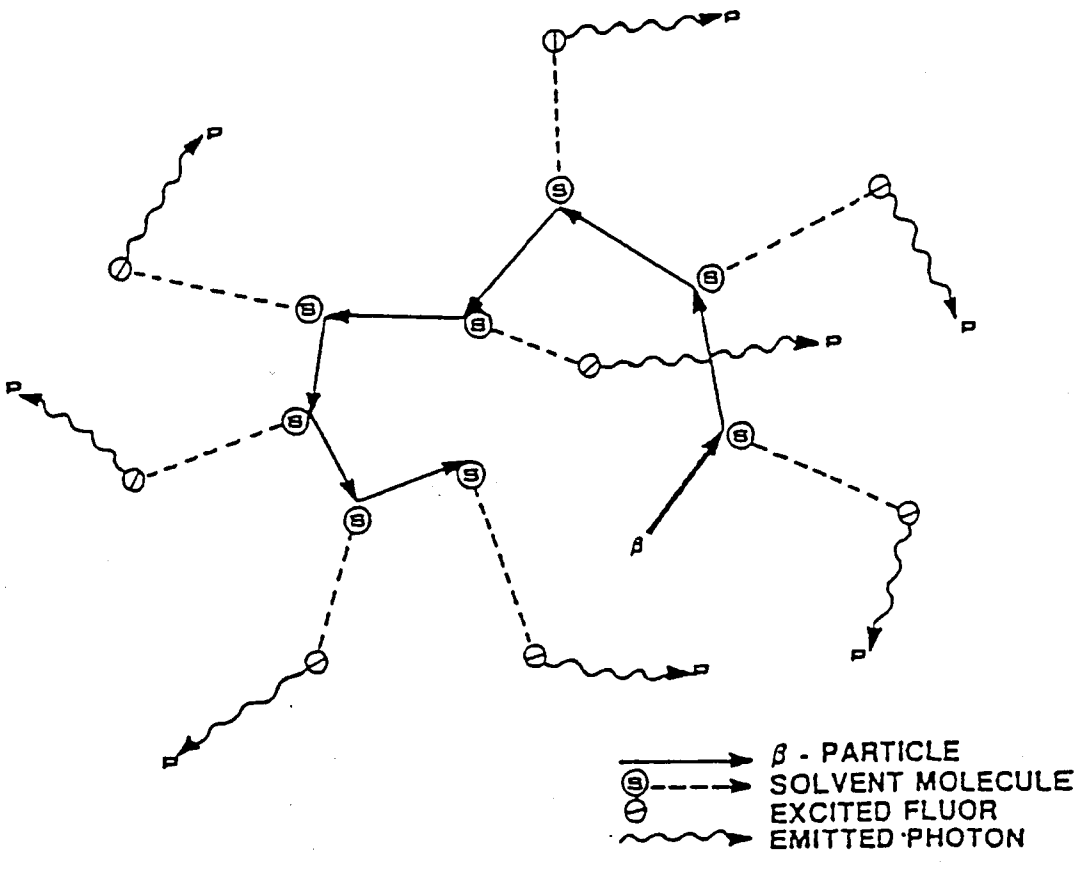


Figure 3.1 Illustration of the Collision Process

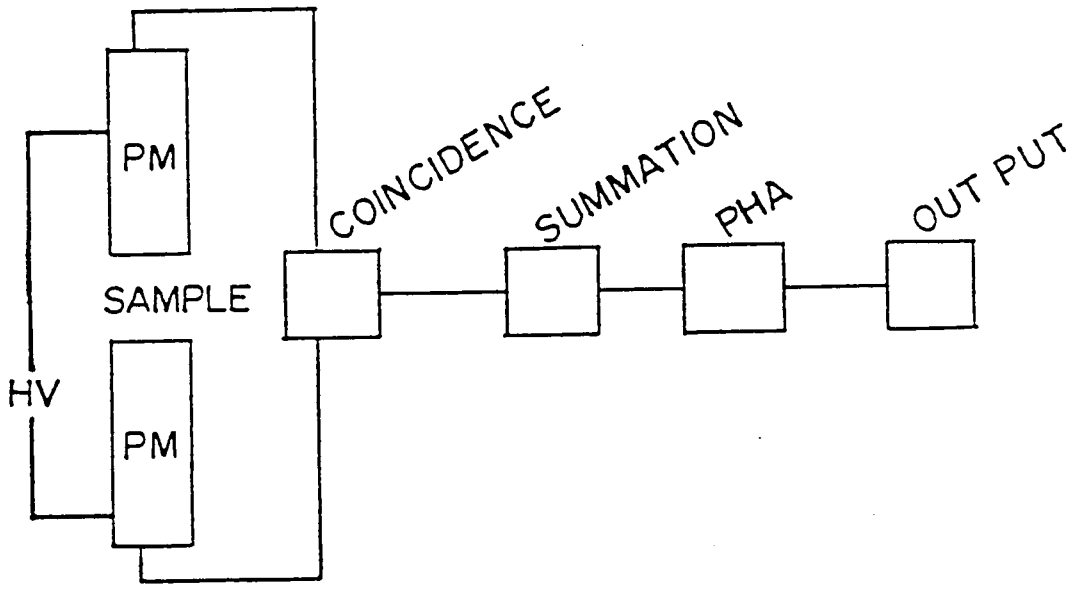


Figure 3.2 A Schematic of Liquid Scintillation Counting

The coincidence circuit prevents some single-photon events from passing on for analysis. These non-nuclear, single-photon events include electrical "dark noise" which originates from the photomultiplifier tubes, inevitable background produced by environmental radiation, chemical reactions that generate chemiluminescence and/or photoluminescence in the sample.

The so called "internal liquid scintillation counting" (the radioactive material is in direct contact with the scintillation) and coincidence counting offers many unique measurement advantages including homogeneous sample geometry, no absorption effects for beta radiation, and maximum radionuclide counting efficiency.

3.2.2 Components of Counting System

The system used at UTK is a Packard 2000, which functionally consists of the following major parts.

1. Scintillation detector.

2. Varisette™ sample changer which provides the means for sample movement to and from the detector.

3. Spectralyzer™ spectrum analyzer. The coincident summed pulses from the detector system are accumulated and analyzed in a spectrum analyzer circuit. The spectralyzer spectrum analyzer also provides a method to determine the efficiency of the system. A spectral index of the sample(SIS) is calculated and is related to the quenching level of the sample.

4. IBM compatible PC which controls all instrument functions. Defining or

editing a protocol program can simply be accomplished using the keyboard.

5. A printer for the outputs.

3.2.3 Performance Tests of Detector

Three performance verifications should be conducted daily. They are: 1) ^{14}C efficiency check, 2) ^{3}H efficiency check, and 3) background check. The performance verification specifications include the follows. 1) A minimum acceptable efficiency for unquenched ^{14}C is 90%. 2) A minimum acceptable efficiency for unquenched ^{3}H is 58%. 3) A background in the range of 0-19 KeV should be below 30 CPM.

3.3 P-32 Counting Efficiency Determination

This section will discuss the factors affecting the liquid scintillation counting efficiency, interferences to the liquid scintillation process, and the hair ^{32}P efficiency determination.

3.3.1 Quenching

In liquid scintillation counting, the terms of quenching and counting efficiency are closely related. There are in essence two different types of quenching: chemical quenching and color quenching. Chemical quenching interferes in the scintillation process by deexcitation of the solvent. Thus, it causes energy losses in the beta energy transfer from solvent to solute before the beta energy is converted to photons

[24]. Color quenching is the attenuation of light photons in the solution. Thus, it lessens the probability of transfer of photons to the cathode of the PMT [24]. All of these cause energy loss in the liquid scintillation solution. As a result, the energy spectrum detected from the beta emitter shifts toward lower energies as illustrated by Figure 3.3.

Due to this change in energy distribution, it appears that the counting efficiency depends on the degree of quenching, and thus on the nature of the sample, the scintillator used, and the sample preparation method.

The energy of beta particles plays an important role in determining the counting efficiency. The coincidence requirement that each PMT produces a response sets a limit of detection. The beta particle must have sufficient energy to produce at least two photons, and one must interact with each PMT. Inevitably, because the photons are radiated in all directions, some will be lost. Thus, the probability of a photon entering each PMT decreases with decreasing beta particle energy [12]. High-energy beta particles produce excited and ionized solvent molecules which are relatively isolated from each other. The magnitude of each pulse produced is proportional to the energy deposited in the scintillator. Low-energy beta particles produce them in close space in regions of high ionization density in which energy is dissipated in nonradiative transitions. This process is referred as "ionization quenching" by Birks [19]. It will reduce the efficiency of the low energy beta particle counting. Since ^{32}P has a very high maximum beta energy, the efficiency lost at lower energy is less than most of the other beta nuclides, such as ^{14}C. This

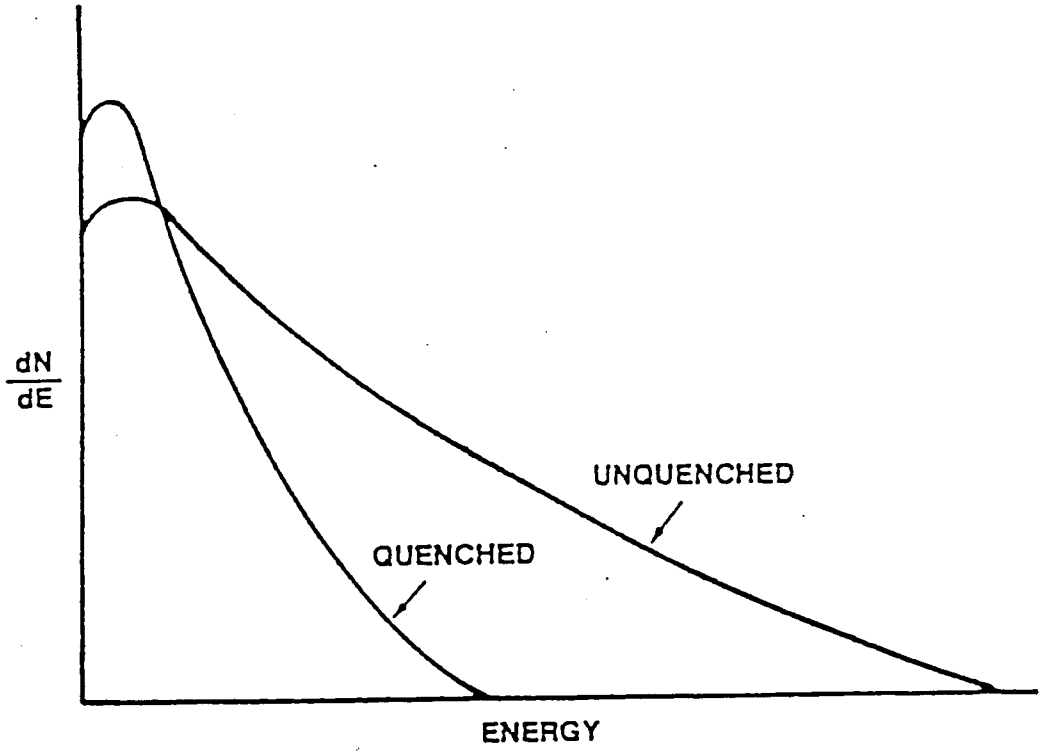


Figure 3.3 Quenching Effect

advantage can be used to trace ^{32}P counting efficiency by using ^{14}C quenched standards, which will be discussed in Section 3.3.3.

The application of high resolution spectrum analysis of the Packard 2000 allows the calculation of two efficient and very accurate parameters to monitor quenching levels: the Spectral Index of the Sample (SIS) and the Transformed Spectral Index of the Internal Standard Spectrum (tSIE).

3.3.2 Counting Interference

The following interferences are common to the liquid scintillation process: 1) chemiluminescence, 2) photoluminescence 3) static electricity, 4) heterogeneous samples, 5) background produced by environmental radiation, and 6) random electric noise.

Chemiluminescence is the production of light as a result of chemical reaction. This occurs typically in samples of alkaline pH and/or containing peroxides. A 30% hydrogen peroxide will be used in hair sample preparation. "Photoluminescence results from the activation of the cocktail and/or vial by ultraviolet light, such as sunlight or UV light sources used in the laboratory. Since a luminescence spectrum is quench independent and is a single photon event, it is easy to distinguish from a beta energy spectrum using spectrum analysis. [24]" The Packard 2000 counter can correct the counting results for luminescence influences.

Static electricity is another common source of counting interference, especially in dry weather. The buildup and subsequent discharge of static electricity on liquid

scintillation vials is independent of quenching and the pulse height is limited to 10-12 keV.

Heterogeneous effects are encountered for insoluble samples or for two phase samples. This could occur when we prepare ashed hair samples using Triton if the solution in the vial is not homogeneous prior to counting, which will be discussed in Section 3.4.3. The efficiency of insoluble samples will be decreased and unstable. When two phases are present, each phase will have its own counting efficiency. The Packard 2000 counter warns the user when heterogeneous samples are encountered.

3.3.3. Tracing Hair-^{32}P Counting Efficiency

For the determination of ^{3}H and ^{14}C absolute activity, commercially manufactured quench standards are available. These standards can be used to generate quench curves, either manually or automatically, for the calculation of activity values of unknown samples of the same radionuclide. However, no commercial quench standards for ^{32}P are available since it has a relative short radioactive half-life. The laboratory preparation of such quench standards is time consuming and not practical in an emergency situation. Comparing ^{14}C quenching with ^{32}P quenching will be used to estimate the quenched ^{32}P counting efficiency.

There are two methods, SIS and tSIE, for relating the efficiency and quenching levels in a Packard 2000. The Packard 2000 uses the distribution of the counts along the energy axis to monitor quench. By weighting each pulse by its energy, the mean pulse of the spectrum for any sample can be determined. This mean pulse, called

SIS, is correlated with counting efficiency or quenching. For an unquenched sample of any radionuclide, SIS value is close to its theoretical maximum energy. The Packard 2000 also uses an external standard quench correction system, tSIE. This method is based on the fact that when both the sample vial and solution are irradiated by a gamma source, Compton electrons are produced within the sample. "The basic principle is that these Compton electrons behave as the beta particles emitted by the radioactive sample in solution and any quenching in the sample results in a proportional quenching of the Compton electrons. The number of Compton electrons produced is related to the strength of the gamma source which is adjusted to produce a statistically significant number within an additional period of counting time. [12]" An important advantage of tSIE method is its independence from sample activity. Most hair samples have a low count rate, thus, the tSIE will be used in our measurements to determine the quenching level index, tSIE. Typical tSIE quench curves for ^{14}C and ^{3}H are shown in Figure 3.4 as a function of quenching level. The tSIE value for any unquenched radionuclide is 1000.

As shown in Figure 3.4, for the same tSIE values or same quenching levels, the efficiency of ^{14}C is much higher than ^{3}H since ^{14}C has much higher beta energy than ^{3}H. The maximum beta energy of ^{14}C is 156 KeV. The maximum energy of ^{3}H is 18.6 KeV. Above 300 tSIE, the efficiency for counting ^{14}C is almost constant and not effected much by the change of quenching level. The maximum efficiency for ^{14}C is 94%. Therefore, since the maximum beta energy of ^{32}P is 1700 KeV, which is much higher than ^{14}C maximum energy, we can confidently assume that the counting

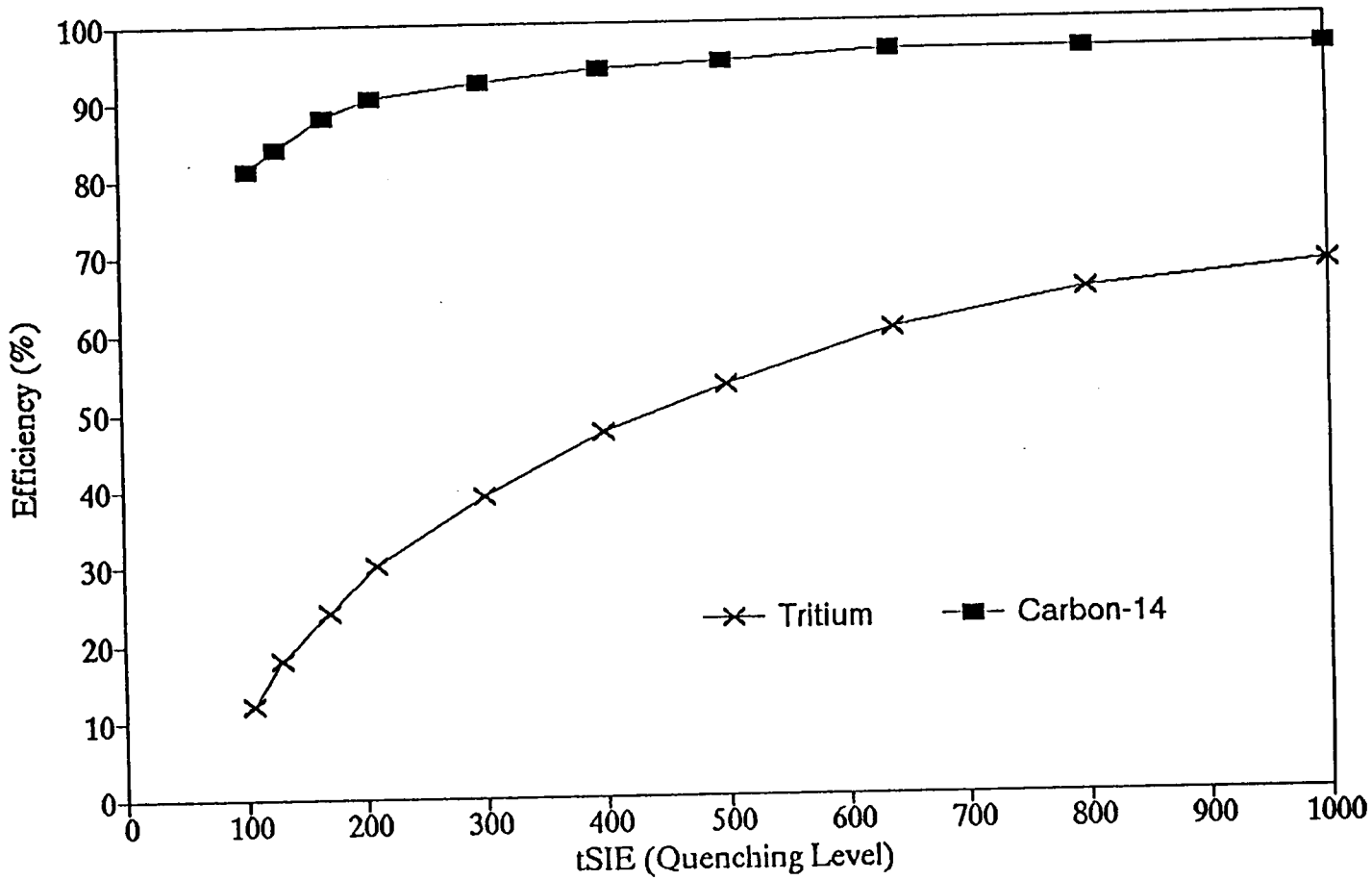


Figure 3.4 Efficiency Curves for Tritium and Carbon-14

efficiency of P-32 is constant within a wide range of quench levels and near its maximum efficiency. A 95% counting efficiency can be conservatively given to hair-^{32}P activity measurement when the quenched ^{32}P standards are not available.

To verify this assumption, a series of experiments were conducted. The degree of quenching in the chemically prepared hair samples is determined by the amount of chemical dissolving material and the hair weight handled by the solubilization method. In this case, the counting efficiency is affected by the chemical quenching, color quenching, and the degree of solubilization of the sample. Eight hair samples, with different amounts of hair in similar glass vials, dissolved by different amounts of chemical materials, and with the same activity of P-32 isotope added using digital pipe, were counted. The quenching level is increased as a function of the amount of hair dissolved and of the chemical materials, as shown in Table 3.1. Significant quenching occurs when more than 0.5 gm of hair is dissolved. The slight variation of ^{32}P count rates is probably caused by the errors of the ^{32}P dilution process since a very small amount of ^{32}P isotope was transferred with a digital pipe.

3.4 Hair Sample Preparation

The efficient measurement of radioactivity in biological material by a liquid scintillation counter requires close contact between the sample and counting solution to reduce self-absorption. The hair samples should be pretreated before counting. Chemical dissolution and high temperature ashing were evaluated for establishing the

Table 3.1 Relationship Between Quenching and Hair Sample Weight

Sample ID	Sample weight (g)	tSIE	cpm
1	0.0338	380	43170.4
2	0.0502	356	44544.9
3	0.0725	332	42273.9
4	0.0979	344	43243.9
5	0.1341	229	43726.4
6	0.2149	223	44470.9
7	0.3140	195	42870.9
8	0.5053	100	41908.4

analysis procedures.

3.4.1 Hair Washing

If the hair sample is to be counted shortly after the accident, even though not contaminated by fission products, the hair should be washed. ^{31}Si is produced from oil, dust particles, dry skin, etc. on the surface of the hair [10], and ^{31}Si has a half-life of 2.6 hrs.

3.4.2 Chemical Dissolution of Hair

The major considerations in evaluating the methods utilized for producing homogenous counting solutions from hair by chemical dissolution are: (1) ease of sample preparation, (2) maximum or optimal hair weight and volume handled by the solubilization method, (3) maximum efficiency related to hair weight, and (4) chemiluminescence.

The chemical solutions used are: (1) SX-10 Tissue Solubilizer, (2) 30% Hydrogen Peroxide, and (3) DTT (Dithiothreitol). All of these are made by the Fisher Scientific Corporation, and the functions of each material are listed in Table 3.2. A series of experiments were conducted to obtain optimal amounts of the hair, and chemical materials, along with detailed analysis procedures.

Based on the experiments, it is concluded that one gram of hair needs 12000 - 14000 μl tissue solubilizer, 6000 - 7000 μl hydrogen peroxide, and 0.12 gm DTT.

Table 3.2 Description of Chemical Materials Used

Chemical Materials	Description
Hydrogen Peroxide 30%	Acid solution helps tissue solubilizer to dissolve hair sample completely
ScintiGest* Tissue Solubilizer	Ready-to-use 0.6N solution specifically formulated for rapid solubilization of tissue homogenates. Usually yields clear solution, rather than viscous, cloudy gels produced by other types of solubilizers.
DTT (Dithiothreitol)	Six grades of agarose and the highest grades of acrylamide, bisacrylamide and associated reagents are available for separation of proteins and nucleic acids by electrophoresis.

Heating about 3-4 hours at 50-60 ^{0}C is also needed. The preferred, optimal order for adding chemical materials is hydrogen peroxide, tissue solubilizer, and DTT. The maximum amount of the hair solubilized without severe chemical quenching and completely solubilized within four hours is 0.3 gm.

3.4.3 Ashing Hair

Ashing hair is another choice for making a good counting solution. A Muffle furnace and some crucibles are required in the ashing process. The experiments were conducted at temperatures ranging from 600-1000^{0}C. Excessive amounts of char are developed below 700^{0}C, and much of the hair volatilized at 1000^{0}C. The residual ash associated with the experiments performed at a temperature of approximately 800^{0}C indicates that no char was produced and that an appreciable amount of ash remained in the crucibles. One gram of hair will become 0.008 gram after ashing. Care must be taken in transferring the ashed hair to the liquid scintillation vial to assure that little ashed hair is lost in the process. The loss of the ashed hair will affect the calculation of specific ^{32}P activity remarkably when the sample contains a small amount of hair.

The ashed hair remains in a fine powder. Triton-100 is used for suspending the powders in the counting solution.

Based upon a comparison of the above hair preparation methods, chemical dissolving is recommended when the hair sample weighs below 0.3 gm since the chemical quenching is relatively small. If a large hair sample is available, ashing hair

is recommended due to less quenching. The consistency of ashing depends on the degree of suspension and careful operation.

The procedures for preparing background samples are the same as for the hair sample. The background sample should simulate as closely as possible the chemical composition and physical form of the irradiated hair sample solution being measured except it is "blank". The "blank" hair can be obtained from an unirradiated individual.

3.5 Hair Sample Counting and ^{32}P Activity Calculation

A series of hair samples were irradiated by a bare Cf-252 neutron source. The counting window (counting energy range) was set at 5-1700 keV. The counts below 5 keV were cut off since data were unstable. This was caused by some random "noise pulses" from PMT, surrounding background, and unknown effects from chemical reactions. The print-outs from the counting system include the count rate of sample and background count rate in the region of interest, counting time, quenching indicator (SIS, tSIE), and chemical luminacence indicator. Using the measured count rate, the ^{32}P activity is calculated by

$$A = \frac{C}{2.22\times10^{6} e^{-\lambda t} E_f m} \quad (\mu Ci/g) \tag{3.1}$$

where A = ^{32}P activity induced in hair, dpm/g,

C = cpm associated with the specified window setting,

λ = ^{32}P decay constant,

t = elapsed time from the end of the accident until the start of

counting,

E_f = counting efficiency for ^{32}P, and

m = the amount of hair (gm).

One standard deviation of calculated ^{32}P activity is given by

$$\sigma_A = A\sqrt{\frac{G_c+B_c}{C^2 \times T}}, \tag{3.2}$$

where G_c = gross cpm associated with the specified window setting,

B_c = background cpm associated with the specified window setting,

σ_A = one standard deviation of A, and

T = counting time, which is the same for sample and background counting (min.).

The measured and calculated results are listed in Table 3.3. The highest neutron dose used was 541 rads, and the lowest was 66 rads. The largest sample contains about 1.0 gram of hair. The smallest sample has about 0.16 gram of hair. The ratios between ^{32}P specific activity and dose vary slightly between 3.1×10^{-7} μCi/g per rad and 3.8×10^{-7} μCi/g per rad except samples LA1-A, 4-C, and 8-A. The minor variation corresponds to the repeatability of the measurement process. LA1-A, 8-A are small ashed samples and 4-C is a large chemiclly dissolved sample. They have relatively lower specific activities compared with other samples. This fact further confirmes the conclusions in Section 3.4 that small ashed samples (below 0.3 g) and large chemically dissolved sample (above 0.5 g) will cause an activity loss if the operation process is not performed very careful. Some inconsistent results for the

Table 3.3 Measured and Calculated Results for Hair Samples

Irradiated by Different Neutron Dose.

Sample ID	Sample Weight (g)	t_1 [1] (hrs)	T [2] (min)	Net CPM	A [3] ($x10^{-5}$)	Total Dose (rads)	A/Dose[4] ($x10^{-7}$)	σ_A [5] ($x10^{-6}$)	σ_A/A (%)
11-C*	0.1746	88.32	20	14.2	4.65	134	3.474	7.43	15.6
33-C	0.166	126.1	40	28.65	10.64	339	3.14	6.16	5.789
55-C	0.1768	126.45	40	53.5	18.675	541	3.452	6.41	3.34
2-A**	0.5344	65.82	60	34.48	3.494	102	3.409	1.468	4.2
2-A	0.5344	73.02	30	33.47	3.446	102	3.36	2.144	5.79
4-C	0.5343	93.45	60	26.83	2.875	102	2.82	1.74	6.7
6-C	0.1619	169.1	60	10.95	3.966	102	3.88	5.68	13.91
8-A	0.1618	117.5	60	7.27	2.7	102	2.65	4.93	18
10-A	1.0563	77.133	30	55.53	3.28	102	3.275	1.4	4.2
10-A	1.0563	78.283	30	56.34	3.23	102	3.152	1.34	4.14

Table 3.3 (continued)

Sample ID	Sample Weight	t_1 (hrs)	T (min)	Net CPM	A ($x10^{-5}$)	Total Dose	A/Dose ($x10^{-7}$)	σ_A ($x10^{-6}$)	σ_A/A (%)
LA1-A	0.2135	132.03	60	6.55	1.92	66	2.9	3.84	20.4
L1-C	0.2142	133.03	60	8.6	2.51	66	3.81	4.81	19
LA2-A	0.5192	131.03	60	19.28	2.32	66	3.51	1.71	7.47
LA2-A	0.5192	150.4	60	16.4	2.05	66	3.1	1.76	8.6
AN1-A	0.5	161.67	40	17.2	2.28	66	3.45	2.23	9.8

Notes: * Sample is chemically dissolved.

** Sample is ashed.

1. t1 = elapsed time after irradiation and before starting counting,

2. T = counting time,

3. A = ^{32}P specific activity, μCi/g hair,

4. A/Dose ($x10^{-7}$) = ratio of ^{32}P specific activity and measured total neutron dose, μCi/g per rad,

5. σ_A ($x10^{-6}$) = one standard deviation of A, μCi/g hair.

same samples counted twice, such as LA2-A, are caused by the heterogenous ashed sample solution. The ashed solution should be shaken before each counting since the Triton material in the solution can only be effective for one to two hours each time.

The larger statistical counting error is associated with low count samples or small samples. According to Equation (3.2), counting error can be reduced by increasing counting time.

3.6 Sensitivity of Measurement System

According to the theory in Section 2.6, the LLD for the hair ^{32}P counting will be

$$LLD = 4.66\sqrt{B_c T}\ , \tag{3.3}$$

where B_C is the background count rate and T is counting time in minutes.

The MDA is in the form of

$$MDA = \frac{4.66\sqrt{B_C}}{2.22\times10^6 E_f \sqrt{Tm}} \quad \mu Ci/g, \tag{3.4}$$

where the MDA is prototional to the square root of the background count rate and inverse to the sample weight and square root of the counting time. To investigate the relationship among the background count rate, counting time and sample weight, a series of experiments using "blank" hair samples were conducted.

Table 3.4 lists the experimental results from chemically dissolved "blank" hair samples. The background count rate does not change significantly with different

Table 3.4 Background Count Rate from Chemically Dissolved "Blank" Hair Samples with Different Amount of Hair and Counting Time in Window (5-1700 KeV)

Sample weight (g)	Counting Time (mins)	Background CPM
0.1618	30	70.67
0.161	30	67.63
0.1605	60	65.75
0.2034	60	77.88
0.2021	60	75.38
0.2002	60	74.83
0.2056	30	77.08
0.5023	30	84.43
0.5054	60	85.45
0.51	30	89.13
0.5055	30	89.1

counting times, but it increases as the sample weight (or chemical material) increases. The averaged background count rate for hair samples of about 0.16 gram is 68 cpm; for samples of 0.2 gram, 76.3 cpm; and for samples of 0.5 gram, 87 cpm.

Table 3.5 lists the background count rate from ashed "blank" hair samples. The measured background count rates are almost constant regardless of the counting time and sample weight. The averaged background count rate is 50.3 cpm. This value is near the "blank" cocktail count rate, which is about 45 cpm in the window (5-1700 KeV). The background count rate for the counter itself is 36 cpm in the same window.

The following conclusions are based on a comparison of results in Table 3.4 and Table 3.5: 1) the background count rate of chemically dissolved hair samples increases as the weight of the hair in the sample increases, 2) the background count rate of ashed samples is almost constant and similar to the count rate of the cocktail solution, 3) the background count rate of chemically dissolved samples is higher than ashed samples, and 4) the background count rates for both methods do not change significantly with different counting time.

The calculated MDAs based on the above conclusions are listed in Table 3.6. The lowest MDA is 2.02E-6 μCi/g hair, which is from 1.0 gram of ashed sample counted for 60 minutes. If we take the bare Cf-252 spectrum as a reference spectrum, about six to seven rads of total neutron dose can be measured from one gram of hair sample with 95% confidence level.

Table 3.5 Background Count Rate from Ashed "Blank" Hair Samples with Different Amount of Hair and Counting Time in Window (5-1700 KeV)

Sample Weight (g)	Counting Time (mins)	Background CPM
0.1620	30	49.2
0.1615	60	49.3
0.22	60	52.78
0.2015	30	50.75
0.2022	60	51.02
0.5011	30	51.2
0.5111	60	49.27
0.5023	60	48.05
1.05	30	50.23
1.08	60	53.03

Table 3.6 Minimum Detectable Activity for Hair ^{32}P Counting

Sample preperation	Sample weight (g)	Background count rate	Counting time (min.)	LLD (counts)	MDA (μCi/g)
Chemical dissolution	0.16	68	30	210	2.07E-5
			60	297	1.46E-5
Ashing	0.16	50.3	30	181	1.78E-5
			60	256	1.26E-5
Chemical dissolution	0.2	76.3	30	222	1.75E-5
			60	315	1.24E-5
Ashing	0.2	50.3	30	181	1.43E-5
			60	256	1.01E-5
Chemical dissolution	0.5	87	30	238	7.52E-6
			60	336	5.3E-6
Ashing	0.5	50.3	30	181	5.72E-6
			60	256	4.04E-6
Ashing	1.0	50.3	30	181	2.85E-6
			60	256	2.02E-6

CHAPTER VI

DEVELOPMENT OF ACCIDENT NEUTRON DOSE ASSESSMENT SYSTEM

4.1 Introduction

The production of ^{24}Na in the blood by neutrons is a function of total neutron dose, the accident neutron spectrum, the individual body size and body weight, the specific ^{24}Na concentration in an individual's blood, and the person's orientation during the accidents. When an accident happens, detailed and accurate information such as that stated above is difficult to obtain within a few hours after the accident. However, a rapid accident neutron dosimetry system for initial dose assessment is necessary and important for doctors to treat the victims as soon as possible.

The most important and difficult step in the initial dose assessment is to determine the accident neutron spectrum within a few hours after the accident. Area dosimeter stations and computerized calculations can be used to obtain spectral information. However, they can not satisfy the limited time requirement [1].

The IAEA report entitled "Compendium of Neutron Spectra and Detector Responses for Radiation Protection Purposes" [4] and Data Base files from ORNL [13] contain a large number of spectra of fission neutrons transmitted through different thicknesses of various materials which have been calculated by a Monte Carlo method [4]. These encompass the most likely neutron spectra encountered in

nuclear accidents. These data provide a basis for a methodology to quickly approximate the actual spectrum in a criticality accident from sets of spectra after accidents.

This chapter discusses the development of an accident neutron dose assessment system using these neutron spectra and measured blood activity, the special functions of hair activation in accident neutron dosimetry, and quantities affecting the accuracy of the derived neutron dose.

4.2 Discussion of Neutron Spectra

One hundred seventeen different neutron spectra were supplied by ORNL in May 1991 in the form of Data Base files. Most of them can be found in Reference 4. Ninety-eight of them can be readily transfered from the Data Base files to ASCII files.

4.2.1 Spectrum Description

In a nuclear accident, the geometry and material composition of the critical assembly and its environment can be very complex. Two approximations were assumed in the use of the 98 neutron spectra [4]:

1. The actual spectrum corresponds directly to that from the critical assembly or to one filtered by various materials. Multiple scattering from the room or from surrounding objects to the location of the individual is not considered.

2. The composition and thickness of the shielding material are much more important in determining the shape of the leakage spectrum than geometry of the critical assembly [14].

Ninety-eight neutron spectra are grouped according to shielding configurations, as listed in Table 4.1. Each group includes different radius of shielding and shielding materials.

4.2.2 Plots of Representative Spectra

All spectra are presented in the form of fluence per unit lethargy (per unit logarithmic energy) versus neutron energy in MeV. "The lethargy unit is preferred since neutron spectra, when plotted as fluence per unit energy, often display a steep negative slope at lower energies due to a roughly inverse-energy type of dependence and require many decades on the fluence axis for complete presentation. The lethargy unit essentially weights the fluence by the corresponding neutron energy, so the negative slope is changed to an approximately horizontal line which is simple to present graphically. [4]"

Ninety-eight spectra must be interpolated with the same energy boundaries since each spectrum in Data Base files has its own energy groups and energy boundaries. The integrating energy boundaries are 620 groups ranging from 10E-10 MeV to 18 MeV. A linear interpolation is used. Both original and interpolated uncollided fission spectra are shown in Figure 4.1 and Figure 4.2. The shape and magnitude of both plots are identical. This verifies the interpolation.

Table 4.1 Spectra Description

1. Spectra from selected critical assemblies

   Uncollided fission spectrum
   Unshielded HPRR
   Concrete shielded HPRR at 3 meters
   Plexiglass shielded HPRR
   Steel shielded HPRR at 3 meters

2. Spectra from critical solutions

   Fissile H_2O solution
   Fissile D_2O solution

3. Spectra of fission neutrons through shielding

   Fission neutrons through H_2O
   Fission neutrons through D_2O
   Fission neutrons through graphite
   Fission neutrons through polyethylene
   Fission neutrons through 1% borated polyethylene
   Fission neutrons through Be
   Fission neutrons through Al
   Fission neutrons through concrete
   Fission neutrons through concrete + 10% Fe
   Fission neutrons through concrete + 50% Fe
   Fission neutrons through Fe
   Fission neutrons through Cu
   Fission neutrons through Pb
   Fission neutrons through ^{238}U

4. Spectra of H_2O-moderated fission neutrons through shielding
   H_2O-moderated fission neutrons through Be
   H_2O-moderated fission neutrons through Al
   H_2O-moderated fission neutrons through concrete
   H_2O-moderated fission neutrons through Fe
   H_2O-moderated fission neutrons through Cu
   H_2O-moderated fission neutrons through Pb

5. Selected spectra

   Bare Cf-252
   D_2O moderated Cf-252

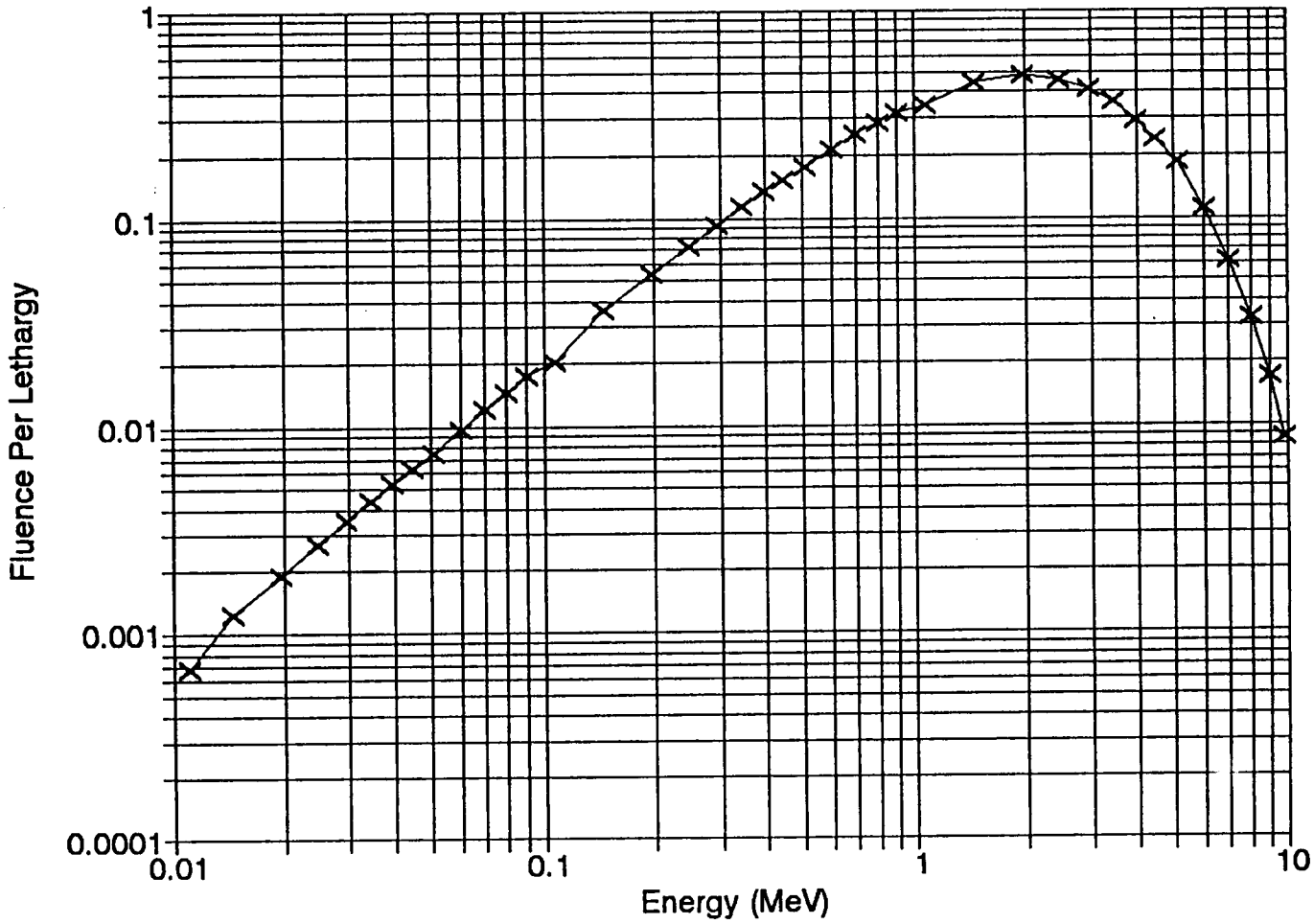


Figure 4.1 Uncollided Fission Spectrum (original)

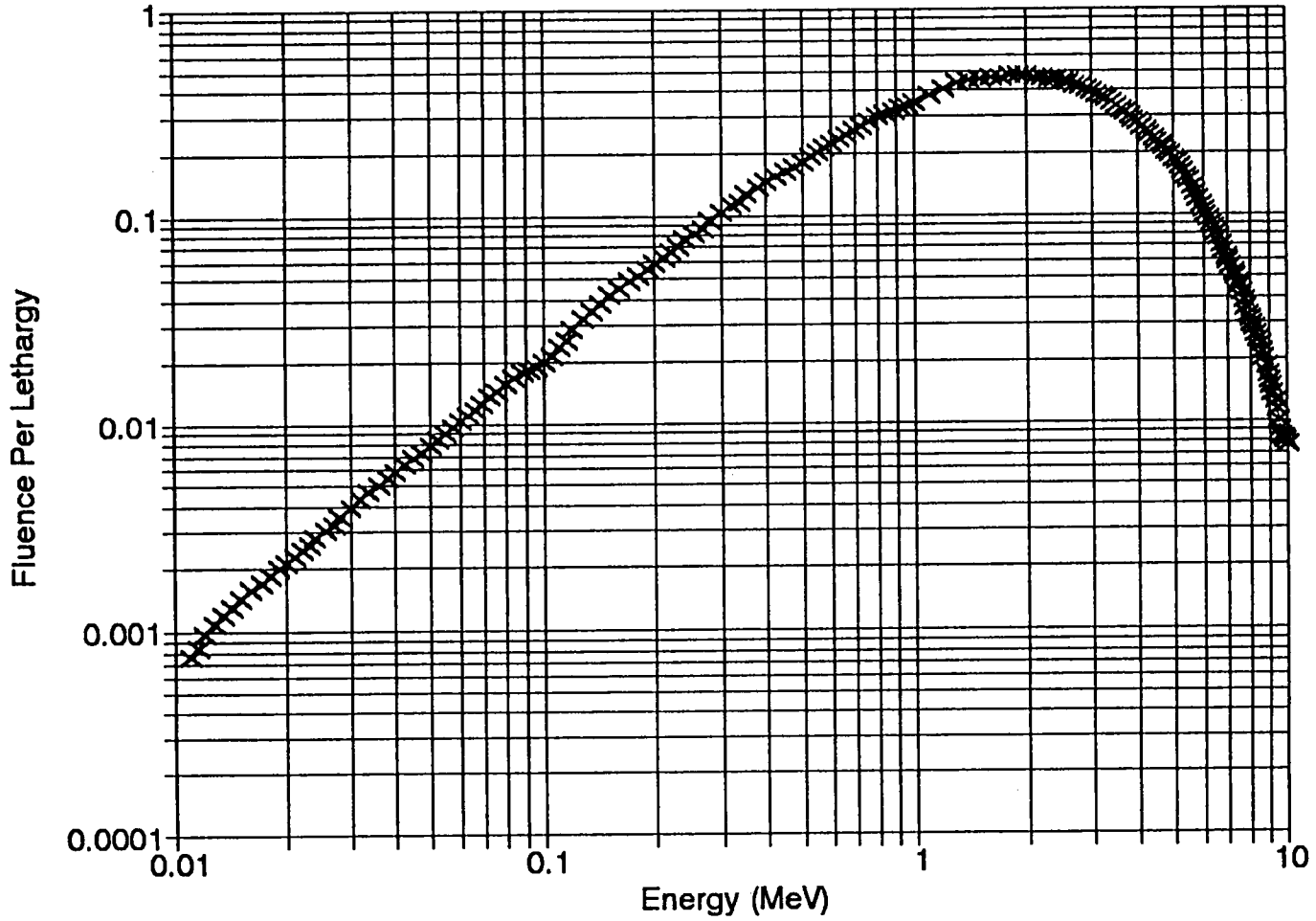


Figure 4.2 Uncollided Fission Spectrum (interpolated)

4.3 Neutron Dosimetry Using Blood

A collection of 98 neutron spectra is utilized to develop a method for estimating neutron dose by the induced ^{24}Na activity in blood without the difficulty of an exact spectrum measurement and calculation. The intention is to convert the blood activity-to-fluence relation into an activity-to-dose relation by means of the known fluence-to-dose conversion factors. Thus, the neutron dose can be directly related to the blood activity based on the 98 neutron spectra information.

4.3.1 Blood Activity-to-Fluence

Many calculations and experiments have been conducted to determine the relationship between the incident neutron fluence and the induced specific activity of ^{24}Na in the blood. An intermediate step in the relation between fluence and the specific activity of ^{24}Na is the Capture Probability [15,16], which is the fraction of neutrons striking a phantom that is captured at thermal energy.

4.3.1.1 Capture Probability

"The human body is several mean free paths thick for fast neutrons. Thus, the probability that a fast neutron will be captured as a thermal neutron is not very sensitive to its initial energy. [15]" Table 4.2 lists the calculated capture probabilities as a function of incident neutron energy for a Bomab phantom [1]. A schematic of a Bomab phantom is illustrated in Figure 4.3. Basically, the Bomab phantom is a set

Table 4.2 Capture Probabilities for a Bomanb Phantom.

They are for a broad, parallel beam of neutrons

incident normally on the front of the phantom.

Neutron Energy (MeV)	Capture Probability
2.5E-8	0.186
1.0E-6	0.301
1.0E-5	0.338
1.0E-4	0.335
1.0E-3	0.313
1.0E-2	0.296
1.0E-1	0.292
2.0E-1	0.293
3.0E-1	0.294
3.5E-1	0.290
4.5E-1	0.251
5.0E-1	0.303
6.0E-1	0.302
8.0E-1	0.288
1.0E+0	0.244
1.2E+0	0.270
1.4E+0	0.266
1.8E+0	0.250
2.0E+0	0.242
2.4E+0	0.230
3.0E+0	0.210
3.4E+0	0.200
4.0E+0	0.184
4.5E+0	0.178
6.0E+0	0.147
10.0	0.140
14.0	0.127

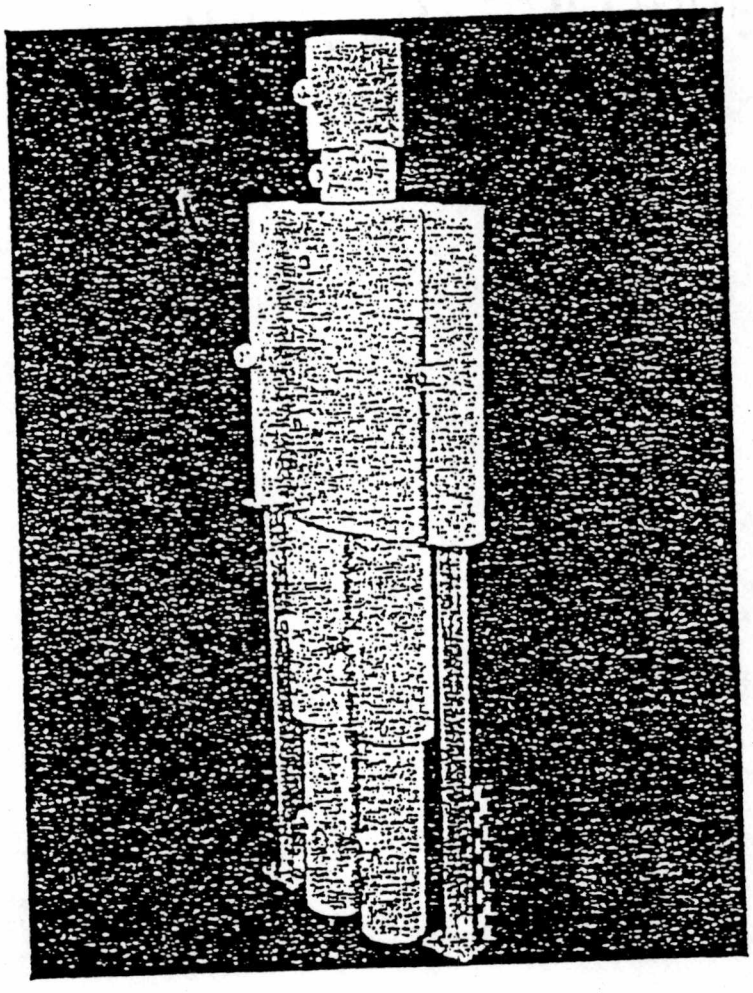


Figure 4.3 A Schematic of Bomab Phantom

of 10 NaCl solution-filled polythelyne bottles. Some of the bottles are elliptical and some are cylindrical. The shape and size of the Bomab phantom will be used as a reference man in our calculations.

The moderation of the body to the incident neutrons is so strong that the interaction of $^{23}Na(n,\gamma)^{24}Na$ is mainly determined by the body capture probability, not the absorption cross-section of ^{23}Na. This is well illustrated by Figure 4.4, Capture probability as a function of neutron energies and Figure 4.5, Cross-section of ^{23}Na as a function of neutron energy.

4.3.1.2 Relation Between Fluence and ^{23}Na Activation

When a beam of neutrons incident normal to the axis of the phantom, the number of neutrons in the energy interval dE striking the phantom is $S\phi(E)dE$, where S is the projected area of the phantom to the beam. Of the total number of neutrons striking the phantom, a fraction $\xi(E)$ (capture probability) will be captured in the phantom and the fraction of these which will undergo reaction of $^{23}Na(n,\gamma)^{24}Na$ is Σ_{Na}/Σ_t, where Σ_{Na} is the macroscopic absorption cross-section of ^{23}Na in tissue and blood, and Σ_t is the total absorption cross-section in the body [15]. Thus, the total number of ^{24}Na atoms produced in the phantom is

$$\frac{\Sigma_{Na}}{\Sigma_t}\int_0^{\infty}\xi(E)S\phi(E)dE \qquad (4.1)$$

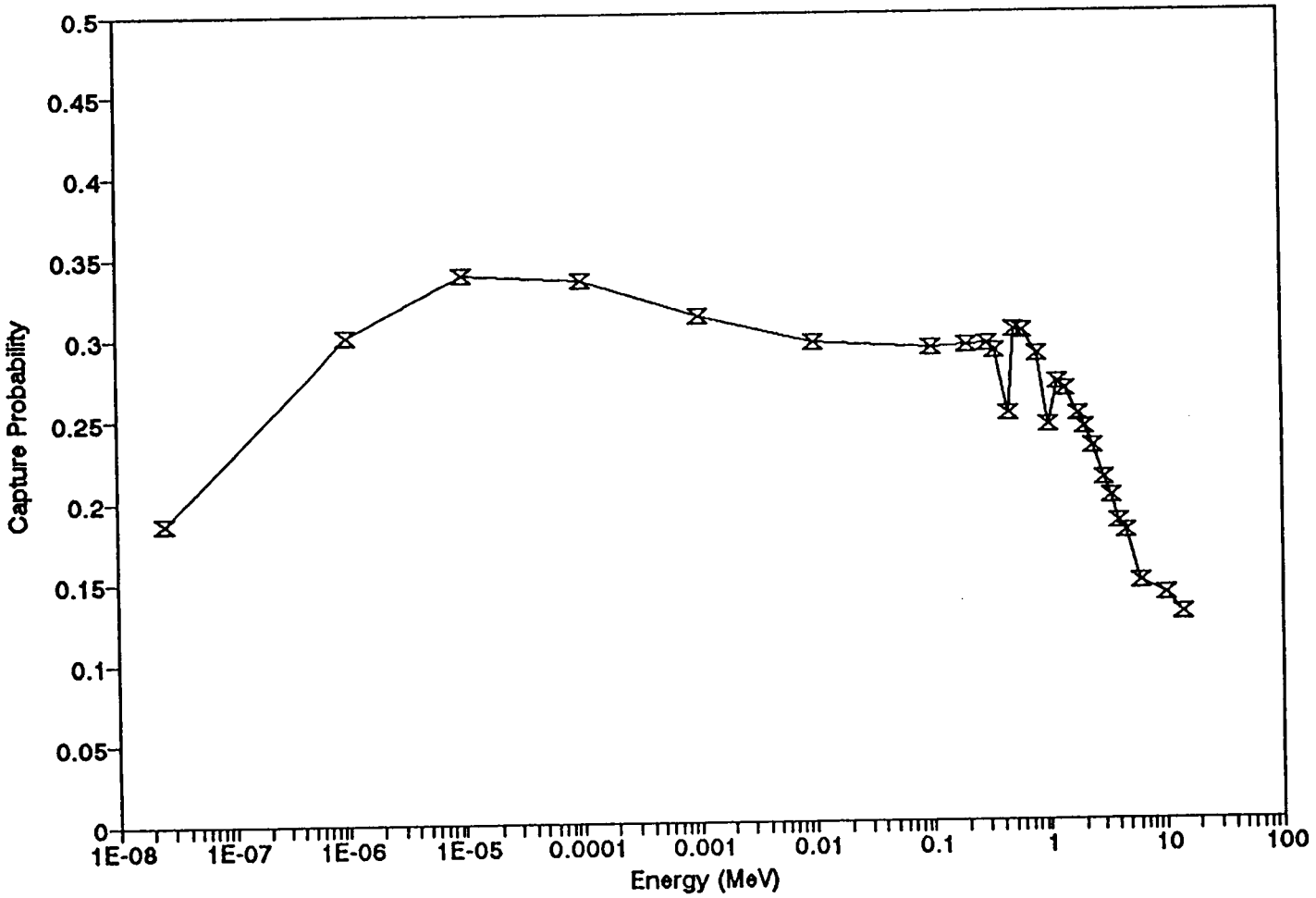


Figure 4.4 Capture Probability As A Function of Neutron Energy

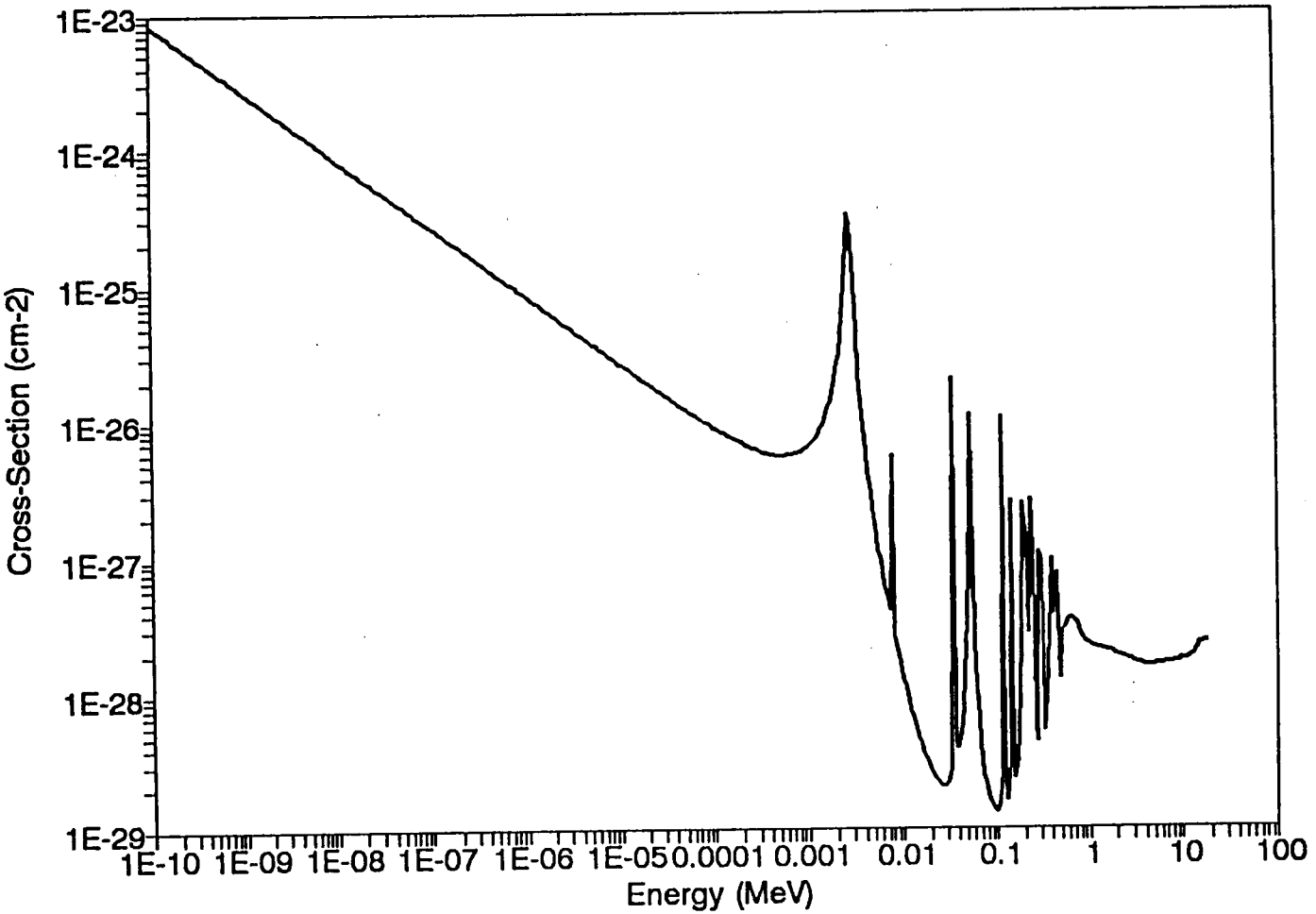


Figure 4.5 Cross Section of $^{23}Na(n,\gamma)^{24}Na$

If the volume of the phantom is V and the ^{24}Na decay constant is λ, the specific activity of ^{24}Na per unit volume induced in the phantom is

$$A = \lambda\left(\frac{S}{V}\right)\left(\frac{\Sigma_{Na}}{\Sigma_t}\right)\int_0^{\infty}\xi(E)\phi(E)dE \quad \mu Ci/ml \tag{4.2}$$

This equation was first given by Hurst [15] and is used widely in the calculation of ^{24}Na activation. Since the ratio of the concentration of ^{24}Na and ^{23}Na, ($^{24}Na/^{23}Na$), in circulated blood is equal to the ratio in the whole body [17], we can conclude that the specific activity of ^{24}Na per unit volume of whole body is same as the specific activity of ^{24}Na per unit volume of the blood.

The thermal spectrum-averaged macroscopic cross section of ^{23}Na in Equation (4.2) is given by

$$\Sigma_{Na} = \frac{6.023\times10^{23}}{23}\sigma_{Na}m_{Na} \tag{4.3}$$

where 6.023E+23 = Avogadro's number,

23 = atomic weight of sodium,

σ_{Na} = the thermal-neutron microscopic cross section of ^{23}Na (0.534 barns), and

m_{Na} = the mass of ^{23}Na per cm^3 of the solution in the phantom.

The total absorption cross-section (Σ_t) is calculated from the elemental abundance in the standard man and is equal to 0.02339 cm^{-1} [14].

Since the ratio of Σ_{Na}/Σ_t is proportional to the ^{23}Na concentration according to Equation (4.3), it is convenient to give specific ^{24}Na activity in terms of ^{24}Na/mg

^{23}Na which is essentially independent of the ^{23}Na concentration in each individual's blood. Thus, Equation (4.2) also can be expressed as

$$A = \lambda\left(\frac{\Sigma_{Na}}{m_{Na}\Sigma_t}\right)\frac{S}{V}\int_0^{\infty}\xi(E)\phi(E)dE \quad \mu Ci^{24}Na/g^{23}Na \tag{4.4}$$

Using the shape and size of Bomab phantom, for neutron radiation normally incident upon the front, the projected area (S) of body normal to the incident neutron beam is 5690 cm^2. The total volume (V) of the body is 68.28×10^3 cm^3. The relation between neutron fluence and blood activation is given by

$$A = 1.81\times10^{-14}\int_0^{\infty}\xi(E)\phi(E)dE \quad \mu Ci^{24}Na/mg^{23}Na \tag{4.5}$$

4.3.2 Fluence-to-Neutron Dose Conversion Factor

Before discussing fluence-to-dose conversion factors, it is important and necessary to state the meaning of the "dose" used in this research.

There are several kinds of "dose" used in accident dosimetry. One is the surface absorbed dose. This is the absorbed dose from neutrons interacting close to the surface of the body where the neutrons are incident [1]. This concept has the convenience of being consistent with the one used for the routine interpretation of the badge dosimeters. Another is the depth dose. This is the absorbed dose at the depth where the maximum radiation damage could occur [18]. Surface absorbed doses are categorized according to two reactions: 1) surface absorbed heavy charged

particle (recoils and $^{14}N(n,p)^{14}C$) dose, and 2) surfaced absorbed $^{1}H(n,\gamma)^{2}D$ dose. The variation of surface absorbed dose and depth dose with incident neutron energy is given in Figure 4.6. At energies above 0.1 MeV the surface absorbed dose comes mainly from recoils and heavy charged particles. While below 0.01 MeV most of it comes from gamma rays produced by capture in hydrogen. Since the surface absorbed dose from fast neutrons is of primary concern, it is customary to express the surface absorbed dose using surface absorbed recoil dose. The neutron fluence-to-dose conversion factors for depth and surface absorbed doses are listed in Table 4.3.

4.3.3 ^{24}Na Activity-to-Dose Conversion Factors For different Spectra

The total neutron dose received by the person per specific activity of ^{24}Na due to a fluence, is given by

$$\frac{D}{A} = \frac{\int_0^{\infty} R(E)\phi(E)dE}{\lambda\left(\frac{\Sigma_{Na}}{m_{Na}\Sigma_t}\right)\left(\frac{S}{V}\right)\int_0^{\infty}\xi(E)\phi(E)dE} \qquad (4.6)$$

The equation used for computer calculations is of the form,

$$\frac{D}{A} = \frac{\sum_1^K R(E_i)\phi(E_i)(E_{i+1}-E_i)}{1.81\times10^{-8}\sum_1^N \xi(E_j)\phi(E_j)(E_{j+1}-E_j)} \quad \frac{Rad}{pCi^{24}Na/mg^{23}Na} \qquad (4.7)$$

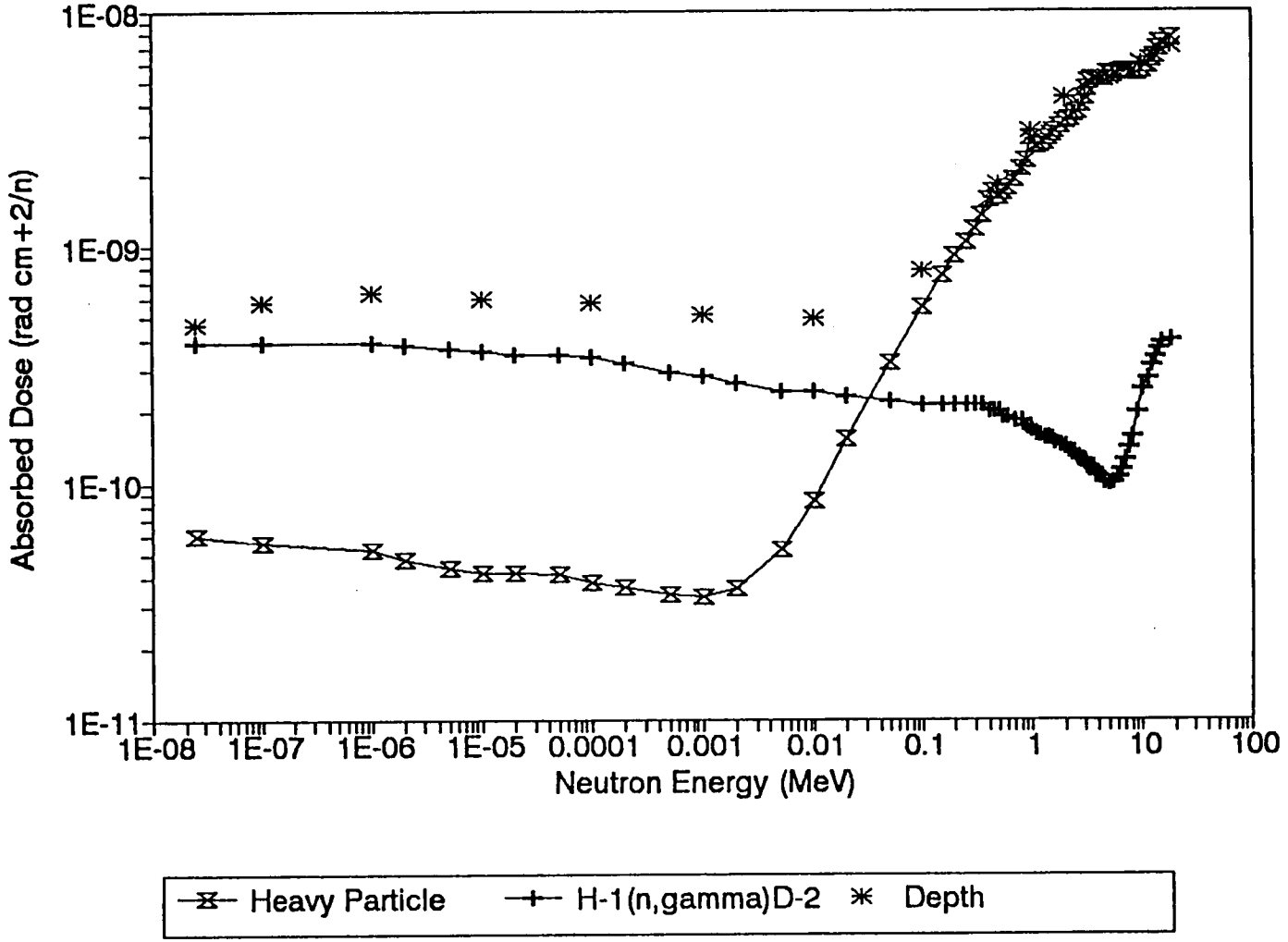


Figure 4.6 Fluence-to-Dose Conversion Factors

Table 4.3 Neutron Fluence to Dose Conversion Factors

Neutron Energy (MeV)	Surface Absorbed Dose per unit fluence ($rad.cm^2.n^{-1}$)		Deapth Absorbed Dose per unit fluence ($rad.cm^2.n^{-1}$)
	Heavy particle	$^1H(n,\gamma)^2D$	
2.5e-8	0.600e-10	3.9e-10	4.65e-10
1.0e-7	0.560e-10	3.9e-10	5.79e-10
1.0e-6	0.520e-10	3.9e-10	6.31e-10
2.0e-6	0.475e-10	3.8e-10	
5.0e-6	0.435e-10	3.7e-10	
1.0e-5	0.420e-10	3.6e-10	6.04e-10
2.0e-5	0.420e-10	3.5e-10	
5.0e-5	0.410e-10	3.5e-10	
1.0e-4	0.380e-10	3.4e-10	5.79e-10
2.0e-4	0.365e-10	3.2e-10	
5.0e-4	0.340e-10	2.9e-10	
1.0e-3	0.330e-10	2.8e-10	5.14e-10
2.0e-3	0.360e-10	2.6e-10	
5.0e-3	0.520e-10	2.4e-10	
1.0e-2	0.840e-10	2.4e-10	4.96e-10
2.0e-2	1.510e-10	2.3e-10	
5.0e-2	3.200e-10	2.2e-10	
1.0e-1	5.500e-10	2.1e-10	7.82e-10
1.5e-1	7.500e-10	2.1e-10	
2.0e-1	9.000e-10	2.1e-10	
2.5e-1	10.40e-10	2.1e-10	
3.0e-1	11.80e-10	2.1e-10	
3.5e-1	13.40e-10	2.1e-10	
4.0e-1	15.50e-10	2.0e-10	
4.5e-1	16.80e-10	2.0e-10	
5.0e-1	16.00e-10	2.0e-10	1.80e-9
5.5e-1	16.60e-10	1.9e-10	
6.0e-1	17.60e-10	1.9e-10	
7.0e-1	19.20e-10	1.8e-10	
8.0e-1	21.00e-10	1.8e-10	
9.0e-1	23.10e-10	1.7e-10	
1.0e0	28.50e-10	1.65e-10	3.08e-9
1.1	26.40e-10	1.6e-10	
1.2	26.70e-10	1.57e-10	
1.3	27.50e-10	1.54e-10	
1.4	28.70e-10	1.52e-10	

Table 4.3 (Continued)

Neutron Energy (MeV)	Surface Absorbed Dose per unit fluence (rad.cm^2.n^{-1})		Deapth Absorbed Dose per unit fluence (rad.cm^2.n^{-1})
	Heavy particle	$^1H(n,r)^2D$	
1.5	29.70e-10	1.50e-10	
1.6	30.60e-10	1.47e-10	
1.8	32.40e-10	1.43e-10	
2.0	33.80e-10	1.4e-10	4.27e-9
2.2	35.00e-10	1.35e-10	
2.4	36.20e-10	1.32e-10	
2.6	37.60e-10	1.28e-10	
2.8	40.10e-10	1.25e-10	
3.0	43.00e-10	1.22e-10	
3.2	47.00e-10	1.18e-10	
3.4	49.80e-10	1.15e-10	
3.6	51.20e-10	1.12e-10	
3.8	51.50e-10	1.09e-10	
4.0	51.80e-10	1.06e-10	
4.5	51.70e-10	1.01e-10	
5.0	54.70e-10	1.0e-10	5.24e-9
5.5	53.20e-10	1.01e-10	
6.0	54.70e-10	1.05e-10	
6.5	55.10e-10	1.12e-10	
7.0	55.90e-10	1.24e-10	
7.5	55.80e-10	1.38e-10	
8.0	54.80e-10	1.56e-10	
9.0	54.80e-10	1.96e-10	
10.0	55.80e-10	1.45e-10	6.0e-9
11.0	58.60e-10	2.76e-10	
12.0	61.80e-10	3.1e-10	
13.0	64.60e-10	3.4e-10	
14.0	69.10e-10	3.7e-10	
15.0	73.30e-10	3.89e-10	
18.0	77.00e-10	4.0e-10	7.12e-9

Where $R(E_i)$ is the fluence-to-dose conversion factor.

The calculated ^{24}Na activity-to-depth dose conversion factors and activity-to-surface absorbed dose conversion factors are listed in Table 4.4 and Table 4.5 separately. The conversion factors are expressed in two units. One is pCi ^{24}Na/mg ^{23}Na per rad which is independent on the ^{23}Na concentration in blood. The other is Rad per pCi ^{24}Na/ml blood. The sodium-23 concentration used is 1.91 mg ^{23}Na/ml blood for a standard man [5]. The activity-to-surface absorbed recoil dose conversion factors varies widely with a factor of 30 for the different spectra. A factor of 9 is associated with the variation of activity-to-depth dose conversion factors. These conversion factors are only valid for the neutrons incident on the front or back of the individual.

The person's orientation can be determined from hair sample specific activity. Four hair samples are taken from the front, back, left, and right of the head. The side where the hair sample is taken has the highest specific ^{32}P activity faces the incident neutrons. The correction of the lateral irradiation to the blood activation will be discussed in Section 4.5.

The procedures to calculate the total neutron dose based on Table 4.4 and Table 4.5 are simple if the following information required is available: 1) the form of the fission material such as metal or solution, 2) the type of the shielding materials such as Fe, Pb, concrete, or graphite, 3) the thickness of the shielding, and 4) the type of the moderator. According to this information, an actual accident spectrum can be quickly approximated from 98 neutron spectrum. Thus, the needed activity-

Table 4.4 Activity to Depth Dose Conversion Factors for 98 Ntutron Spectra

Spectrum Description	pCi^{24}Na per mg ^{23}Na per rad	Rad/μCi ml^{-1}
UNCOLLIDED FISSION SPECTRA	1.195	442235
FISSILE SOLUTION, 2 CM RADIUS SPHERE, H2O	1.429	369852
FISSILE SOLUTION, 5 CM RADIUS SPHERE, H2O	1.722	306874
FISSILE SOLUTION, 10 CM RADIUS SPHERE, H2O	1.846	286193
FISSILE SOLUTION, 30 CM RADIUS SPHERE, H2O	1.894	278993
FISSILE SOLUTION, 50 CM RADIUS SPHERE, H2O	1.909	276729
FISSILE SOLUTION, 2 CM RADIUS SPHERE, D20	1.366	386811
FISSION SOLUTION, 30 CM RADIUS SPHERE, D2O	3.381	156298
FISSILE SOLUTION, 50 CM RADIUS SPHERE, D2O	3.542	149190
UNSHIELDED HPRR SPECTRA	2.565	206008
CONCRETE SHIELDED HPRR AT 3 METERS	4.874	108403
PLEXIGLAS SHIELDED HPRR SPECTRA	2.569	205726
STEEL SHIELDED HPRR AT 3 METERS	3.545	149068
FISS.THR. 5 CM H2O	1.935	273069
FISS.THR. 10 CM H2O	1.607	328768
FISS.THR. 30 CM H2O	1.410	374713
FISS.THR. 50 CM H2O	1.243	425154
FISS.THR. 2 CM H2O AT SURFACE	1.690	312600
FISS.THR. 2 CM D2O	1.447	365244
FISS.THR. 5 CM D2O	3.222	164003
FISS.THR. 10 CM D2O	5.295	99795
FISS.THR. 30 CM D2O	6.009	87941
FISS. THR. 2 CM D2O AT SURFACE	1.540	343018
FISS.THR. 5 CM GRAPHITE	1.201	440024
FISS.THR. 10 CM GRAPHITE	1.364	387507
FISS.THR. 20 CM GRAPHITE	2.035	259716
FISS.THR. 40 CM GRAPHITE	4.132	127872
FISS.THR. 60 CM GRAPHITE	5.695	92789
FISS.THR. 10 CM POLYE.	2.213	238786
FISS.THR. 20 CM POLYE.	2.128	248286
FISS.THR. 40 CM POLYE.	1.834	288102
FISS.THR. 60 CM POLYE.	1.668	316793
FISS.THR. 5 CM OF 1% BORATED POLYE.	1.834	288099
FISS.THR. 10 CM OF1% BORATED POLYE.	1.899	278309
FISS.THR. 20 CM OF 1% BORATED POLYE.	1.736	304301
FISS.THR. 40 CM OF 1% BORATED POLYE.	1.502	351917
FISS.THR. 60 CM OF 1% BORATED POLYE.	1.388	380573
FISS.THR. 2.5 CM OF 1% BERYLIUM	1.266	417520
FISS.THR. 5 CM BERYLLIUM	1.469	359818
FISS.THR. 10 CM BERYLLIUM	2.229	237109
FISS.THR. 20 CM BERYLLIUM	4.001	132054
FISS.THR. 30 CM BERYLLIUM	5.250	100657
FISS.THR. 2.5 CM ALUMINUM	1.174	450159

Table 4.4 (Continued)

Spectrum Description	pCi^{24}Na per mg ^{23}Na per rad	Rad/μCi ml^{-1}
FISS.THR. 10 CM ALUMINUM	1.349	391705
FISS.THR. 20 CM ALUMINUM	1.864	283437
FISS.THR. 40 CM ALUMINUM	4.056	130278
FISS.THR. 10 CM CONCRETE	1.875	281809
FISS.THR. 20 CM CONCRETE	2.639	200262
FISS.THR. 30 CM CONCRETE	3.105	170191
FISS.THR. 40 CM CONCRETE	3.100	170469
FISS.THR. 60 CM CONCRETE	2.764	191199
FISS.THR. 5 CM CONCRETE ITH 10% IRON	1.337	395185
FISS.THR. 10 CM CONCRETE ITH 10% IRON	1.704	310159
FISS.THR. 20 CM CONCRETE ITH 10% IRON	2.472	213766
FISS.THR. 60 CM CONCRETE ITH 10% IRON	3.488	151499
FISS.THR. 100 CM CONCRETE ITH 10% IRON	3.696	142953
FISS.THR. 5 CM CONCRETE ITH 50% IRON	1.352	390788
FISS.THR. 10 CM CONCRETE ITH 50% IRON	1.762	299915
FISS.THR. 20 CM CONCRETE ITH 50% IRON	2.723	194087
FISS.THR. 60 CM CONCRETE ITH 50% IRON	4.239	124642
FISS.THR. 100 CM CONCRETE ITH 50% IRON	4.595	115005
FISS.THR. 100 CM OF 100% IRON	9.170	57626
FISS.THR. 5 CM IRON	1.478	357460
FISS.THR. 10 CM IRON	1.834	288055
FISS.THR. 20 CM IRON	2.790	189410
FISS.THR. 30 CM IRON	3.754	140770
FISS.THR. 50 CM IRON	5.322	99286
FISS.THR. 5 CM COPPER	1.653	319623
FISS.THR. 10 CM LEAD	1.481	356793
FISS.THR. 20 CM LEAD	1.897	278596
FISS.THR. 30 CM LEAD	2.414	218910
FISS.THR. 50 CM LEAD	3.715	142248
FISS.THR. 5 CM URANIUM-238	1.746	302648
FISS.THR. 10 CM URANIUM-238	2.444	216177
FISS.THR. 20 CM URANIUM-238	3.951	133745
FISS.THR. 30 CM URANIUM-238	5.266	100352
FISS.,H2O MODERATED THR. 2.5 CM BERYLLIUM	2.450	215666
FISS., H2O MODERATED THR. 5 CM BERYLLIUM	2.638	200272
FISS., H2O MODERATED THR. 10 CM BERYLLIUM	3.300	160137
FISS., H2O MODERATED THR. 20 CM BERYLLIUM	4.713	112117
FISS., H2O MODERATED THR. 10 CM ALUMINUM	3.230	163614
FISS., H2O MODERATED THR. 20 CM ALUMUNUM	4.486	117803
FISS., H2O MODERATED THR. 10 CM CONCRETE	3.049	173294
FISS., H2O MODERATED THR. 20 CM CONCRETE	3.431	154002
FISS., H2O MODERATED THR. 30 CM CONCRETE	3.305	159876
FISS.,H2O MODERATED THR. 20 CM IRON	3.961	133387
FISS.,H2O MODERATED THR. 50 CM IRON	6.203	85182
FISS.,H2O MODERATED THR. 5 CM COPPER	3.087	171171
FISS.,H2O MODERATED THR. 10 CM COPPER	3.660	144384
FISS.,H20 MODERATED THR. 20 CM COPPER	5.035	104940
FISS.,H2O MODERATED THR. 30 CM COPPER	6.438	82082

Table 4.4 (Continued)

Spectrum Description	pCi^{24}Na per mg ^{23}Na per rad	Rad/μCi ml^{-1}
FISS.,H2O MODERATED THR. 50 CM COPPER	8.487	62264
FISS.,H2O MODERATED THR. 5 CM LEAD	2.773	190530
FISS.,H2O MODERATED THR. 10 CM LEAD	2.996	176348
FISS.,H2O MODERATED THR. 30 CM LEAD	4.160	127029
FISS.,H2O MODERATED THR. 50 CM LEAD	5.437	97184
CF-252 BARE	1.149	459710
CF-252 D2O MODERATED	4.459	118503

Table 4.5 Activity to Surface Absorbed Recoil Dose Conversion Factors

for 98 Neutron Spectra

Spectra Description	pCi ^{24}Na per mg ^{23}Na per rad	Rad/μCi ml^{-1}
UNCOLLIDED FISSION SPECTRA	1.391	379780
FISSILE SOLUTION, 2 CM RADIUS SPHERE, H2O	1.694	311882
FISSILE SOLUTION, 5 CM RADIUS SPHERE, H2O	2.093	252423
FISSILE SOLUTION, 10 CM RADIUS SPHERE, H2O	2.280	231798
FISSILE SOLUTION, 30 CM RADIUS SPHERE, H2O	2.349	224956
FISSILE SOLUTION, 50 CM RADIUS SPHERE, H2O	2.364	223499
FISSILE SOLUTION, 2 CM RADIUS SPHERE, D20	1.610	328137
FISSION SOLUTION, 30 CM RADIUS SPHERE, D2O	4.871	108484
FISSILE SOLUTION, 50 CM RADIUS SPHERE, D2O	5.204	101531
UNSHIELDED HPRR SPECTRA	3.363	157137
CONCRETE SHIELDED HPRR AT 3 METERS	9.195	57469
PLEXIGLAS SHIELDED HPRR SPECTRA	3.411	154910
STEEL SHIELDED HPRR AT 3 METERS	4.930	107192
FISS.THR. 5 CM H2O	2.414	218852
FISS.THR. 10 CM H2O	1.951	270870
FISS.THR. 30 CM H2O	1.676	315327
FISS.THR. 50 CM H2O	1.430	369641
FISS.THR. 2 CM H2O AT SURFACE	2.046	258221
FISS.THR. 2 CM D2O	1.709	309261
FISS.THR. 5 CM D2O	4.545	116261
FISS.THR. 10 CM D2O	10.114	52244
FISS.THR. 30 CM D2O	13.304	39719
FISS. THR. 2 CM D2O AT SURFACE	1.827	289218
FISS.THR. 5 CM GRAPHITE	1.390	380024
FISS.THR. 10 CM GRAPHITE	1.590	332363
FISS.THR. 20 CM GRAPHITE	2.493	211969
FISS.THR. 40 CM GRAPHITE	6.602	80034
FISS.THR. 60 CM GRAPHITE	13.352	39576
FISS.THR. 10 CM POLYE.	2.876	183757
FISS.THR. 20 CM POLYE.	2.754	191839
FISS.THR. 40 CM POLYE.	2.275	232317
FISS.THR. 60 CM POLYE.	2.022	261339
FISS.THR. 5 CM OF 1% BORATED POLYE.	2.253	234554
FISS.THR. 10 CM OF1% BORATED POLYE.	2.348	225008
FISS.THR. 20 CM OF 1% BORATED POLYE.	2.106	250925
FISS.THR. 40 CM OF 1% BORATED POLYE.	1.767	299082
FISS.THR. 60 CM OF 1% BORATED POLYE.	1.612	327835
FISS.THR. 2.5 CM OF 1% BERYLIUM	1.465	360574
FISS.THR. 5 CM BERYLLIUM	1.712	308564
FISS.THR. 10 CM BERYLLIUM	2.763	191227
FISS.THR. 20 CM BERYLLIUM	6.297	83919
FISS.THR. 30 CM BERYLLIUM	11.501	45945

Table 4.5 (Continued)

Spectra Description	pCi ^{24}Na per mg ^{23}Na per rad	Rad/μCi ml^{-1}
FISS.THR. 2.5 CM ALUMINUM	1.357	389421
FISS.THR. 10 CM ALUMINUM	1.564	337797
FISS.THR. 20 CM ALUMINUM	2.211	238954
FISS.THR. 40 CM ALUMINUM	5.759	91762
FISS.THR. 10 CM CONCRETE	2.306	229150
FISS.THR. 20 CM CONCRETE	3.519	150144
FISS.THR. 30 CM CONCRETE	4.424	119431
FISS.THR. 40 CM CONCRETE	4.444	118901
FISS.THR. 60 CM CONCRETE	3.838	137671
FISS.THR. 5 CM CONCRETE WITH 10% IRON	1.574	335689
FISS.THR. 10 CM CONCRETE WITH 10% IRON	2.076	254472
FISS.THR. 20 CM CONCRETE WITH 10% IRON	3.299	160187
FISS.THR. 60 CM CONCRETE WITH 10% IRON	5.545	95298
FISS.THR. 100 CM CONCRETE WITH 10% IRON	6.168	85670
FISS.THR. 5 CM CONCRETE WITH 50% IRON	1.587	332878
FISS.THR. 10 CM CONCRETE WITH 50% IRON	2.139	246991
FISS.THR. 20 CM CONCRETE WITH 50% IRON	3.655	144589
FISS.THR. 60 CM CONCRETE WITH 50% IRON	7.056	74884
FISS.THR. 100 CM CONCRETE WITH 50% IRON	8.096	65271
FISS.THR. 100 CM OF 100% IRON	33.951	15564
FISS.THR. 5 CM IRON	1.722	306779
FISS.THR. 10 CM IRON	2.148	245975
FISS.THR. 20 CM IRON	3.398	155521
FISS.THR. 30 CM IRON	4.831	109383
FISS.THR. 50 CM IRON	7.793	67804
FISS.THR. 5 CM COPPER	1.938	272720
FISS.THR. 10 CM LEAD	1.721	306998
FISS.THR. 20 CM LEAD	2.213	238811
FISS.THR. 30 CM LEAD	2.859	184801
FISS.THR. 50 CM LEAD	4.801	110055
FISS.THR. 5 CM URANIUM-238	2.059	256664
FISS.THR. 10 CM URANIUM-238	2.966	178142
FISS.THR. 20 CM URANIUM-238	5.233	100972
FISS.THR. 30 CM URANIUM-238	7.817	67594
FISS.,H2O MODERATED THR. 2.5 CM BERYLLIUM	3.209	164667
FISS., H2O MODERATED THR. 5 CM BERYLLIUM	3.503	150855
FISS., H2O MODERATED THR. 10 CM BERYLLIUM	4.729	111732
FISS., H2O MODERATED THR. 20 CM BERYLLIUM	8.825	59877
FISS., H2O MODERATED THR. 10 CM ALUMINUM	4.638	113930
FISS., H2O MODERATED THR. 20 CM ALUMUNUM	7.366	71736
FISS., H2O MODERATED THR. 10 CM CONCRETE	4.230	124930
FISS., H2O MODERATED THR. 20 CM CONCRETE	5.046	104717
FISS., H2O MODERATED THR. 30 CM CONCRETE	4.832	109351

Table 4.5 (Continued)

Spectra Description	pCi ^{24}Na per mg ^{23}Na per rad	Rad/μCi ml^{-1}
FISS.,H2O MODERATED THR. 20 CM IRON	5.480	96418
FISS.,H2O MODERATED THR. 50 CM IRON	10.412	50749
FISS.,H2O MODERATED THR. 5 CM COPPER	4.165	126881
FISS.,H2O MODERATED THR. 10 CM COPPER	5.069	104243
FISS.,H20 MODERATED THR. 20 CM COPPER	7.721	68442
FISS.,H2O MODERATED THR. 30 CM COPPER	11.668	45288
FISS.,H2O MODERATED THR. 50 CM COPPER	23.485	22499
FISS.,H2O MODERATED THR. 5 CM LEAD	3.701	142758
FISS.,H2O MODERATED THR. 10 CM LEAD	4.037	130879
FISS.,H2O MODERATED THR. 30 CM LEAD	6.019	87793
FISS.,H2O MODERATED THR. 50 CM LEAD	8.959	58983
CF-252 BARE	1.333	396527
CF-252 D2O MODERATED	7.483	70610

to-dose conversion factor can be selected from Table 4.4 or Table 4.5, depending on what kind of dose is used. Then, we divide the measured blood-^{24}Na activity by that factor to obtain the approximate total neutron dose that the person received.

4.4 Estimation of Accident Neutron Dose Using Blood and Hair Activation

If some of the required information above is not available, the activity-to-dose conversion factor can not be simply picked. Since the blood ^{24}Na activation is a function of neutron energies from thermal to fast and hair ^{32}P activation is predominately determined by fast neutrons, the ratio of the measured activities between hair-^{32}P and blood-^{24}Na ($A_{P\text{-}32}/A_{Na\text{-}24}$) can provide additional information about the accident spectrum. Ninety-eight spectra were analyzed. Each spectrum is associated with its unique activity ratio ($A_{P\text{-}32}/Na_{Na\text{-}24}$).

Hair activation is calculated using the following equation.

$$A_P = \frac{m\lambda G}{2.22\times10^6\times W}\int_{2.5MeV}^{\infty}\phi(E)\sigma(E)dE \quad \mu Ci/g \tag{4.8}$$

where A_P is the specific activity of hair ^{32}P, m is the sulphur content per gram of hair (45 mg/g hair), G is Avogadro's number (6.023E+23), W is the atomic weight of sulphur (32 g), σ(E) is the activation cross-section of sulphur as a function of neutron energy, which is illustrated in Figure 4.7, and λ is ^{32}P decay constant.

The equation for calculating the ratio between blood and hair activities for

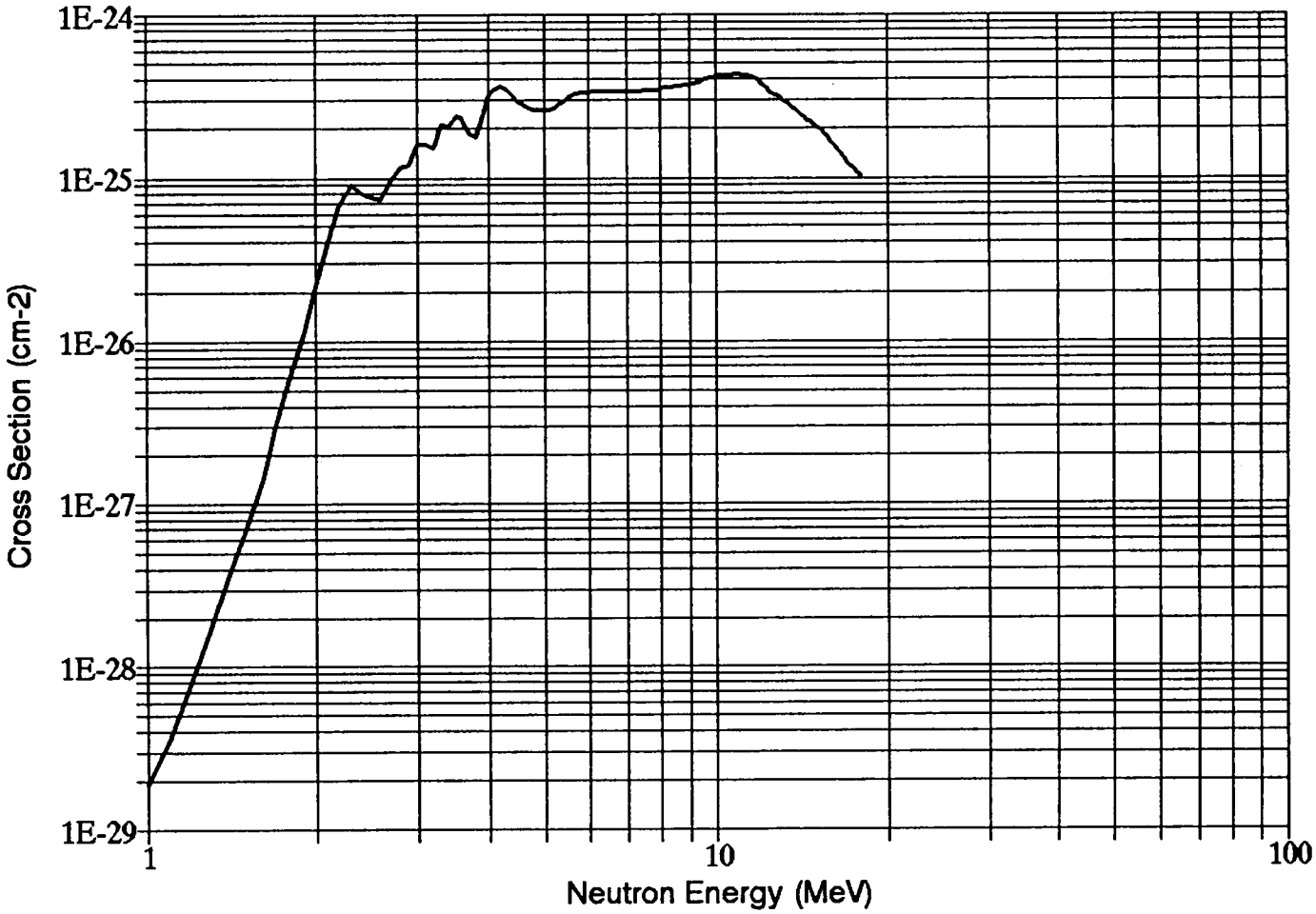


Figure 4.7 Cross Section of $^{32}S(n,p)^{32}P$

each spectrum is

$$R = 7.14\times10^{23}\frac{\int_{2.5}^{\infty}\phi(E)\sigma(E)dE}{\int_{0}^{\infty}\xi(E)\phi(E)dE}\quad\frac{\mu Ci^{32}P/g\ hair}{\mu Ci^{24}Na/g^{23}Na} \tag{4.9}$$

The calculated activity ratios for 98 spectra are listed in Table 4.6. In addition, the ratio between fast neutron fluence (above 2.5 MeV) and total neutron fluence for each spectrum is also listed in Table 4.6. To relate the activity ratio to neutron dose, the activity ratios are plotted versus the blood-sodium activation per rad of dose (activity-to-dose conversion factors) in Figure 4.8. The relationship between activity ratio and dose has an obvious trend in the range from 8.0E-8 to 1.0E-6 $\mu Ci^{32}P/g$ hair per $pCi^{24}Na/mg^{23}Na$, which covers the neutron spectra lightly shielded. The widely scattered points on the left side of the trend in Figure 4.8 are from spectra heavily shielded. More detailed figures describing the relationship between dose and activity ratio for each type of shielding are presented in Figures 4.9 (a) to 4.9 (d). Figure 4.9(a) shows the relation between dose and activity ratios from fission neutrons and fissile solution which are through different radii of H_2O, D_2O, and graphite. Figure 4.9(b) and 4.9(c) illustrates the relation from fission neutrons through different types of shieldings. Figure 4.9(d) presents the relation from H_2O moderated fission neutrons through different types of shieldings.

The procedures to estimate neutron dose using these plots are simple if the ratios from the measured blood and hair activities fall in the range from 8.0E-8 to

Table 4.6 Ratio of Activation of the Hair and Blood & Ratio of Fluence Above 2.5 MeV and Total Fluence for 98 Neutron Spectra

Spectrum Description	$\mu Ci^{32}P$/gm hair per $pCi^{24}Na$/mg ^{23}Na	$\mu Ci^{32}P$/gm hair per $\mu Ci^{24}Na$/ml blood	$\Phi_{Above\ 2.5\ MeV}/\Phi_{Total}$
UNCOLLIDED FISSION SPECTRA	.229E-06	.120E+00	.281E+00
FISSILE SOLUTION, 2 CM RADIUS SPHERE, H2O	.186E-06	.976E-01	.246E+00
FISSILE SOLUTION, 5 CM RADIUS SPHERE, H2O	.152E-06	.798E-01	.213E+00
FISSILE SOLUTION, 10 CM RADIUS SPHERE, H2O	.141E-06	.740E-01	.204E+00
FISSILE SOLUTION, 30 CM RADIUS SPHERE, H2O	.142E-06	.741E-01	.205E+00
FISSILE SOLUTION, 50 CM RADIUS SPHERE, H2O	.139E-06	.728E-01	.198E+00
FISSILE SOLUTION, 2 CM RADIUS SPHERE, D20	.198E-06	.104E+00	.255E+00
FISSION SOLUTION, 30 CM RADIUS SPHERE, D2O	.649E-07	.340E-01	.110E+00
FISSILE SOLUTION, 50 CM RADIUS SPHERE, D2O	.607E-07	.318E-01	.103E+00
UNSHIELDED HPRR SPECTRA	.700E-07	.367E-01	.108E+00
CONCRETE SHIELDED HPRR AT 3 METERS	.207E-07	.109E-01	.368E-01
PLEXIGLAS SHIELDED HPRR SPECTRA	.787E-07	.412E-01	.122E+00
STEEL SHIELDED HPRR AT 3 METERS	.218E-07	.114E-01	.386E-01
FISS.THR. 5 CM H2O	.144E-06	.756E-01	.208E+00
FISS.THR. 10 CM H2O	.206E-06	.108E+00	.273E+00
FISS.THR. 30 CM H2O	.272E-06	.142E+00	.331E+00
FISS.THR. 50 CM H2O	.397E-06	.208E+00	.413E+00
FISS.THR. 2 CM H2O AT SURFACE	.150E-06	.783E-01	.211E+00
FISS.THR. 2 CM D2O	.182E-06	.955E-01	.238E+00
FISS.THR. 5 CM D2O	.727E-07	.380E-01	.122E+00
FISS.THR. 10 CM D2O	.371E-07	.194E-01	.676E-01
FISS.THR. 30 CM D2O	.317E-07	.166E-01	.564E-01
FISS.THR. 2 CM D2O AT SURFACE	.166E-06	.868E-01	.220E+00
FISS.THR. 5 CM GRAPHITE	.245E-06	.128E+00	.288E+00
FISS.THR. 10 CM GRAPHITE	.197E-06	.103E+00	.242E+00
FISS.THR. 20 CM GRAPHITE	.103E-06	.542E-01	.146E+00
FISS.THR. 40 CM GRAPHITE	.284E-07	.149E-01	.481E-01
FISS.THR. 60 CM GRAPHITE	.108E-07	.568E-02	.184E-01
FISS.THR. 10 CM POLYE.	.137E-06	.719E-01	.183E+00
FISS.THR. 20 CM POLYE.	.163E-06	.851E-01	.201E+00
FISS.THR. 40 CM POLYE.	.228E-06	.119E+00	.259E+00
FISS.THR. 60 CM POLYE.	.275E-06	.144E+00	.297E+00
FISS.THR. 5 CM OF 1% BORATED POLYE.	.165E-06	.864E-01	.221E+00
FISS.THR. 10 CM OF1% BORATED POLYE.	.170E-06	.893E-01	.226E+00
FISS.THR. 20 CM OF 1% BORATED POLYE.	.216E-06	.113E+00	.269E+00
FISS.THR. 40 CM OF 1% BORATED POLYE.	.299E-06	.156E+00	.338E+00
FISS.THR. 60 CM OF 1% BORATED POLYE.	.351E-06	.184E+00	.376E+00
FISS.THR. 2.5 CM OF 1% BERYLIUM	.215E-06	.112E+00	.257E+00
FISS.THR. 5 CM BERYLLIUM	.161E-06	.840E-01	.201E+00
FISS.THR. 10 CM BERYLLIUM	.765E-07	.400E-01	.112E+00
FISS.THR. 20 CM BERYLLIUM	.226E-07	.119E-01	.396E-01
FISS.THR. 30 CM BERYLLIUM	.899E-08	.471E-02	.162E-01
FISS.THR. 2.5 CM ALUMINUM	.257E-06	.134E+00	.298E+00
FISS.THR. 10 CM ALUMINUM	.194E-06	.102E+00	.234E+00
FISS.THR. 20 CM ALUMINUM	.105E-06	.552E-01	.139E+00
FISS.THR. 40 CM ALUMINUM	.221E-07	.116E-01	.361E-01
FISS.THR. 10 CM CONCRETE	.120E-06	.626E-01	.184E+00
FISS.THR. 20 CM CONCRETE	.789E-07	.413E-01	.136E+00
FISS.THR. 30 CM CONCRETE	.582E-07	.305E-01	.110E+00
FISS.THR. 40 CM CONCRETE	.565E-07	.296E-01	.108E+00
FISS.THR. 60 CM CONCRETE	.593E-07	.310E-01	.114E+00

Table 4.6 (Continued)

Spectrum Description	$\mu Ci^{32}P$/gm hair per $pCi^{24}Na$/mg ^{23}Na	$\mu Ci^{32}P$/gm hair per $\mu Ci^{24}Na$/ml blood	$\phi_{Above\ 2.5\ MeV}/\phi_{Total}$
FISS.THR. 5 CM CONCRETE WITH 10% IRON	.231E-06	.121E+00	.286E+00
FISS.THR. 10 CM CONCRETE WITH 10% IRON	.171E-06	.897E-01	.233E+00
FISS.THR. 20 CM CONCRETE WITH 10% IRON	.102E-06	.534E-01	.155E+00
FISS.THR. 60 CM CONCRETE WITH 10% IRON	.547E-07	.286E-01	.853E-01
FISS.THR. 100 CM CONCRETE WITH 10% IRON	.444E-07	.232E-01	.686E-01
FISS.THR. 5 CM CONCRETE WITH 50% IRON	.217E-06	.114E+00	.269E+00
FISS.THR. 10 CM CONCRETE WITH 50% IRON	.150E-06	.785E-01	.205E+00
FISS.THR. 20 CM CONCRETE WITH 50% IRON	.764E-07	.400E-01	.119E+00
FISS.THR. 60 CM CONCRETE WITH 50% IRON	.285E-07	.149E-01	.504E-01
FISS.THR. 100 CM CONCRETE WITH 50% IRON	.212E-07	.111E-01	.389E-01
FISS.THR. 100 CM OF 100% IRON	.854E-13	.447E-07	.258E-06
FISS.THR. 5 CM IRON	.126E-06	.659E-01	.169E+00
FISS.THR. 10 CM IRON	.678E-07	.355E-01	.961E-01
FISS.THR. 20 CM IRON	.184E-07	.964E-02	.294E-01
FISS.THR. 30 CM IRON	.475E-08	.249E-02	.813E-02
FISS.THR. 50 CM IRON	.256E-09	.134E-03	.499E-03
FISS.THR. 5 CM COPPER	.110E-06	.577E-01	.149E+00
FISS.THR. 10 CM LEAD	.106E-06	.554E-01	.149E+00
FISS.THR. 20 CM LEAD	.394E-07	.206E-01	.645E-01
FISS.THR. 30 CM LEAD	.132E-07	.692E-02	.237E-01
FISS.THR. 50 CM LEAD	.185E-08	.968E-03	.374E-02
FISS.THR. 5 CM URANIUM-238	.111E-06	.579E-01	.149E+00
FISS.THR. 10 CM URANIUM-238	.538E-07	.282E-01	.805E-01
FISS.THR. 20 CM URANIUM-238	.160E-07	.836E-02	.248E-01
FISS.THR. 30 CM URANIUM-238	.630E-08	.330E-02	.102E-01
FISS.,H2O MODERATED THR. 2.5 CM BERYLLIUM	.859E-07	.450E-01	.127E+00
FISS., H2O MODERATED THR. 5 CM BERYLLIUM	.695E-07	.364E-01	.105E+00
FISS., H2O MODERATED THR. 10 CM BERYLLIUM	.403E-07	.211E-01	.648E-01
FISS., H2O MODERATED THR. 20 CM BERYLLIUM	.146E-07	.767E-02	.256E-01
FISS., H2O MODERATED THR. 10 CM ALUMINUM	.565E-07	.296E-01	.892E-01
FISS., H2O MODERATED THR. 20 CM ALUMUNUM	.267E-07	.140E-01	.452E-01
FISS., H2O MODERATED THR. 10 CM CONCRETE	.688E-07	.360E-01	.118E+00
FISS., H2O MODERATED THR. 20 CM CONCRETE	.589E-07	.308E-01	.106E+00
FISS., H2O MODERATED THR. 30 CM CONCRETE	.593E-07	.311E-01	.110E+00
FISS.,H2O MODERATED THR. 20 CM IRON	.109E-07	.570E-02	.190E-01
FISS.,H2O MODERATED THR. 50 CM IRON	.540E-09	.283E-03	.907E-03
FISS.,H2O MODERATED THR. 5 CM COPPER	.530E-07	.278E-01	.855E-01
FISS.,H2O MODERATED THR. 10 CM COPPER	.277E-07	.145E-01	.464E-01
FISS.,H20 MODERATED THR. 20 CM COPPER	.738E-08	.386E-02	.125E-01
FISS.,H2O MODERATED THR. 30 CM COPPER	.192E-08	.101E-02	.369E-02
FISS.,H2O MODERATED THR. 50 CM COPPER	.116E-08	.609E-03	.175E-02
FISS.,H2O MODERATED THR. 5 CM LEAD	.693E-07	.363E-01	.112E+00
FISS.,H2O MODERATED THR. 10 CM LEAD	.466E-07	.244E-01	.794E-01
FISS.,H2O MODERATED THR. 30 CM LEAD	.669E-08	.350E-02	.135E-01
FISS.,H2O MODERATED THR. 50 CM LEAD	.833E-09	.436E-03	.181E-02
CF-252 BARE	.267E-06	.140E+00	.312E+00
CF-252 D2O MODERATED	.490E-07	.257E-01	.847E-01

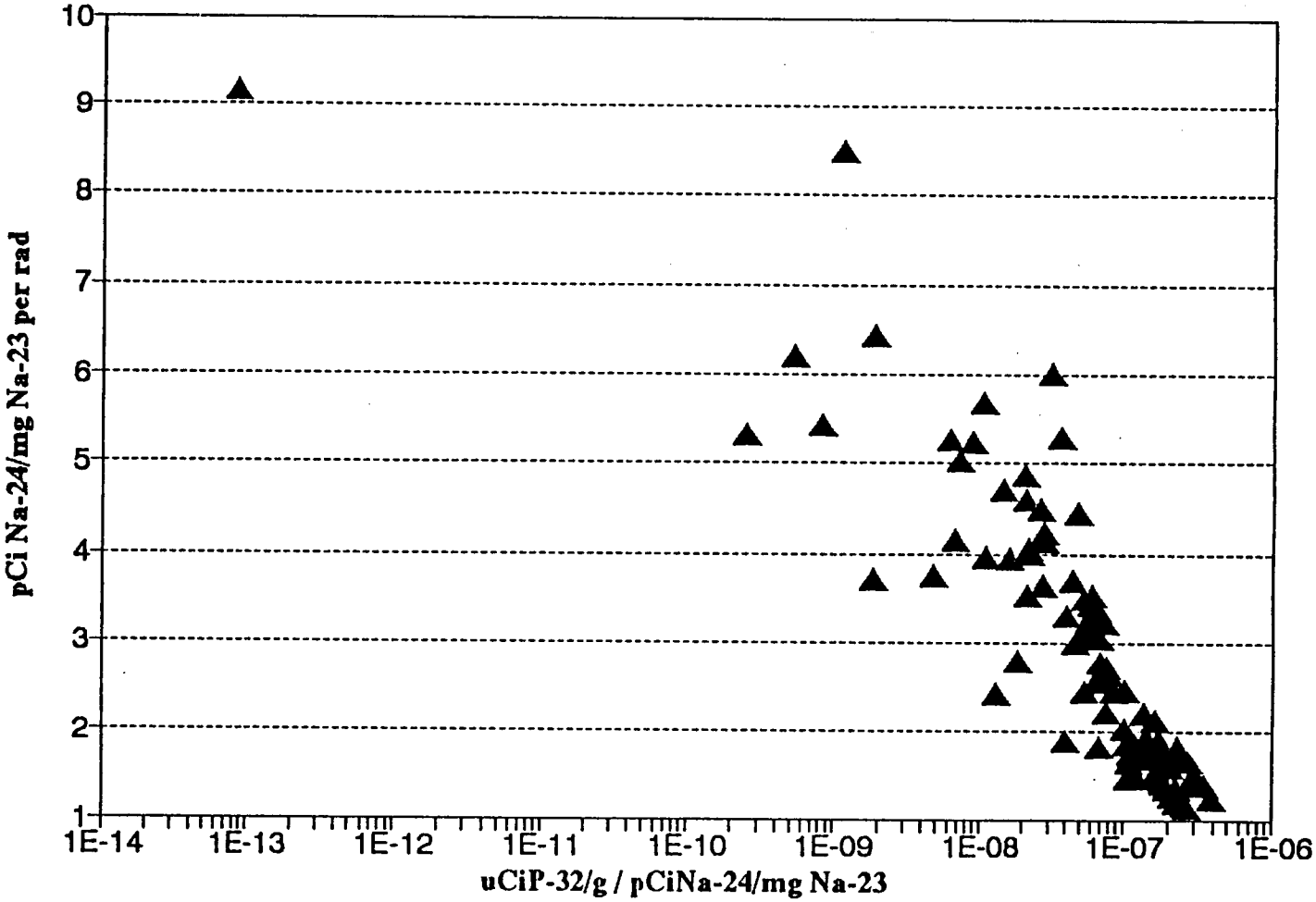


Figure 4.8 Relation Between Activity Ratio ($A_{P\text{-}32}/A_{Na\text{-}24}$) and Depth Dose For 98 Neutron Spectra

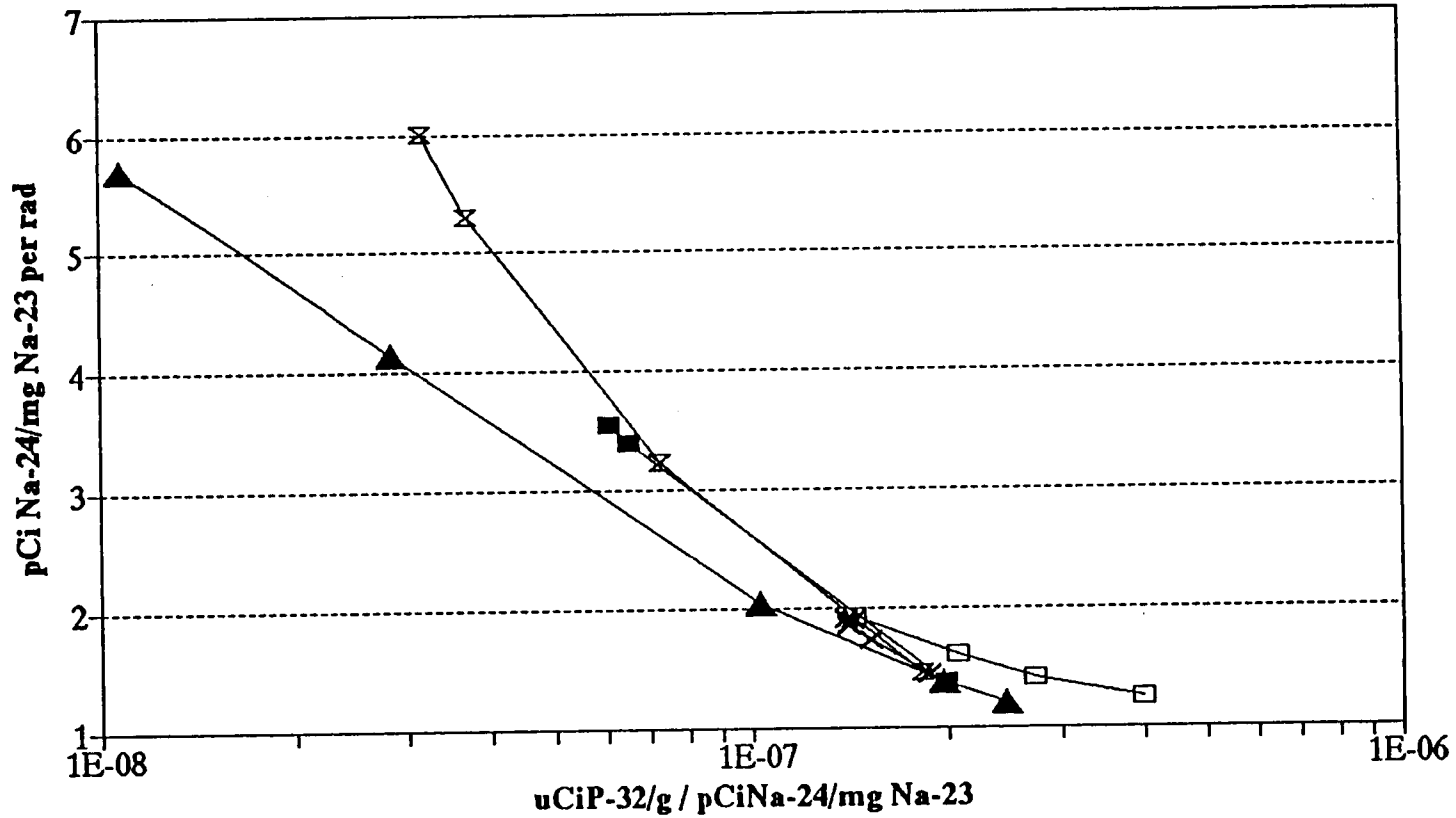
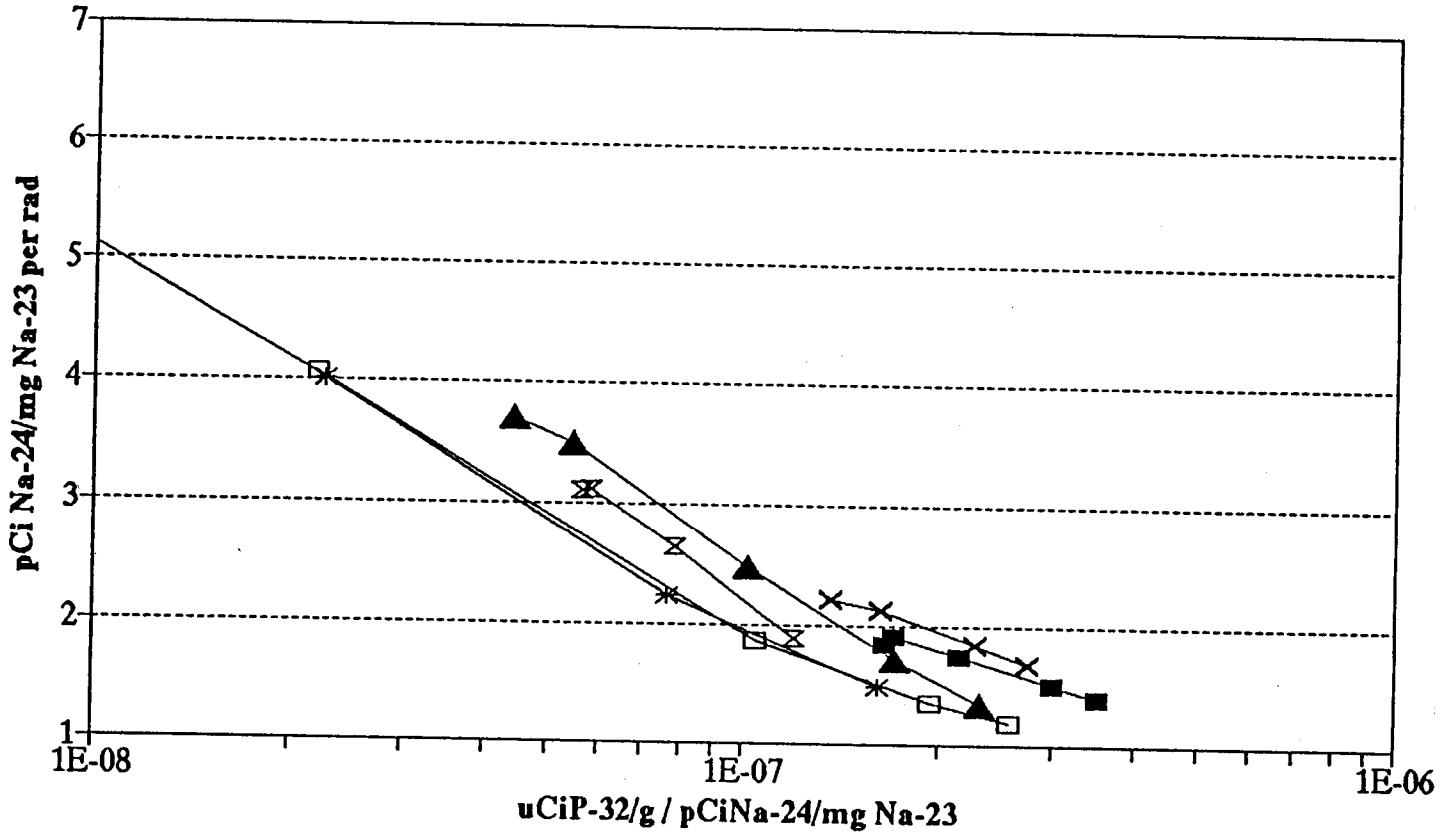
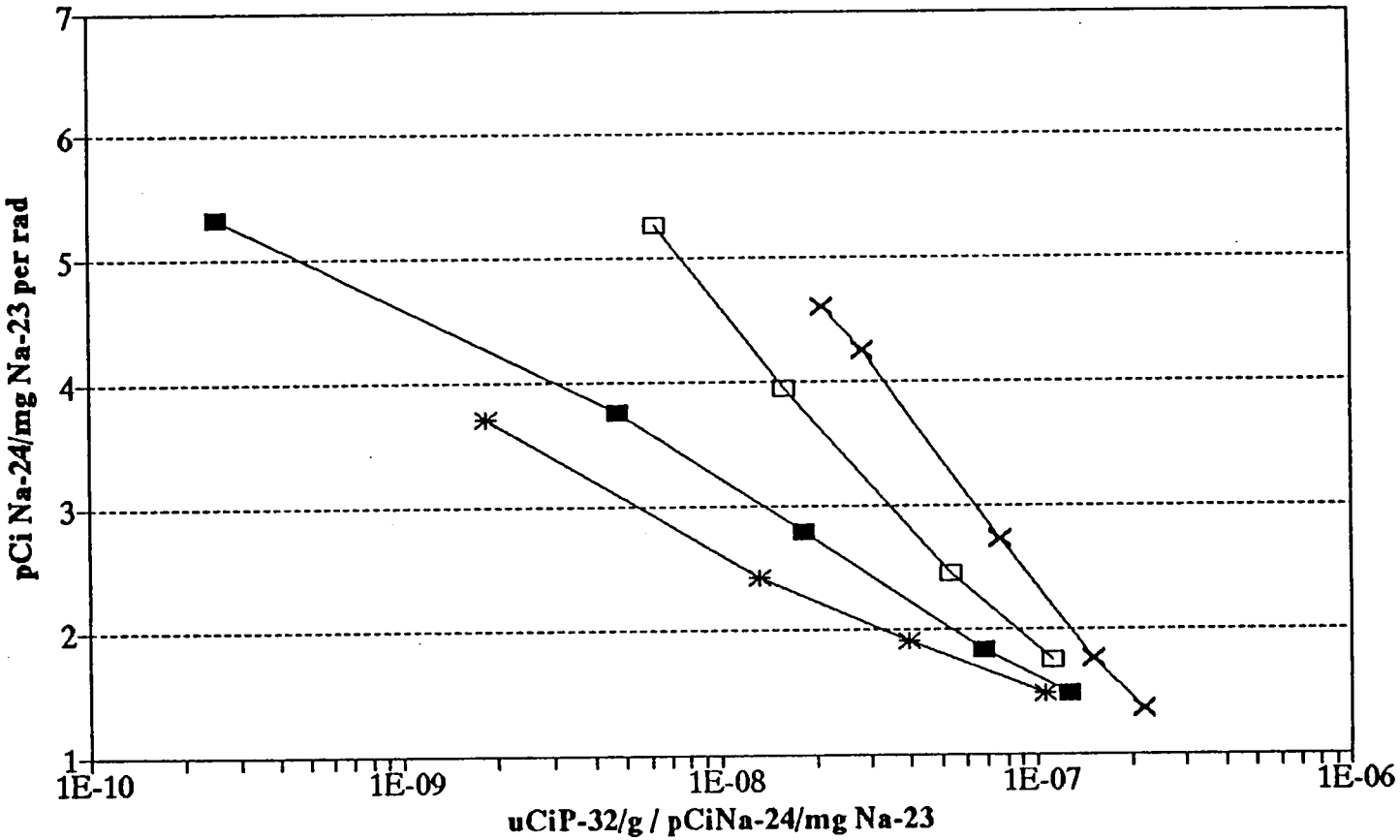


Figure 4.9 Relation Between Activity Ratio and Depth Dose



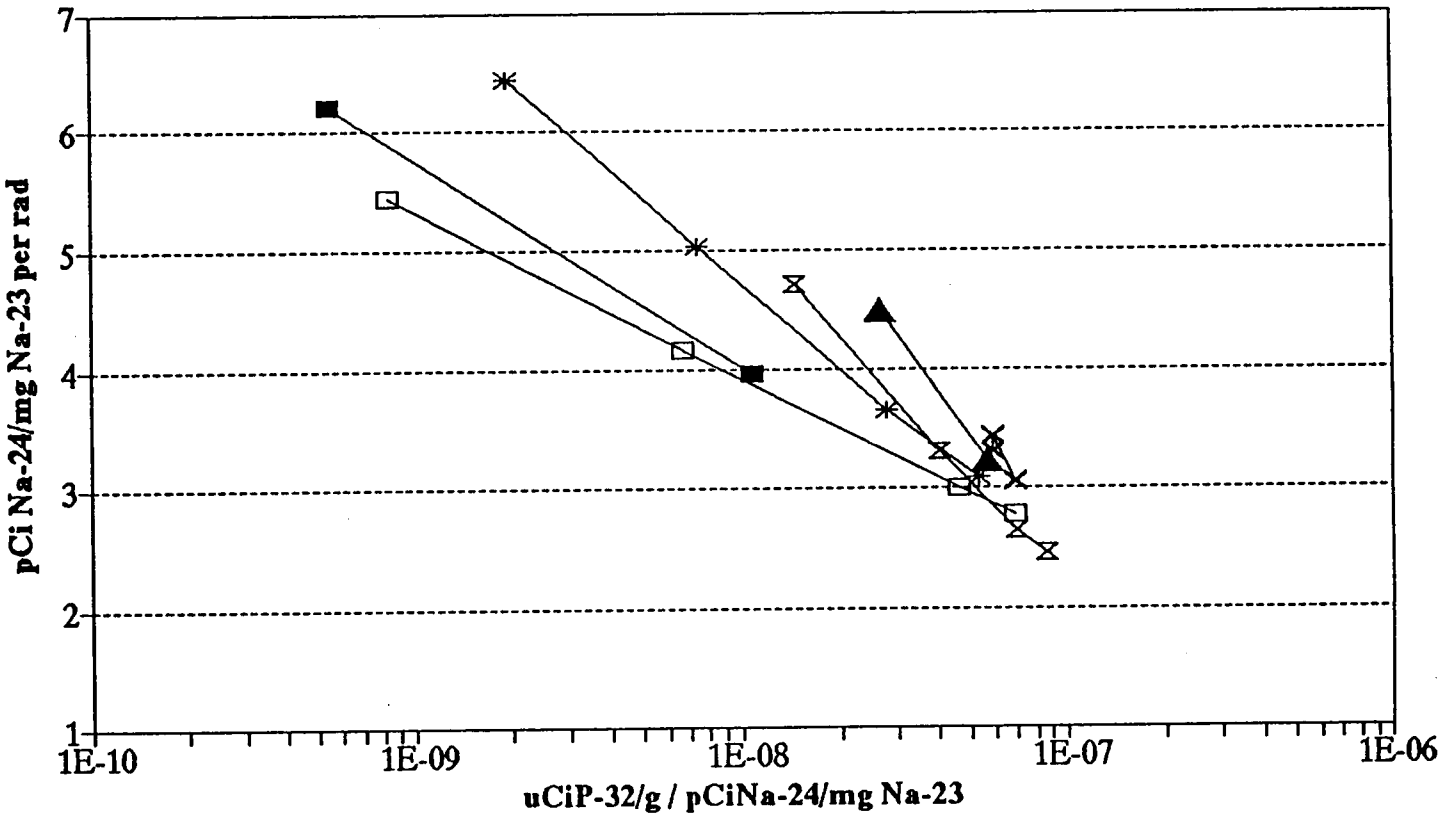
(b) FISS.THR.POLYE. FISS.1% BORAT POLYE FISS.THR.Be
FISS.THR.Al FISS.THR.CONCRETE FISS.THR.CON.10%Fe

Figure 4.9 (continued)



(c) FISS.THR.CON. FISS.THR.Fe FISS.THR.Pb FISS.THR.U-238

Figure 4.9 (continued)



(d) FISS.H2O.THR.CON. FISS.H2O.THR.Fe FISS.H2O.THR.Cu
FISS.H2O.THR.Pb FISS.H2O.THR.Be FISS.H2O.THR.Al

Figure 4.9 (continued)

1.0E-6 $\mu Ci^{32}P/g$ hair per $pCi^{24}Na/mg^{23}Na$. First, read the blood activation ($pCi^{24}Na/mg^{23}Na$ per rad) from the trend on Figure 4.8 at the point corresponding to the activity ratio (A_{P-32}/A_{Na-24}). Then, divide the measured blood activity by that quantity to obtain the estimated neutron dose. This procedure is recommended when the only informations obtained after an accident are the measured blood and hair activities without other informations related to accident neutron source. If the activity ratios fall out that range, one or two more informations such as the type of shielding materials (Pb, Cu,....), are needed to estimate the dose from Figure 4.9(a) to 4.9(d).

4.5 Interpretation of the Derived Neutron Dose

Except the leakage neutron spectrum, the activation of the blood-^{24}Na will be also effected by the floor scattering neutrons, the orientation of individual, and the individual's size.

4.5.1 Floor Scattering Neutrons

The effects of the floor scattered neutrons to the activation depends on the leakage spectrum itself, the distance of the assembly to the person, the height of the source, and the orientation of the person in the vertical plane if the neutrons incident on the front of the person. Most of the scattered neutrons are thermalized and will contribute siginificantly to the body activation, but they will contribute relatively little

to the induced neutron dose. Thus, the estiamted neutron dose based on the data from Table 4.4 and from measured blood activity will be overestimated. Scattering correction factors for the 98 neutron spectra could be calculated for particular geormetry configuation at the time of an accident. In 1981, Cross [16] conducted experiments using a phantom irradiated by fission neutron source at 3 meters to see the effect of scattering. The shift of the incident spectrum is shown in Figure 4.10. The conclusion is that floor-scattered neutrons increase the activity produced by the direct, frontally-incident neutrons by a factor of 1.43.

4.5.2 Orientation of Individual in the Moment of Excursion

Orientation affects the body activation in two ways. First, the different irradiation direction, front or lateral, causes the geometrical factor (S/V) in Equation (4.2) to change because the irradiation areas differ 2.04 times as many neutrons strike a Bomab phantom from the front as from the side. Second, capture probabilities are different for neutrons incident on the front of a phantom or on the side. The calculated results using Monto Carlo method shows that the capture probability is about 20% greater for frontal irradiation than lateral irradiation [16]. Thus, most of the variation caused by person's orientation arises from the geometrical factor rather than from the capture probability.

If the person is irradiated laterally (determined from hair samples) in an accident, the measured blood activity should be multiplied by a factor 2 before using the activity-to-dose conversion factors in Table 4.4 or Table 4.5 to determine the

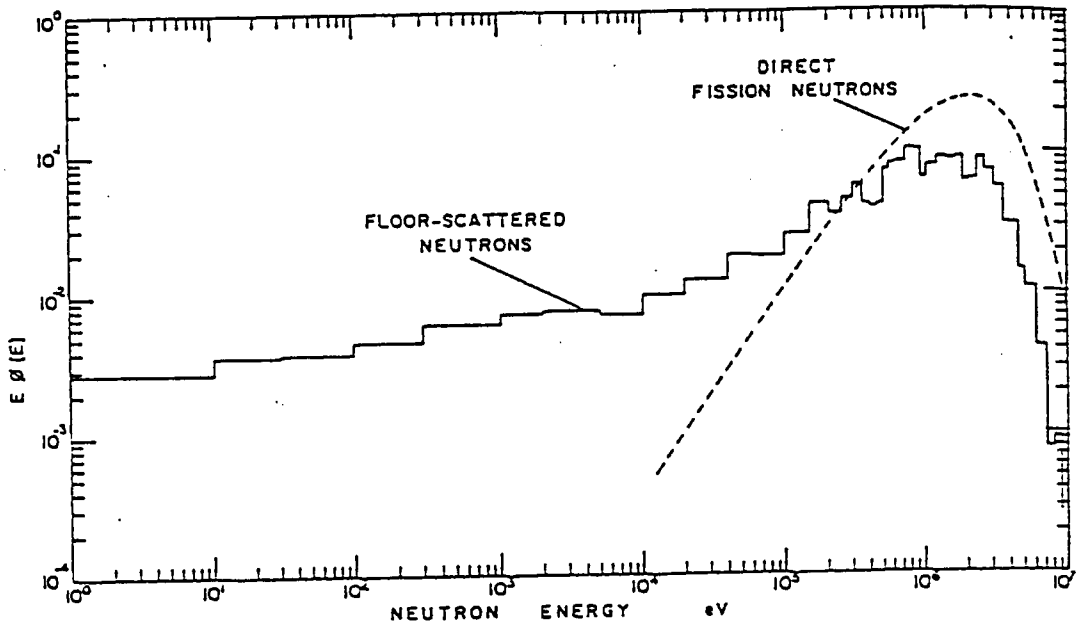


Figure 4.10 Spectra of the "Direct" and Floor-Scattered Components of Neutrons Striking a Phantom 3 m from a Fission Source. The source is 1.5 m above the Floor.

total neutron dose received.

4.5.3 Person's Size

If the person's size is larger than the Bomab phantom, the capture probabilities should be increased since the large volume will provide more opportunities for neutrons to be absorbed. However the specific activity is not significantly increased because the smaller surface area to volume ratio nearly compensates for the larger capture probability [16]. Consequently, the body size dose not contribute significantly to the variation in body activation.

CHAPTER V

CONCLUSIONS AND SUGGESTIONS FOR FURTHER WORK

5.1 Conclusions

Measurement procedures of blood-^{24}Na and hair-^{32}P activities for accident dosimetry system at ORNL are established. The measurement procedure for blood is presented in Appendix A. The one for hair is stated in Appendix B. After accidents, these procedures can be followed to quickly provide the activity information within two to six hours.

The sensitive obtained for counting 20 ml saline samples using HPGe detector is one to two rads of total neutron dose for hard spectra and below 0.5 rads for soft spectra for counting 30 to 60 minutes.

A procedure or direct counting hair samples using liquid scintillation detector was established. About six to ten rads of total neutron dose can be measured from one gram of hair sample using this measurement procedure. The simplicity of the analytical method, the small sample required (0.1g to 1.0g), and the lower Minimum Detectable Activity make the established measurement procedure a practical approch for the determination of of hair ^{32}P activty induced by criticality accidents.

The established neutron dose assessment system using blood and hair is based on a collection of 98 neutron spectra. It does not require the large amount of information necessary for other types of personnel dosimetry, permits an estimate of the individual's neutron dsoe to be made within a few hours.

5.2 Suggestions for Further Work

Ideally the estimate of neutron dose the individual received should be obtained by different dosimetry techniques. It is very meaningful to calculate the TLD responses from from 98 spectra and combine the results with the dosimetry system established by this research.

Uncertainties associated with the established dose assessment system should be analyzed quantitatively. This would involve additional experiments and analysis.

REFERENCES

1. IAEA, "Dosimetry for Criticality Accidents," Vienna, 1982.

2. G. E. Thoma, Jr. and N. Wald, "The Diagnosis and Management of Accidental Radiation Injury," Journal of Occupational Medicine, August 1959.

3. L. H. Hempelmann, H. Lisco, and J. G. Hoffman, Ann. Int. Med., 36, 279 (1952).

4. R. V. Griffith, J. Palfalvi, and V. Maphvamath, "Compendium of Neutron Spectra and Detector Responses for Radiation Detection Purposes," IAEA, Vienna, 1990.

5. Z. Ubovic and I. Miric, "Blood - Sodium Measurements for Nuclear Accident Dosimetry," IAEA-SM-229/49.

6. W. S. Snyder and M. J. Cook, "Report of Task Group on Reference man," International Commission on Radiological Protection, Number 23.

7. B. Altshuler and B. Pasternack," Statistical Measures of the Lower Limit of Detection of a Radioactivity Counter," Health Physics, Volume 9, 1963.

8. D. F. Peterson, V. E. Mitchell, and W. H. Langhman, "Estimation of Fast Neutron Doses in Man by ^{32}S (n,β) ^{32}P Reaction in Body Hair," Health Physics, Volume 6, 1961.

9. D. F. Peterson, "Personnel Dosimetry for Radiation Accidents," IAEA, Vienea, 1965.

10. D. E. Hankins, "Direct Counting of Hair Sample for ^{32}P Activation," Health Physics, Volume 17, 1969.

11. PACKARD Instrument Company. "TRI-CARB Liquid Scintillation Analyzers."

12. D. L. Horrocks, "Applications of Liquid Scintillation Counting," Academic Press, 1974.

13. Dr. Casson's Notes on Data Base Files.

14. H. Ing and W. G. Cross, Spectra and Dosimetry of Neutrons from Moderation of ^{235}U and ^{252}Cf Fission Sources In H_2)," Health Physics, Volume 29, 6, 1975.

15. G. S. Hurst, R. H. Ritchie, and L. C. Emerson, "Accidental Radiation Protection Excursion at the Oak Ridge Y-12 Plant-III," Health Physics, Volume 2, 1959.

16 W. G. Cross, "Neutron Activation of Sodium in Phantoms and the Human Body," Health Physics, Volume 41, 1981.

17. F. W. Sanders and J. A. Auxier, "Neutron Activation of Sodium in ANTHROPOMORPHOUS Phantoms," Health Physics, Volume 8, 1962.

18. International Commission on Radiological Protection (ICRP) Publication No. 21.

19. J. B. Birks, "The Theory and Practice of Scintillation Counting," The Macmillan Company, New York, 1964.

20. Y. Feng, L. F. Miller, and M. Thein, "Blood (Na-24) and Hair (P-32) Measurements for Nuclear Accident Dosimetry," 36th Annual Conference on Bioassay, Analytical & Environmental Radiochemistry, Oak ridge, Tennessee, December 1990.

21. L. F. Miller, Y. Feng, W. Casson, M. Thein, and G. Mei, "Determination of Neutron Dose from Criticality Accidents with Bioassays for Na-24 and P-32," Proceeding of Third Conference on Radiation Protection & Dosimetry, Orlando, Florida, October 1991.

22. U. S. Department of Energy, ORDER 5480.11, "Radiation Protection for Occupational Workers," Washington, D.C., December 1988.

23. "Certificate of Calibration of Mixed Radionuclide Gamma-Ray Reference Solution, M 23529," Amersham.

24. "Operation Manual for TRI-CARB Liquid Scintillation Analyzers, Models 2000CA and 2000CA/LL," Packard Instrument Company.

25. "Operational Manual for HPGe Spectra Analyzer" EG&G.

APPENDIXES

APPENDIX A

BLOOD ACTIVITY MEASUREMENT PROCEDURE

1.0 Purpose

This procedure describes a method for the determination of ^{24}Na in human blood for estimation of the neutron dose as a result of a criticality accident.

2.0 Scope

In the event an individual is exposed to neutrons, the induced activity of ^{24}Na in blood can be readily measured. This information can be used in conjunction with knowledge of the neutron spectrum to obtain an estimate of the neutron dose. If an individual has not worn proper dosimeters during an accident, ^{24}Na activity in blood can provide important information for the neutron dose evaluation.

3.0 Responsibility

A laboratory that is capable of providing dose estimates from criticality accidents must maintain appropriate equipment, records, traceability of calibration sources, and computational methods support. In addition, it must demonstrate this capability by accurate determination of neutron induced ^{24}Na activity in blind tests.

4.0 Summary of Methods

4.1 All information that will be useful for determining the accident neutron spectrum should be recorded since the activation of blood sodium is a strong function of the energy distribution of the neutrons. The composition and location of all objects in the area is very useful for obtaining accurate information on the neutron spectrum. The victim's orientation is also important for correlating dosimetry information with neutron dose and for determining other parameters, such as projected area, used in dose calculations.

4.2 A minimum of 20 ml of blood should be obtained from the exposed individual by qualified medical personnel.

4.3 The gamma spectroscopy system selected for use in determining the induced activity should be under a quality assurance program, and the applicable quality assurance tests of the equipment should be performed prior to measuring the induced ^{24}Na activity.

4.4 An efficiency calibration spectrum should be obtained for a liquid sample in the same geometry and volume as the sample from the exposed individual. A National Institute of Standards and Technology (NIST) traceable source should be used for calibration.

4.5 Determine the counting time required for measuring ^{24}Na activity to the desired accuracy according to the requirement of Minimum Detectable Activity (MDA). Use the equation for MDA in Section 9.3.

4.6 Obtain a gamma-ray spectrum from the sample of the exposed individual.

4.7 Use the 1.368 MeV photopeak counts to calculate the induced ^{24}Na activity in the blood.

4.8 Estimate the total neutron dose the individual received according to Section 11.0.

5.0 References

5.1 ICRP Report No.23

5.2 NCRP Report No.58

6.0 Materials and Equipment

6.1 The recommended gamma-ray spectroscopy system includes:

(1) a high purity Germanium detector with its liquid nitrogen cryostat,

(2) detector bias supply, linear amplifier, multichannel analyzer and data readout device,

(3) gamma-ray spectroscopy data acquisition and analysis software,

(4) a low background shield facility,

(5) liquid gamma-ray standard source, traceable to NIST, and

(6) 20 ml containers of the same geometry as the standard source.

7.0 Preparation of Detection System

The gamma-ray spectroscopy system shall be checked prior to use and all results should fall into the predetermined limits.

NOTE - The performance tests should include: the system energy calibration; the system count rate reproducebility; and the system energy resolution. All of performance tests should be conducted with a certified check source whose energies that span the 1368 KeV photopeak.

8.0 Efficiency Calibration of Detection System

8.1 Preparation of the liquid efficiency calibration source

The liquid calibration source should have the same geometry and volume as the blood sample. Detailed techniques for quantitative sampling a liquid standard source are discussed in Section 5.1.2 NCRP No.58[2].

8.2 Obtain gamma-ray spectrum using the liquid calibration source at a desired and reproducible source-to-detector distance. It is desirable that about 1000 net counts are accumulated in each full-energy gamma-ray peak to be used in the analysis.

8.3 Calculate the efficiency, E_{pi}, as follow:

$$E_{pi} = \frac{C_{net}}{A_i \, I_i}$$

where E_{pi} = full-energy peak efficiency of each nuclide.

C_{net} = net gamma-ray count rate in the full-energy peak. (counts per second live time)

A_i = gamma-ray emission rate at counting time (gamma-rays/s).

I_i = gamma-ray intensity at a certain energy for each nuclide.

8.4 Plot the values for full-energy efficiency versus gamma-ray energy (E_{pi}) on log-log graph or fit to an appropriate mathematical function.

9.0 Measurement of the ^{24}Na Activity in Blood Sample

9.1 Determine the proper counting time for the blood samples refer to the requirement of Minimum Detectable Activity (MDA) given by followed equation:

$$MDA = \frac{4.66\sqrt{C_B}}{2.22\times10^6 T E_f V}$$

where MDA = required Minimum Detectable Activity, μCi/ml,

C_B = background counts,

T = counting time,

E_f = efficiency at interested energy peak, and

V = volume of blood sample, ml.

The specified MDA corresponds to a 95% statistical confidence level.

9.2 Verify that the blood samples from the irradiated individuals are properly identified.

9.3 Document the time the accident happened and the time elapsed between the accident excursion and the blood sample taken.

9.4 Place the blood sample on the detector to be measured at the source-to-detector distance used for efficiency calibration.

9.5 Accumulate the gamma-ray spectrum and record the elapsed time from the end of the irradiation to the start of the counting and elapsed time from the end of irradiation to the end of the counting.

9.6 Counting times of 30 to 60 minutes may be required to obtain a LAUDE that corresponds to one or five lid dose for typical counting systems.

9.7 Record the net counts in the 1.368 MeV energy peak.

10.0 Calculation of ^{24}Na Concentration in Blood Sample

The concentration of Na-24 in blood sample and one standard deviation of calculated activity are given by

$$A_{Na} = \frac{\lambda C_{Na} F_a}{2.22\times10^6 (e^{-\lambda t_1} - e^{-\lambda t_2}) E_f I_r V R_t}$$

$$\sigma_A = A_{Na} \sqrt{\frac{G_{B+C} + C_B}{C_{Net}^2}}$$

where A_{Na} = ^{24}Na concentration in blood sample, μCi/ml,

C_{Net} = the number of the net counts at 1.368 MeV energy peak,

λ = decay constant of ^{24}Na, 0.00077 min^{-1},

t_1 = elapsed time from the end of irradiation to start of the counting, mins,

t_2 = elapsed time from the end of irradiation to the end of the counting, mins,

E_f = detection system efficiency at 1.368 MeV,

I_I = gamma-ray intensity at 1.368 Mev, 100%,

V = total volume of blood sample, ml,

G_{B+C} = number of gross counts at 1.368 MeV,

C_B = number of the background counts in the region corresponding to the peak area of G_c,

σ_A = one standard deviation of A,

R_t = metabolic correction factor, and

F_a = decay correction factor.

The correction for ^{24}Na radioactive decay is needed if irradiation time is longer than one hour. The derived correction factor is
where F_a = decay correction factor,

λ = ^{24}Na decay constant, 0.00077 min^{-1}, and

$$F_a = \frac{\lambda t_a}{1 - e^{-\lambda t_a}}$$

t_a = irradiation time, mins.

The metabolic half-life for ^{24}Na from the body is 12 days. If a correction is necessary, R_t can be taken to be

$$R_t = 4.87e^{-0.0815t} + 0.51e^{-0.0513t} + 0.0027e^{-0.0015t}$$

Where R_t is the fraction of the initial ^{24}Na remaining in the body at the time the sample is collected, t days after the accident.

APPENDIX B

HAIR ACTIVITY MEASUREMENT PROCEDURE

1.0 Purpose

This procedure describes a method for the determination of ^{32}P activity in human head hair for estimation of neutron dose above 2.5 MeV from a nuclear criticality accident.

2.0 Scope

In the event of an individual being is exposed to neutrons, the induced activity of ^{32}P in hair can be readily measured. This information can be used in conjunction with knowledge of the neutron spectrum to obtain an estimate of the total neutron dose. The neutron dose above 2.5 MeV can be obtained directly from the ^{32}P activity measurement. The irradiated hair also provides information on the person's orientation in the accident.

3.0 Responsibility

A laboratory that is capable of providing dose estimates from criticality accidents must maintain appropriate equipment, records, traceability of calibration sources, and computational methods support. In addition, it must demonstrate this capability by accurate determination of neutron dose in blind tests.

4.0 Summary of Methods

4.1 All information associated with the accident that influences the neutron energy distribution should be recorded. The location of the exposed personal, the orientation, shielding, and actions of the person following the excursion. Composition and location of all objects in the area are very useful for obtaining accurate information on the neutron spectrum.

4.2 Four head hair samples from different parts around the head of the exposed person should be obtained, and a minimum of 0.1 gm hair is needed for each location sample.

4.3 The liquid scintillation counting system selected for use in determining the induced activity should be under a quality assurance program, and the applicable quality assurance tests of the equipment should be checked for performance prior to measuring the induced ^{32}P activity.

4.4 If a National Institute of Standards and Technology (NIST) liquid ^{32}P source (or a equivalent maximum β energy traceable liquid source) is available, an accurate efficiency calibration of liquid scintillation counter can be obtained. If not, an efficiency tracing method may be used.

4.5 Hair samples should be dissolved or ashed to obtain the background measurement.

4.6 Determine the counting time required for measuring ^{32}P activity based on the equation for Minimum Detectable Activity (MDA) in Section 9.2.

4.7 Obtain ^{32}P net count rate from the sample of the exposed individual and calculate the activity of ^{32}P using the method in Section 9.2.

5.0 Materials and Equipment

5.1 Liquid Scintillation Counter.

5.2 Hair Dissolving Materials

5.2.1 Hydrogen peroxide 30%
5.2.2 Tissue solubilize
5.2.3 DTT (Dithiothreitol)
5.2.4 Heater

5.3 Hair Ashing Materials

5.3.1 High temperature muffle furnace
5.3.2 Crucibles
5.3.3 Triton-10

5.4 Hair Cleaning Materials

5.4.1 Detergent
5.4.2 Distilled Water
5.4.3 Ethanol

5.5 Scintillation cocktail for biological materials, with high efficiency and low chemiluminescence.

5.6 Scintillation Glass Bottles (20 ml).

5.7 Analytical balance.

5.8 Digital pipett, and test tubes.

6.0 Preparation of Hair Sample

6.1 Take the hair samples from the front, back, left, and right of the victim's head and put the name tag on each sample.

6.2 Document the detailed position on head the hair removed, the time the accident happened, and the time elapsed before the hair sample taken.

6.3 Wash the hair removed with detergent, distilled water and ethanol, and then dried in an oven with the temperature below 80^0C.

6.4 Cut the washed hair as tiny as possible. Be careful, not to mix the different samples.

6.5 Weight each sample accurately, and document the weight.

6.6 Hair Sample Treatment

Chemical dissolving or ashing may be used for preparing hair for liquid scintillation counting. The chemical dissolving method is recommended if the amount of hair in the sample is less than 0.3 gm, otherwise choose the ashing method.

6.6.1 Chemical Dissolution Hair

6.6.1.1 Put the weighted hair into a scintillation glass vial. Add the dissolving materials: hydrogen peroxide 30%, tissue solubilize, and DTT orderly.

One gram of hair may need 14000 μl tissue solubilizer, 7000 μl hydrogen peroxide 30%, and 0.12g DTT.

6.6.1.2 Swirl the vial gently and digest at the constant 50 ^{0}C-60 ^{0}C until the hair completely dissolved. Usually need three to four hours.

6.6.1.3 Put 20 ml cocktail into vial, and wait for 20 minutes until the solution is transparent.

6.6.2 Ashing Hair

6.6.2.1 Preheat the muffle furnace until the temperature is 800 ^{0}C. Usually this process needs one to two hours.

6.6.2.2 Put the weighted hair into a crucible and then put the crucible into

the muffle furnace.

6.6.2.3 Keep the temperature about 800 °C to 815 °C. The heating time depends on the amount of hair, 15 minutes for 0.5 gm and 20 minutes for 1 gm.

6.6.2.4 Put the hot crucible on a heat isolating material and wait about 20 minutes until the crucible cooling down.

6.6.2.5 Collect all of the ashed powder and place it in a scintillation glass vial. Put 5 ml of cocktail into the crucible and gently stir the solution and another 10 ml of cocktail in the scintillation glass vial.

If the glass vial can work under a high temperature (800°C), direct ashing hair in a scintillation vial ia recommended.

6.6.2.6 To get a relative homogeneous sample, put 5 ml of triton-10 into the glass vial. Cap the vial and then shake it vigorously to mix until the solution begins to jell. Place the vial into the counting system.

7.0 Preparation of Background Sample

The same procedures should be used for preparation of the background samples as used for the irradiated samples.

8.0 Measurement Procedures

8.1 It is recommended that the liquid scintillation counter be under quality control program. If not, conduct performance tests before using the counter. The tests should include the QIP/^{14}C efficiency check, ^{3}H efficiency check and background check. The detailed procedures can refer to the operation manual of the counting system.

8.2 Perform an efficiency calibration if quenched ^{32}P liquid standards are available. When edit DPM protocol program, set counting time of interest, window 1 (energy region A) on 5 keV-1710 keV, and window 2 (energy region B) on 50 keV-1700 keV.

If all of the process follows the above procedures, the 95% efficiency can be directly used in the following counting and calculation instead of the efficiency calibration, which will reduce the preparation time and simplify the counting process with a reasonable accuracy.

8.3 Edit the protocol program[1]. Suggested inputs for the Packard 2000 are shown below.

Count Time[2]	30, 60, or 90 mins.
# Counts/vial	1
# Vials/Standard	1
# Vials/sample	1
1st Vial background	Yes
Radio-nuclide	^{32}P
Region A: LL-UL	5.0 - 1700 KeV
Region B: LL-UL	50.0 - 1700 KeV
QIP	tSIE
ES Terminator	Count
Data Mode	CPM
Luminescence Correction	On
Heterogeneity Monitor	Yes
Printout	Count Time, CPMA, CPMB, 2S%, tSIE, SIS, and LUM%

Notes:

1. All operational information on the following Table is concerning Packard Tri-Carb 2000CA and 2000CA/LL liquid scintillation systems.

2. The count time of interest should be basically satisfied with MDA.

8.4 Count samples at least twice using the same procedure.

9.0 ^{32}P Activity Calculation

9.1 ^{32}P activity induced in hair and one standard deviation of calculated activity are given by

$$A = \frac{C}{2.22\times10^{-6}e^{-\lambda t}E_f m}, \quad (\mu Ci/g),$$

$$\sigma_A = A\sqrt{\frac{G_c+B_c}{TC^2}}$$

where A = ^{32}P activity induced in hair, dpm/g, or μCi/g,

C = CPM in energy region A,

If the data in region A looks unreasonable large, using the CPM in region B. There may be some unknown chemical reactions happened in solution.

λ = ^{32}P decay constant,

t = elapsed time from the end accident until the start of counting,

E_f = counting efficiency for ^{32}P,

m = the amount of hair (g),

G_c = gross cpm in energy region A,

B_c = background cpm in energy region A,

σ_A = one standard deviation of A, and

T = counting time, which is same for sample and background (min.).

9.2 Minimum Detectable Activity

$$MDA = \frac{4.66\sqrt{B_c}}{2.22\times10^6 E_f T m}, \quad (\mu Ci/g).$$

Where B_c = background cpm,

T = counting time, which is same for sample and background (min.).

E_f = counting efficiency,

m = the amount of hair sample (g), and

MDA = Minimum Detectable Activity, $\mu C_i/g$, at a confidence level of 95%.

APPENDIX C.1

FORTRAN PROGRAM FOR INTERPOLATING 98 NEUTRON SPECTRA

THIS PROGRAM IS TO INTERPOLATE 98 NEUTRON SPECTRA WITH SAME ENERGY BOUNDARIES. THE DATA FILES NEEDED ARE: ENERGY OUTPUT FILE'S FILE NAME, FLUENCE OUTPUT FILE'S FILE NAME, NUMBER OF SPECTRA NEEDED TO BE INTERPOLATED, INPUT ENERGY FILE'S FILE NAME, AND INPUT FLUENCE FILE'S FILE NAME.

```
      PROGRAM FOR INTERPOLATING THE FLUENCE
      CHARACTER*70 OUTE, OUTF, IENAME, IFNAME
     * ,ONAMEE, ONAMEF, NAMEE, NAMEF, NAMEOE, NAMEOF
      REAL  PHIU,E
      INTEGER I, J, COUNT,M,N,k,JJ
      DIMENSION EG(621), PHI(100), EAV(100)

      WRITE(*,*) 'ENERGY OUTPUT FILE_S FILE NAME'
      READ(*,'(A)') OUTE

      WRITE(*,*) 'FLUENCE OUTPUT FILE_S FILE NAME'
      READ(*,'(A)') OUTF

      WRITE(*,*) ' NUMBER OF FILES TO INTERPOLATED'
      READ(*,'(A)') NFILES

      WRITE(*,*) 'MIDDLE ENERGY FILE_S FILE NAME'
      READ (*, '(A)') IENAME

      WRITE(*,*) 'MIDDLE FLUENCE FILE_S FILE NAME'
      READ (*, '(A)') IFNAME

      OPEN(30, FILE=IENAME, STATUS='OLD')
      OPEN(40, FILE=IFNAME, STATUS='OLD')

      OPEN(16, FILE=OUTE, STATUS='OLD')
      OPEN(17, FILE=OUTF, STATUS='OLD')

      OPEN(12, FILE='ER621', STATUS='OLD')
      READ(12,*) EG

      DO JJ=1, NFILES
```

```
      READ(30,'(A)') NAMEE
      READ(40,'(A)') NAMEF
      OPEN(10,FILE=NAMEE,STATUS='OLD')
      OPEN(11,FILE=NAMEF,STATUS='OLD')

      READ(16,'(A)') NAMEOE
      READ(17,'(A)') NAMEOF
      OPEN(14, FILE=NAMEOE, STATUS='UNKNOWN')
      OPEN(15, FILE=NAMEOF, STATUS='UNKNOWN')

      I=1
      DO while (.TRUE.)
      READ(10, *, END=99) EAV(I)
      READ(11,*,END=99) PHI(I)
      I=I+1
      END DO
99    COUNT=I-1
      write(14,*) EAV(1)
      CLOSE (10)
      CLOSE(11)

      k=1
      DO 300 J=2, COUNT

      DO 400 I=k, 621
            IF (EG(I).GT.EAV(J-1) .AND. EG(I).LE.EAV(J)) THEN
   PHIU=PHI(J-1)+((PHI(J)-PHI(J-1))/(EAV(J)-EAV(J-1)))*
     >         (EG(I)-EAV(J-1))

       E=EG(I)
          WRITE(15,*) PHIU
       WRITE(14,*) E

      ELSE IF (EG(I).GT.EAV(J)) THEN
      GOTO 500
            ELSE
      END IF

400   CONTINUE

500   N=I+1
       K=N-1

300   CONTINUE
```

```
END DO

STOP
END
```

APPENDIX C.2

FORTRAN PROGRAM FOR CALCULATING

ACTIVITY RATIO BETWEEN HAIR ^{32}P TO BLOOD ^{24}Na

FOR 98 NEUTRON SPECTRA

THIS PROGRAM IS TO CALCULATE ACTIVATION RATIO BETWEEN HAIR-^{32}P AND BLOOD-^{24}Na. THE DATA FILES NEEDED ARE: NUMBER OF FILES TO BE INTERPOLATED, ENERGY BOUNDARY FILE'S FILE NAME, FLUENCE FILE'S FILE NAME, AND SPECTRUM NAME LIST.

```
      PROGRAM CANVERSION FACTOR CALCULATION
      CHARACTER*70, NAMEFF, NAMEFE,ICNAME,
*           ONAME,FENAME,FFNAME,DNAME
      REAL  PHITOT, ANA1,A1,AP,SUMPHIU,
      INDEX1,FPHI,SUL_B,SUL_A,R,
     >      ANA2,A2,INDEX2,ASIGMA,FFPHI
      INTEGER I,J,N,COUNT,K,JJ
      DIMENSION  EB(1000), PHIU(1000), EC(28), CAP(27),SIGMAP(155)
      DATA ASIGMA/240E-27/

      WRITE(*,*) 'OUTPUT FILE NAME'
      READ(*, '(A)') ONAME

      WRITE(*,*) 'NUMBER OF FILES TO BE CALCULATED '
      READ(*,*) NFILES

      WRITE(*,*) 'ENERGY BOUNDARY FILE_S FILE NAME'
      READ(*,'(A)') FENAME

      WRITE(*,*) 'FLUENCE FILE_S  FILE NAME'
      READ(*,'(A)') FFNAME

      WRITE(*,*) 'SPECTRUM NAME LIST'
      READ(*,'(A)') DNAME

      OPEN(30, FILE=FENAME,STATUS='OLD')
      OPEN(40,FILE=FFNAME,STATUS='OLD')
      OPEN(20, FILE=DNAME,STATUS='OLD')
```

```
      OPEN(12, FILE='UE28.PHA', STATUS='OLD')
      READ(12,*) EC

      OPEN(15,FILE='P32CS.25', STATUS='OLD')
      READ(15,*) SIGMAP

      OPEN(14,FILE='UCS27.PHA', STATUS='OLD')
      READ(14,*) CAP

      OPEN(13, FILE=ONAME, STATUS='NEW')

      DO JJ=1,NFILES
      READ(30,'(A20)') NAMEFE
      READ(40,'(A20)') NAMEFF
      READ(20,'(A70)') DNAME

      OPEN(10,FILE=NAMEFF, STATUS='OLD')
      OPEN(11,FILE=NAMEFE,STATUS='OLD')

      I=1
      DO 50 n=1,1000
      READ(11,*,END=99) EB(I)
      I=I+1

50    CONTINUE

99    COUNT=I-1

      J=1
      DO 60 I=1,1000
      READ(10,*,END=98) PHIU(J)
      J=J+1

60    CONTINUE

98    PHITOT=0
      DO 200 I=2, COUNT
            PHITOT=PHITOT+PHIU(I-1)*(LOG(EB(I))-
     >           LOG(EB(I-1)))

200   CONTINUE

      DO 300 I=1,COUNT
            IF(EB(I).EQ.2.5) THEN
```

```
            M=I+1
            ELSE
            END IF

300   CONTINUE

      AP=0
      ANA1=0
      A1=0
      FPHI=0
      J=M-1
      A2=0
      ANA2=0

      DO 400 I=M, COUNT

      AP=AP+(1.293E+10)*PHIU(I-1)*SIGMAP(I-J)*(LOG(EB(I))
     >       -LOG(EB(I-1)))

      FPHI=FPHI+PHIU(I-1)*(LOG(EB(I))
     >       -LOG(EB(I-1)))

400   CONTINUE
      R=FPHI/PHITOT

      N=1
      DO 5000 J=2,28
            SUMPHIU=0
      DO 4000 I=N,COUNT
            IF (EB(I-1).GE.EC(J-1).AND.EB(I-1).LT.EC(J)) THEN

            SUMPHIU=SUMPHIU+PHIU(I-1)*(LOG(EB(I))
     >            -LOG(EB(I-1)))

            ELSE IF (EB(I-1).GE.EC(J)) THEN
            GOTO 1000
            ELSE
            END IF

4000  CONTINUE

1000  N=I+1

      A1=CAP(J-1)*SUMPHIU*(1.81667E-8)
```

```
      ANA1=ANA1+A1
      ANA2=(ANA1/1.81667E-8)* (3.47E-14)

5000  CONTINUE

      INDEX1=AP/ANA1
      INDEX2=AP/ANA2
      FFPHI=AP/(1.293E+10 * ASIGMA)
      SUL_A=FFPHI/ANA1
      SUL_B=FPHI/ANA1

      WRITE(13,1) DNAME,INDEX1,INDEX2,R
1     FORMAT( A43, E9.3, 2X, E9.3, 2X, E9.3)

      END DO

      STOP
      END
```

APPENDIX C.3

FORTRAN PROGRAM FOR CALCULATING

BLOOD ACTIVITY-TO-DOSE CONVERSION FACTORS

FOR 98 NEUTRON SPECTRA

THIS PROGRAM IS TO CALCULATE BLOOD ACTIVITY-TO-DOSE CONVERSION FACTORS. THE DATA FILES NEEDED ARE: NUMBER SPECTRA TO BE ANALYZED, ENERGY BOUNDARY FILE'S FILE NAME, FLUENCE FILE'S FILE NAME, AND SPECTRUM NAME LIST.

```
      PROGRAM  DOSE CANVERSION FACTOR CALCULATION

      CHARACTER*70, NAMEFF, NAMEFE,ICNAME,
     *  ONAME,FENAME,FFNAME,DNAME
      REAL  K, PHISUM, PHITOT, ATOTAL,A,D,DTOTAL,SUMPHIU,W
      INTEGER I,J,N,COUNT,ICOUNT,JJ
      DIMENSION C(14), EB(1000), PHIU(1000), E(15), EC(28), CAP(27)
      DATA C/3.9E-10, 3.9E-10, 3.9E-10, 3.6E-10, 3.4E-10, 2.8E-10,
     *       2.4E-10, 2.1E-10, 2.0E-10, 1.65E-10, 1.4E-10,
     *          1.0e-10, 2.45E-10, 3.7E-10/
      DATA E/2.50E-8, 1.0E-7, 1.0E-6, 1.0E-5, 1.0E-4, 1.0E-3,
     *       1.0E-2, 1.0E-1, 5.0E-1, 1.0E+0, 2.0E+0,
     *         5.0E+0, 10.0E+0, 14.0E+0,20.0E+0/


      WRITE(*,*) 'OUTPUT FILE NAME'
      READ(*, '(A)') ONAME

      WRITE(*,*) 'NUMBER OF FILES TO BE CALCULATED'
      READ(*,*) NFILES

      WRITE(*,*) 'ENERGY BOUNDARY FILE_S FILE NAME'
      READ(*,'(A)') FENAME

      WRITE(*,*)'FLUENCE FILE_S FILE NAME'
      READ(*,'(A)') FFNAME

      WRITE(*,*) 'FILES_NAME LIST'
      READ(*,'(A)') DNAME
```

```
      OPEN(30, FILE=FENAME, STATUS='OLD')
      OPEN(40, FILE=FFNAME, STATUS='OLD')
      OPEN(20, FILE=DNAME, STATUS='OLD')

      OPEN(12, FILE='UE28.PHA', STATUS='OLD')
      READ(12,*) EC

      OPEN(14,FILE='UCS27.PHA', STATUS='OLD')
      READ(14,*) CAP

      OPEN(13, FILE=ONAME, STATUS='NEW')

      DO JJ=1,NFILES
      READ(30,'(A20)') NAMEFE
      READ(40,'(A20)') NAMEFF
      READ(20,'(A70)') DNAME

      OPEN(10, FILE=NAMEFF, STATUS='OLD')
      OPEN(11, FILE=NAMEFE, STATUS='OLD')

      I=1
      DO 50 n=1,1000
      READ(11,*,END=99) EB(I)
      I=I+1
50    CONTINUE

99    COUNT=I-1
      CLOSE (11)

      J=1
      DO 60 I=1,1000
      READ(10,*,END=98) PHIU(J)
      J=J+1
60    CONTINUE
      CLOSE(10)

98    PHITOT=0
      DO 300 I=2, COUNT
            PHITOT=PHITOT+PHIU(I-1)*(LOG(EB(I)*1000000)-
     >          LOG(EB(I-1)*1000000))
300   CONTINUE

      N=1
```

```
      DTOTAL=0
      K=0
      A=0
      D=0
      ATOTAL=0

      DO 500 J=2, 15

        PHISUM=0

        DO 400 I=N, COUNT

          IF (EB(I-1).GE.E(J-1).AND.EB(I-1).LT.E(J)) THEN
           PHISUM=PHISUM + PHIU(I-1)*(Log(EB(I)*1000000)
     >       -Log(EB(I-1)*1000000))

           ELSE IF (EB(I-1).GE.E(J)) THEN
          GOTO 100
          ELSE
          END IF

400     CONTINUE

100    N=I+1

       D=C(J-1)*PHISUM
       DTOTAL=DTOTAL+D
500    CONTINUE

      N=1
      DO 5000 J=2,28
            SUMPHIU=0
      DO 4000 I=N,COUNT
            IF (EB(I-1).GE.EC(J-1).AND.EB(I-1).LT.EC(J)) THEN
            SUMPHIU=SUMPHIU+PHIU(I-1)*(LOG(EB(I)*1000000)
     >          -LOG(EB(I-1)*1000000))
            ELSE IF (EB(I-1).GE.EC(J)) THEN
            GOTO 1000
            ELSE
            END IF

4000  CONTINUE

1000  N=I+1
```

```
      A=CAP(J-1)*SUMPHIU
      ATOTAL=ATOTAL+A

5000  CONTINUE

      K=1.81667E-8 * (ATOTAL/DTOTAL)
      W=2.90867E+13 *(DTOTAL/ATOTAL)

      WRITE(13,1) DNAME,K,W
1     FORMAT(A45,1X,F10.3,6X,F10.3)
      END DO

      STOP
      END
```

APPENDIX D

ADDITIONAL BIBLIOGRAPHY

1. J. E. Turner, "Atoms, Radiation, and Radiation Protection," Pergamon Press, Inc, 1986.

2. A. B. Brodsky, "CRC Handbook of Radiation Measurements and Protection, Section A, Volume I: Physical Science and Engineering Data," CRC Press, Inc., 2255 Palm Beach Lakes Boulevard, West Palm Beach, Florida 33409, 1978.

3. E. D. Bransome, Jr., "The Current Status of Liquid Scintillation Counting," Grune & Stratton, Inc., 757 Third Avenue, New York, New York 10017, 1970.

4. H. J. M. Bowen and D. Gibbons, "Radiation Analysis," Oxford at the Clarendon Press, 1963.

5. International Atomic Energy Agency, "Neutron Monitoring for Radiation Protection Purposes," Proceeding of a Symposium on Neutron Monitoring for Radiation Protection Purposes, Vol. I and Vol. II, IAEA, Vienna, Austria, 1973.

6. International Atomic Energy Agency, "Selected Topics in Radiation Dosimetry," Proceedings of the Symposium on Selected Topics in Radiation Dosimetry, IAEA, Vienna, Austria, June 1960.

7. J. M. A. Lenihan, S. J. Thomson, and V. P. Guinn, "Advances in Activation Analysis," Academic Press, Inc., 1972.

8. J. B. Briks, "The Theory and Practice of Scintillation Counting," A Pergamon Press Book, The Macmillan Company, New York, 1964.

9. International Atomic Energy Agency, "Neutron Monitoring for Radiation Protection Purposes," Proceeding of a Symposium on Neutron Monitoring for Radiation Protection Purposes, IAEA, Vienna, Austria, September 1966.

10. W. J. Gray and A. M. James, "Radiochemical Methods," John Wiley & Sons, 1986.

VITA

I was born in Beijing, China. I graduated from Beijing University of Science & Technology, in August, 1984 with a Bachelor of Science Degree in Mechanical Engineering. I had been a mechanical engineer in Beijing Institute of Nuclear Engineering for five years before I came to the Unite States of American. In fall of 1989, I entered the University of Tennessee, Nuclear Engineering Department, as a full time graduate student in Radiation Protection Engineering (Health Physics). I expect to be awarded the Master of Science Degree with a major in Nuclear Engineering and a minor in Statistics, in December, 1991.